Bifurcations and Linear Stability of Families of Relative Equilibria With A Dominant Vortex

A THESIS
SUBMITTED TO THE FACULTY OF THE GRADUATE SCHOOL
OF THE UNIVERSITY OF MINNESOTA
BY

Alanna Hoyer-Leitzel

IN PARTIAL FULFILLMENT OF THE REQUIREMENTS
FOR THE DEGREE OF
DOCTOR OF PHILOSOPHY

Richard Moeckel

July, 2014

Acknowledgements

I would like express my gratitude to the following people for their help while I wrote this dissertation:

Anna Barry, who let me use her idea for my thesis. My advisor, Rick Moeckel, who answered my never ending questions with insightful mathematical advice. My committee, Dick McGehee, Arnd Scheel and Peter Rejto. The SIAM Arnold Reading Group for explaining forms to me (again) and encouraging me to calculate my first ever symplectic pullback. Julie, Samantha, and Bryan, without whom I'd never have taken a dynamical systems class. Julie, again, for long walks in the cold and her encouraging words. Kate Friday, for regularly feeding me, talking to me about things that aren't math, and reminding me that there's life outside of grad school. Alex and Maggie, who helped me keep pushing through at the very end, and Alex, again, for fixing all my TeX problems. All the UMN Mathematics Graduate Students (seriously, all of you, but namely, Madeline, Joe, Dmors1&2, Heidi, Nicole, James) who are so full of love and support. I wouldn't have done this (or wanted to do this) with you. XOXOXO. My UCCS Dissertation Support Group. Zac & Weefy - Dr. Bites is finally an appropriate name to call me. Mom - JWTDP. Dad - Thank you.

Abstract

Studying the dynamics of vortex configurations with one large vortex with and N smaller vortices has applications to physical electromagnetic systems and atmospheric science, as well as being a historically interesting problem. The existence, and linear stability of relative equilibria configurations of the $(1 + N)$-vortex problem are examined. Such configurations are shown to be critical points of a special potential function, and their linear stability depends on the weighted Hessian of this potential. Algebraic geometry and some numerical methods are used to examine the bifurcations of critical points and stability specifically in the case of $N = 3$.

Contents

List of Tables

List of Figures

Chapter 1

Introduction

Vorticity in a fluid is a measure of how much the fluid spins or swirls. Point vortices arise when an inviscid incompressible fluid has vorticity equal to 0 everywhere except at a finite set of points. This is analogous to the point masses used in the n-body problem to model the motion of celestial bodies under gravitational attraction. Similar to the n-body problem, the differential equations for the n-vortex problem can be given by a Hamiltonian system of differential equations; however for point vortices, the Hamiltonian function is logarithmic and the system has half as many degrees of freedom.

A relative equilibrium is a configuration of vortices (or masses) that maintains a rigid shape and size as it translates through the plane and rotates around the center of vorticity (center of mass).[1] These types of solutions are commonly studied in both the n-vortex and n-body problems, as the assumptions about the shape of the configuration and periodicity of the solution simplify otherwise seemingly unsolvable problems. Further common simplifications are to study configurations of N equal vortices (or masses) with regular polygonal shapes or to study configurations of vortices (or masses) with one large vortex and N smaller vortices.

Such configurations are not just simplifications of mathematical imagination, but are found in physical applications. The first theories of point vortices arose from work in electromagnetism, where physicists, who at the time were also leading mathematicians, theorized that electromagnetic fields were actually fluids that conducted current [1].

[1] The n-vortex problem is also studied on the sphere or in bounded domains of $\mathbb{R}^2$, but here we look only at the n-vortex problem in the plane.

This is not far from reality and for electron columns in a magnetized field, like that in a Malmberg-Penning trap, the equations are that of a two-dimensional ideal fluid with point vortices. Durkin and Fajans [2] experimentally found ring configurations with and without a central vortex and tested their stability. Vortices in a ring with and without a central vortex also show up in models of hurricane eye walls [3, 4], and so point vortices also have applications to atmospheric science.

We will consider the special case of the $(N+1)$-vortex problem where one of the vortices is much larger than the other N and especially the limiting case when the N small vortices tend to zero. In the gravitational setting, Hall called this limiting case the $(1+N)$-body problem, thus we will consider the $(1+N)$-vortex problem. For example, the $(1+3)$-vortex problem refers to the limiting case of one large and three small vortices as the three small vortices tend to zero. Figure 1.2 shows relative equilibria of the $(1+3)$-vortex problem.

This dissertation takes an approach to fluid dynamics that is strongly influenced by the gravitational n-body problem, arguably the most famous Hamiltonian system. Poincare and his work on the n-body problem credited with generating the modern theory of dynamical systems, but even the famous celestial mechanist did work on the n-vortex problem [5]. Thus the history of the $(N+1)$-vortex problem dates back to 1856 with Maxwell's Adams Prize winning essay on the gravitational $(N+1)$-body problem used to model the rings of Saturn. Maxwell proved that neither a solid nor a fluid ring is stable, and considered a regular polygonal ring of N equal masses around a center mass. A few years later, the n-vortex problem was first formulated as the problem of point vortices in a Hamiltonian system by Kirchhoff in his *Lectures on Mathematical Physics* [6]. This inspired Thomson (Lord Kelvin) to propose a (now discredited) point vortex atomic theory. Soon after Thomson looked at vortex rings of polygonal configurations of N equal vortices for the Adams Prize essay of 1883 [7].

Over 100 years after Maxwell and Thomson, Hall initiated studies of relative equilibria in the $(1+N)$-body problem [8]. Hall generalized previous work to study all possible limiting configurations, not only ring configurations. He emphasized the importance of considering configurations in the restricted case of $1+N$ bodies as limits of configurations of $N+1$ bodies: "...if we neglect completely the interaction of the small particles then we have N-central force problems, all independent." Not all solutions of

these decoupled central force problems are limits of the solutions with the small particles having positive mass. Hall defined relative equilibria of the $(1+N)$-body problem as follows:

Definition 1.1. *Suppose for $k \to \infty$, we have a sequence $\epsilon_k \to 0$ and $q_0^k, ..., q_N^k \in \mathbb{R}^2$ are positions of $N+1$ point masses such that $q_0^k, ..., q_N^k$ is a relative equilibrium configuration for masses $m_0 = 1, m_1 = ... = m_N = \epsilon$, then if $\bar{q}_j = \lim_{k\to\infty} q_j^k$, $j = 0, ..., N$, then $\bar{q}_0, ..., \bar{q}_N$ is a relative equilibrium configuration of the $(1+N)$-body problem.*

Hall used this definition and the equations for relative equilibria to prove that the large mass limits to the origin, the small masses limit to a circle around the origin, and assuming that $q_i \neq q_j$, that the rate of convergence is $\mathcal{O}(\epsilon)$. He developed a special potential function for the limiting positions on the circle, and proved that a relative equilibrium of the $(1+N)$-vortex problem is a critical point of the function

$$U(\rho) + I(\rho) = \sum_{i<j} \frac{1}{\rho_{ij}} + \frac{1}{2} \sum_{i<j} \rho_{ij}^2, \quad \rho_{ij} = |q_i - q_j|, \quad i, j = 1, ..., N. \tag{1.1}$$

Later, Moeckel [9] continued Hall's work on the gravitational $(1+N)$-body problem by using the special potential function of Hall's to characterize the linear stability of nearby configurations with sufficiently small positive masses. Moeckel found that the Hessian of Hall's potential function turns up in the linearized system of the $(N+1)$-body problem. Such a configuration is linearly stable if and only if the limiting configuration is a local minimum of Hall's potential function. In this way Moeckel corrected Maxwell's result regarding the stability of the $(N+1)$-body problem for $N \geq 7$.

Similar work was recently done in the n-vortex problem. Cabral and Schmidt [10] examined the stability of regular polygonal configurations in the $(N+1)$-vortex problem with N equal vortices and one central vortex. Using a normal form expansion of the Hamiltonian, which is possible because of the assumptions on the regularity of the shape of the configurations, they found local Liapunov stability for ratios of circulations between the large and smaller vortices in a certain interval. They proved that the ring with central vortex configuration is not stable if the vortices on the ring are much smaller than the central vortex.

Barry [11] then applied the ideas of Hall's potential function for the gravitational $(1+N)$-body problem to the n-vortex problem, examining configurations with a large

central vortex and N small equal vortices. She defined relative equilibria of the $(1+N)$-vortex problem in the same way Hall did for the gravitational setting, and proved that the large vortex limits to the origin, the small vortices limit to a circle around the origin, and that the rate of convergence is $\mathcal{O}(\epsilon)$. Barry found that the relative equilibria of the $(1+N)$-vortex problem are critical points of the function

$$V(\theta) = -\sum_{i<j} \left(\cos(\theta_i - \theta_j) + \tfrac{1}{2}\log(2 - 2\cos(\theta_i - \theta_j)\right), \tag{1.2}$$

where θ_i is the angular position of the ith vortex on the circle around the origin. Barry then used the potential function to characterize linear stability of nearby configurations of the full unrestricted problem. She found that for all positive (negative, resp.) circulations of the small vortices, configurations in the $(1+N)$-vortex problem continued to stable relative equilibria of the $(N+1)$-vortex problem if the limiting configuration is a nondengerate minimum (maximum, resp.) of the special potential function. Here she was able to explore the regular N-gon with a central vortex (again finding it unstable for small vortices on the ring) and to numerically find families of relative equilibria for large N.

Most recently, Roberts [12] continued the tradition of using techniques from the literature on the n-body problem to study the n-vortex problem. Applying Moeckel's techniques [13] to the n-vortex problem with all positive circulations, he found linear and nonlinear stability for all planar relative equilibria that are nondegenerate minima of the Hamiltonian restricted to the level surface of angular impulse, analogous to moment of inertia in the gravitational case.

We raise several questions for relative equilibria with one large and N small vortices with not necessarily equal nor positive circulations: How many the relative equilibria configurations are there and what are they? Are any of these relative equilibria linearly stable? We look specifically at the case when $N = 3$ and find the bifurcations of families of relative equilibria and of stability.

It is interesting to note that the 3-vortex problem is completely integrable and does not display chaos. Grobli's dissertation completely solves the problem [14]. As Aref, Rott, and Thomann write, "In a sense, the three-vortex problem plays the same role in vortex dynamics as the two-body Kepler problem does in the theory of gravitationally interacting mass points" [15]. Thus the 4-vortex problem is the next step, and this is

the reason this thesis focuses on the $(1+3)$-vortex problem, looking at a special case of the 4-vortex problem. Under certain conditions, the 4-vortex problem is also integrable. Assuming zero net vorticity and zero total momentum, Eckhardt [16] and Rott [17] analyze the stability of relative equilibrium by reducing the system to one dimension. Other work on relative equilibria in the 4-vortex problem includes finding upper bounds on the number of configurations [18, 19], and most recently counting and classifying all relative equilibria with 2 pairs of equal vortices [20]. Hampton *et al* applied techniques from computational algebraic geometry similar to those utilized in this thesis. The work in this thesis is novel for finding specific numbers of relative equilibria for certain values of the circulations of the four vortices, for looking at configurations of four vortices that are not symmetric in the choice of circulations, and examining the linear stability of such configurations.

Chapter 2 introduces the equations of motion and Hamiltonian formalism of the n-vortex problem. Chapter 3 outlines the problem of relative equilibria and the $(1+N)$-vortex problem and develops the potential function used for finding relative equilibria configurations. Because of the mixed signs and unequal strengths of the small vortices, the relative equilibria are the null set of a "weighted" gradient.

Chapters 4 and 5 contain the main results of the thesis. Chapter 4 examines the relative equilibria configurations for the $(1+3)$-vortex problem in particular and finds bifurcations in the numbers of relative equilibria based on the circulation parameters. By normalizing the three circulation parameters to the unit sphere, it is determined that there are regions with 14, 10, and 8 families of relative equilibria (up to symmetry). An exact count of components in the bifurcation diagram (Figure 1.1), as well as an exact count of the number of relative equilibria in each component are done using exact symbolic calculations rather than numerically. To do so, techniques for counting roots of polynomial equations from algebraic geometry are used. Chapter 5 considers at the linear stability of relative equilibria in the $(N+1)$-vortex problem which continue for $\epsilon > 0$ from relative equilibria configurations in the $(1+N)$-vortex problem. Linear stability occurs if the "weighted" Hessian of the potential function at a critical point has $N-1$ positive eigenvalues (and one 0 eigenvalue corresponding to rotational symmetry). This theorem is applied to the case where $N = 3$ by using the unique (up to scaling) relationship between the position variables and the circulation parameters for critical

points of the potential function. Regions where the circulation parameters give a stable family of relative equilibria in the 4-vortex problem with three sufficiently small vortices and one larger vortex are found numerically.

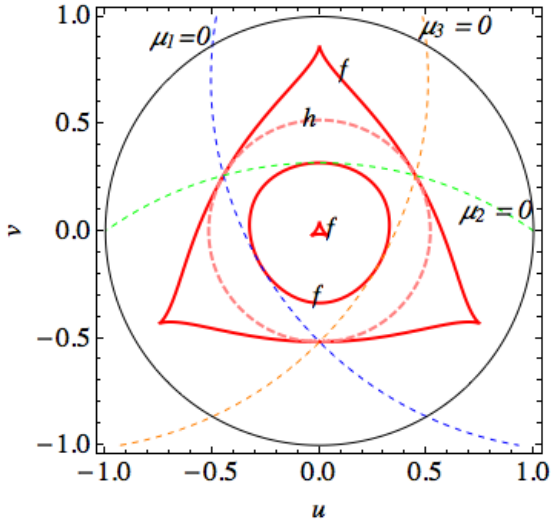

Figure 1.1: Bifurcation diagram for the number of relative equilibria in the $(1+3)$-vortex problem

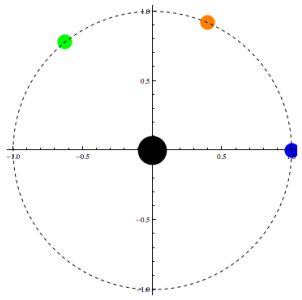

(a) $\mu_1 = -1$, $\mu_2 = -3$, $\mu_3 = 10$

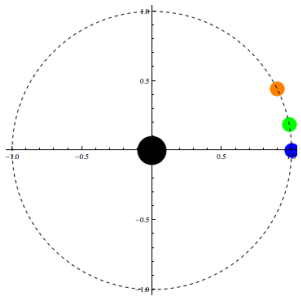

(b) $\mu_1 = 2$, $\mu_2 = -1$, $\mu_3 = 3$

Figure 1.2: Stable Relative Equilibria with Vortices of Mixed Signs

Chapter 2

The n-Vortex Problem and Hamiltonian Systems

Consider a system of n point vortices moving in the plane, each with circulation $\Gamma_i \neq 0$ and positions $q_i = (x_i, y_i) \in \mathbb{R}^2$. The differential equations for this system are Hamiltonian and are given by

$$\Gamma_i \dot{q}_i = J \nabla_i H = \sum_{j \neq i} \Gamma_i \Gamma_j \frac{(q_i - q_j)^\perp}{r_{ij}^2} \tag{2.1}$$

where H is the Hamiltonian function

$$H(q) = -\sum_{i<j} \Gamma_i \Gamma_j \log r_{ij}, \qquad r_{ij} = ||q_i - q_j|| \tag{2.2}$$

and $J = \begin{bmatrix} 0 & 1 \\ -1 & 0 \end{bmatrix}$ and $(x, y)^\perp = (-y, x)$.

2.1 Hamiltonian Systems

A general Hamiltonian system can be described by a smooth, real-valued function $H(q)$ for $q \in \mathbb{R}^{2n}$ and the differential equation $\dot{q} = \mathcal{J} \nabla H(q)$ where $\mathcal{J}$ is the $2n \times 2n$ block diagonal matrix

$$\mathcal{J} = \begin{bmatrix} 0 & I \\ -I & 0 \end{bmatrix}$$

and I is the $n \times n$ identity. The matrix $\mathcal{J}$ gives a skew inner product on the phase space: $\Omega(v, w) = v^T \mathcal{J} w$, making the space a symplectic manifold [21].

The n-vortex problem is a Hamiltonian system with a nonstandard symplectic structure. For the system of differential equations (2.1), the symplectic form is $\sum \Gamma_i dy_i \wedge dx_i$ which has the block diagonal matrix representation with $\Gamma_i J$ along the diagonal. This can also be written as

$$\Gamma \dot{q} = K \nabla H(q) \tag{2.3}$$

where K is $2n \times 2n$ block diagonal matrix with J on the diagonal and
$\Gamma = Diag(\Gamma_1, \Gamma_1, ..., \Gamma_n, \Gamma_n)$.

2.1.1 Symmetries and Integrals

While not all Hamiltonian systems have symmetries and integrals, the n-vortex problem does, and they are useful for understanding the degeneracy that occurs when studying relative equilibria solutions. For an autonomous Hamiltonian system $\dot{q} = \mathcal{J} \nabla H(q)$, a symmetry is a symplectic map ψ on $\mathbb{R}^{2n}$ such that $H(q) = H(\psi(q))$ for all q. Examples of such a map would be translation or rotation. An integral is a smooth, real-valued function F on $\mathbb{R}^{2n}$ that is constant on solutions of the Hamiltonian. Conserved physical quantities of systems, e.g. energy or momentum, are integrals. Integrals can be used to reduce the dimension of a Hamiltonian system by fixing a level set of the integral. For examples of this reduction, see [22, 21]. A famous theorem relates symmetries and integrals.

Theorem 2.1 (Noether's Theorem)**.** *Let ψ_t be a symplectic symmetry for the Hamiltonian H for all t. Then $\psi(t, q) = \psi_t(q)$ is the solution to a Hamiltonian system $\dot{q} = \mathcal{J} \nabla F(q)$, where F is a smooth, real-valued function on $\mathbb{R}^{2n}$ and F is an integral for the Hamiltonian system.*

Conversely, if a F is an integral, then the flow it defines is a symmetry of the Hamiltonian.

There are three independent first integrals of the n-vortex problem in addition to the Hamiltonian [23]. The invariance under time translation corresponds to conservation of energy (the Hamiltonian). Invariance under translations in space corresponds to

conservation of linear momentum, and hence the center of vorticity gives two integrals:

$$Q = (X, Y) = \sum_{i=1}^{n} \Gamma_i q_i. \tag{2.4}$$

Invariance under rotations corresponds to conservation of angular momentum, and hence angular impulse

$$I = \sum_{i=1}^{n} \Gamma_i ||q_i||^2 \tag{2.5}$$

is an integral.

The Poisson bracket of two functions (for the nonstandard symplectic structure in the n-vortex problem) is defined by

$$\{f, g\} = \sum_{i=1}^{n} \frac{1}{\Gamma_i} \left(\frac{\partial f}{\partial x_i} \frac{\partial g}{\partial y_i} - \frac{\partial f}{\partial y_i} \frac{\partial g}{\partial x_i} \right) = \nabla f^T \Gamma^{-1} K \nabla g. \tag{2.6}$$

Theorem 2.2. *If two functions f and g are integrals, then $\{f, g\}$ is also an integral.*

So we see that $\{X, Y\} = \sum_{i=1}^{n} \Gamma_i$, $\{X, I\} = 2Y$, $\{Y, I\} = -2X$. And therefore the Possion bracket gives no new integrals [24]. For $n \leq 3$, the n-vortex problem is fully integrable.

Note: The sum $\sum_{i=1}^{n} \Gamma_i$ is called the *total circulation* of the system of n vortices.

2.1.2 Stability and Hamiltonian Systems

Hamiltonian systems never have asymptotically stable equilibrium points or periodic solutions because the phase flow preserves volume [25]. Studying nonlinear stability or Liaponov stability is possible, but is often difficult. Unless the fixed point of the Hamiltonian system is a maximum or a minimum of the Hamiltonian, the phenomenon of Arnold diffusion most likely makes the point unstable [26]. This thesis focuses on linear stability.

In the case of a linear Hamiltonian system $\dot{z} = Az$, the matrix A is called a *Hamiltonian* matrix. The following are equivalent definitions for Hamiltonian matrices:

1. $A^T \mathcal{J} + \mathcal{J} A = 0$.
2. $\Omega(v, Aw) = -\Omega(Av, w)$ where Ω is the skew inner product of 2 vectors, $\Omega(v, w) = v^T \mathcal{J} w$.

3. $A = \mathcal{J}S$ where S is symmetric.

The characteristic polynomial of a Hamiltonian matrix A is an even polynomial [21], so if $\lambda \in \mathbb{C}$ is an eigenvalue of A, then so is $-\lambda$, $\bar{\lambda}$ and $-\bar{\lambda}$. By the general theory of stability of linear systems, a linear Hamiltonian system is stable if all the eigenvalues of A are purely imaginary or 0, and if A is diagonalizable. This gives a kind of "neutral stability" in a Hamiltonian system where nearby orbits are neither coming towards nor going away from the equilibrium point. The weaker, necessary condition that all the eigenvalues of A are purely imaginary or 0 is called *spectral stability*.

In the linearized n-vortex problem, repeated eigenvalues with nontrivial Jordan blocks correspond to symmetries and integrals of the system. Often times we take a definition of linear stability on a subspace that is skew-orthogonal to the subspaces associated with these nontrivial Jordan blocks. This is equivalent to linear stability after quotienting out by symmetry, as Smale outlines in his paper *Topology and Mechanics* [27]. However quotient manifolds are unwieldy and difficult objects with which to work. The instability produced by symmetries are a "drift" in the system, such as a drift in rotation angle or drift in the translation of center of vorticity (mass). If we consider this drift harmless, then ignoring these nontrivial Jordan blocks is a natural thing to do.

The following lemma of Moeckel's [9] gives a stability criterion for linear Hamiltonian systems.

Lemma 2.1. *Suppose A is a Hamiltonian matrix such that every eigenvector $v \in \mathbb{C}^{2m}$ of A satisfies $\Omega(v, \bar{v}) \neq 0$ (where $\bar{v}$ denotes the complex conjugate of v). Then*

- *All of the eigenvalues of A are imaginary.*
- *Every generalized eigenvector of A is an eigenvector.*
- *0 is a stable equilibrium point for the differential equation $\dot{z} = Az$.*

This lemma guarantees that the matrix A is diagonalizable and that there are no nontrivial Jordan blocks. Often this lemma is applied on a subspace that is skew-orthogonal to the subspace associated with any nontrivial Jordan blocks due to symmetry. (If there were nontrivial Jordan blocks elsewhere, it would not be so natural to ignore them. However, that is the point of the lemma - to show that there are no other nontrivial Jordan blocks.)

Chapter 3

Relative equilibria and the $(1+N)$-Vortex Problem

Of special interest are configurations of n vortices that rotate rigidly around the center of vorticity. These are called relative equilibria solutions because they become fixed points in a rotating coordinate system. Let $N = n - 1$. Given the assumption that the n vortices in the n-vortex problem are one center vortex and N other vortices, this problem is called the $(N+1)$-vortex problem. It is closely related to the $(1+N)$-vortex problem which is a restricted case of the n-vortex problem where the N vortices have 0 circulation. In this chapter, we define coordinates that are useful in these cases, define relative equilibria, particularly in the restricted case, and derive a special potential function that gives the relative equilibria of the $(1+N)$-vortex problem.

3.1 Relative Equilibria

Definition 3.1. *A relative equilibrium solution of the n-vortex problem is a periodic solution with period $2\pi/\omega$ of the form*

$$q_i(t) = e^{-\omega J t} q_i(0) \tag{3.1}$$

where $e^{-\omega J t} = R^{-1}(t) = \begin{bmatrix} \cos(\omega t) & -\sin(\omega t) \\ \sin(\omega t) & \cos(\omega t) \end{bmatrix}$.

One can change to a rotating coordinate system using the following change of coordinates: $\zeta_i(t) = R(t)q_i(t)$.

$$\begin{aligned}\dot{\zeta}_i &= \dot{R}q_i + R\dot{q}_i = \dot{R}R\zeta_i + RJ\tfrac{1}{\Gamma_i}\nabla_i H(q) \\ &= \omega J\zeta_i + \tfrac{1}{\Gamma_i}J\nabla_i H(Rq) = \omega J\zeta_i + \tfrac{1}{\Gamma_i}J\nabla_i H(\zeta)\end{aligned} \tag{3.2}$$

where the third step in the calculation follows from the fact that R and J commute. The new equations of motion are

$$\Gamma_i\dot{\zeta}_i = \omega\Gamma_i J\zeta_i + J\nabla_i H(\zeta_i) \tag{3.3}$$

At a relative equilibrium configuration this becomes $\zeta_i(t) = R(t)R^{-1}(t)q_i(0) = q_i(0)$, hence the periodic relative equilibrium solutions become fixed points in this coordinate system. Recall the function $I(q) = \sum \Gamma_i||q_i||^2$ (which is invariant under rotations). We can rewrite (3.3) at a fixed point as

$$\nabla H + \omega\nabla I = 0 \tag{3.4}$$

Thus configurations for relative equilibria must solve this equation.[1]

Note that any rotation of a relative equilibrium is again a relative equilibrium. In rotating coordinates, this means the equilibrium points are not isolated. Additionally, if q is a relative equilibrium point with angular velocity ω, then any scaling rq, $r \neq 0$ is also a relative equilibrium point with the angular velocity ω/r^2. It is customary to count equivalence classes of relative equilibria by fixing the angular impulse I or the angular velocity ω and then identifying relative equilibria that are identical under rotation.

Another important quantity for the n-vortex problem is the *total vortex angular momentum*

$$L = \sum_{i<j} \Gamma_i\Gamma_j. \tag{3.5}$$

In [12], Roberts proves $\nabla H(z)\cdot z = -L$ by differentiating the identity $H(rz) = H(z) - L\log|r|$ with respect to r and evaluating at $r = 1$. Given this identity and the fact that I is homogenous of degree 2, taking the inner product of equation (3.4) with z

[1] Often times this equation leads to a topological approach for finding relative equilibrium configurations. Relative equilibria are critical points of H restricted to a level surface of I with ω acting as the Lagrange multiplier.

gives that $\omega = L/2I$. This relates the angular impulse and angular velocity of a relative equilibrium, hence fixing one quantity will determine relative equilibrium up to scaling. For this paper we'll set angular velocity to be $\omega = 1$ and allow I to vary.

3.2 The $(N+1)$-vortex problem and Heliocentric Coordinates

Consider the case of relative equilibria where there is one strong vortex and N weak vortices. Let $q_0, q_1, ..., q_N \in \mathbb{R}^2$ be the positions of the $N+1$ vortices with strengths $\Gamma_0 = 1$, $\Gamma_i = \epsilon\mu_i$ where $\mu_i \in \mathbb{R} \setminus \{0\}$ and $0 < \epsilon << 1$.

Heliocentric Coordinates are often used in the n-body problem with one big mass (usually the sun, hence the name "helio") and several small masses. This is reminiscent of the $(N+1)$-vortex problem and so we use it here. The change of coordinates is $Z_0 = q_0$ and $Z_i = q_i - q_0$ for $i = 1, ..., N$. The inverse transformation $F : Z \to q$ is $q_0 = Z_0$ and $q_i = Z_i + Z_0$. The pullback of the symplectic form $\omega = \sum \Gamma_i dy_i \wedge dx_i$ is

$$F^*\omega = \Gamma dY_0 \wedge dX_0 + \sum_{i=1}^{N} \Gamma_i dY_i \wedge dX_i + \sum_{i=1}^{N} \Gamma_i (dY_0 \wedge dX_i + dY_i \wedge dX_i) \tag{3.6}$$

where $\Gamma = \sum_{i=0}^{N} \Gamma_i$ is the total circulation. In the case when $N = 3$, the matrix representation for this is

$$A_1 = \begin{bmatrix} 0 & -\Gamma_0 - \Gamma_1 - \Gamma_2 - \Gamma_3 & 0 & \Gamma_1 & 0 & \Gamma_2 & 0 & \Gamma_3 \\ \Gamma_0 + \Gamma_1 + \Gamma_2 + \Gamma_3 & 0 & -\Gamma_1 & 0 & -\Gamma_2 & 0 & -\Gamma_3 & 0 \\ 0 & \Gamma_1 & 0 & -\Gamma_1 & 0 & 0 & 0 & 0 \\ -\Gamma_1 & 0 & \Gamma_1 & 0 & 0 & 0 & 0 & 0 \\ 0 & \Gamma_2 & 0 & 0 & 0 & -\Gamma_2 & 0 & 0 \\ -\Gamma_2 & 0 & 0 & 0 & \Gamma_2 & 0 & 0 & 0 \\ 0 & \Gamma_3 & 0 & 0 & 0 & 0 & 0 & -\Gamma_3 \\ -\Gamma_3 & 0 & 0 & 0 & 0 & 0 & \Gamma_3 & 0 \end{bmatrix}.$$

We can ignore the coordinates for the big vortex by dropping the first 2 rows and columns of the matrix since they will not appear in the new Hamiltonian. This corresponds to

ignoring the instability that comes from a drift in the center of mass[2] or working in a quotient space. The equations of motion for this system are then

$$\dot{Z} = A_1^{-1}\nabla H(Z), \quad H(Z) = -\sum_{j=1}^{3}\Gamma_0\Gamma_j \log|Z_j| - \sum_{i<j}\Gamma_i\Gamma_j \log|Z_i - Z_j| \tag{3.7}$$

For the $(3+1)$-vortex problem with $\Gamma_0 = 1$ and $\Gamma_i = \epsilon\mu_i$, the equations become

$$\dot{Z} = A(\nabla H_1 + \epsilon \nabla H_2) \tag{3.8}$$

where

$$H = \epsilon\left(-\sum_{j=1}^{3}\mu_j \log|Z_j|\right) + \epsilon^2\left(-\sum_{i<j}\mu_i\mu_j \log|Z_i - Z_j|\right) = \epsilon H_1 + \epsilon^2 H_2 \tag{3.9}$$

and $A = \begin{bmatrix} 0 & \frac{1+\epsilon\mu_1}{\mu_1} & 0 & 1 & 0 & 1 \\ -\frac{1+\epsilon\mu_1}{\mu_1} & 0 & -1 & 0 & -1 & 0 \\ 0 & 1 & 0 & \frac{1+\epsilon\mu_2}{\mu_2} & 0 & 1 \\ -1 & 0 & -\frac{1+\epsilon\mu_2}{\mu_2} & 0 & -1 & 0 \\ 0 & 1 & 0 & 1 & 0 & \frac{1+\epsilon\mu_3}{\mu_3} \\ -1 & 0 & -1 & 0 & -\frac{1+\epsilon\mu_3}{\mu_3} & 0 \end{bmatrix}$.

Writing this out in coordinates we get

$$\dot{Z}_i = (1+\epsilon\mu_i)\frac{Z_i^{\perp}}{|Z_i|^2} + \epsilon\sum_{j\neq i}\mu_j\left(\frac{Z_j^{\perp}}{|Z_j|^2} + \frac{(Z_i - Z_j)^{\perp}}{|Z_i - Z_j|^2}\right) \tag{3.10}$$

where $(x,y)^{\perp} = (-y,x)$.

3.3 Definition of Relative Equilibria in the $(1+N)$-Vortex Problem

We now consider the limiting case as $\epsilon \to 0$. Let ϵ_k be a sequence of real numbers such that $\epsilon_k \to 0$ as $k \to \infty$ and let $q_0^k, ..., q_N^k$ be a sequence of relative equilibria configurations of the $(N+1)$-vortex problem, each with circulations $\Gamma_0^k = 1, \Gamma_i^k = \epsilon_k\mu_i$.

[2] This means we should expect to run into fewer zero eigenvalues and nontrivial Jordan blocks in the linearized system than if we were looking at the full n-vortex problem.

Definition 3.2. *A relative equilibria of the* $(1+N)$*-vortex problem is a configuration* $\bar{q}_0, ..., \bar{q}_N$ *such that there exists a sequence of relative equilibria of the* $(N+1)$*-vortex problem* $q_j^k \to \bar{q}_j$ *as* $k \to \infty$*.*

It is possible that as $\epsilon \to 0$, two or more vortices may converge to the same limiting position. This is not ruled out by the definition of relative equilbria in the $(1+N)$-vortex problem. However, we will assume that the vortices do not collide and so require that they are bounded away from each other by some $m > 0$, i.e. $|q_i - q_j| > m$ for $i \neq j$.[3]

Also the next lemma shows that configurations are bounded, hence there is some $M > 0$ such that $|q_i| < M$ for all i. Note that both M and m do not depend on ϵ, but may depend on N.

Lemma 3.1. *If* $q^k = (q_0^k, ..., q_N^k)$ *is a family of relative equilibria depending on* ϵ^k*, then* $|q^k|$ *is bounded as* $\epsilon^k \to 0$*,* $k \to \infty$*, and so there is a convergent subsequence of relative equilibria, converging to* $(\bar{q}_0, ..., \bar{q}_N)$*.*

Proof. The dependence on ϵ will be suppressed. Suppose, by way of contradiction that there is a subsequence such that $|q| \to \infty$. Define $u = q/|q|$. We take the equations for relative equilibria (3.4) and find that u satisfies

$$|q|\Gamma_i u_i + \frac{1}{|q|} \sum_{j \neq i} \frac{\Gamma_i \Gamma_j (u_i - u_j)^\perp}{|u_i - u_j|^2} = 0. \tag{3.11}$$

Since $|u| = 1$ is bounded, there is a convergent subsequence $u \to \bar{u}$. And since $|\bar{u}| = 1$, $\bar{u} \neq 0$, and there is some $u_i \neq 0$. Since $u_i \neq u_j \ \forall i, j$, the sum is bounded, and hence $|q|$ is bounded, a contradiction.

□

Since any family of relative equilibria $(q_0^k, ..., q_N^k)$ depending on ϵ is bounded, it has a convergent subsequence, converging to a relative equilibria of the $(1+N)$-vortex problem.

Assuming that the center of mass is at the origin, we will see in the next lemma that the large vortex is near the origin and by assuming that the vortices rotate with

[3] As far as I know, no one has proved an n-vortex equivalent of the *Perpendicular Bisector Theorem* for the n-body problem [28]. Hence these assumptions don't rule out the possibility of collinear $(1+N)$-vortex configurations with the same rigor as in the corresponding n-body problem.

angular frequency 1, the small vortices will limit to the unit circle. This lemma also gives rates of convergence for the relative equilibria, which is important when looking at the linearized system in Chapter 5. Also note that this lemma uses heliocentric coordinates, but the definitions of relative equilibria are the same.

Lemma 3.2. *Assuming angular velocity $\omega = 1$, a convergent sequence of relative equilibria $Z_0^k, ..., Z_N^k$ of the $(N+1)$-vortex problem will satisfy $|Z_0| = \mathcal{O}(\epsilon_k)$ and $|Z_i^k|^2 = 1 + \mathcal{O}(\epsilon_k)$, $i = 1, ..., N$ and $|\bar{Z}_i| = 1$ for $i = 1, ..., N$ and $|\bar{Z}_0| = 0$.*

Proof. By changing heliocentric coordinates to a rotating coordinate frame, the differential equations for the $(N+1)$-vortex problem become

$$\dot{\xi}_i = \omega J\xi_i + (1+\epsilon\mu_i)\frac{\xi_i^\perp}{|\xi_i|^2} + \epsilon\sum_{j\neq i}\mu_j\left(\frac{\xi_j^\perp}{|\xi_j|^2} + \frac{(\xi_i-\xi_j)^\perp}{|\xi_i-\xi_j|^2}\right) \tag{3.12}$$

At a relative equilibrium fixed point for $\omega = 1$, we get

$$0 = \omega J\xi_i + (1+\epsilon\mu_i)\frac{\xi_i^\perp}{|\xi_i|^2} + \epsilon\sum_{j\neq i}\mu_j\left(\frac{\xi_j^\perp}{|\xi_j|^2} + \frac{(\xi_i-\xi_j)^\perp}{|\xi_i-\xi_j|^2}\right) \tag{3.13}$$

$$0 = \omega\xi_i + (1+\epsilon\mu_i)\frac{-\xi_i}{|\xi_i|^2} + \epsilon\sum_{j\neq i}\mu_j\left(\frac{-\xi_j}{|\xi_j|^2} + \frac{-(\xi_i-\xi_j)}{|\xi_i-\xi_j|^2}\right) \tag{3.14}$$

$$\xi_i = (1+\epsilon\mu_i)\frac{\xi_i}{|\xi_i|^2} + \epsilon\sum_{j\neq i}\mu_j\left(\frac{\xi_j}{|\xi_j|^2} + \frac{\xi_i-\xi_j}{|\xi_i-\xi_j|^2}\right) \tag{3.15}$$

Then

$$|\xi_i| \leq (1+\epsilon|\mu_i|)\frac{1}{|\xi_i|} + \epsilon\sum_{j\neq i}|\mu_j|\left(\frac{1}{|\xi_j|} + \frac{1}{|\xi_i-\xi_j|}\right) \tag{3.16}$$

$$|\xi_i|^2 \leq (1+\epsilon|\mu_i|) + \epsilon|\xi_i|\sum_{j\neq i}|\mu_j|\left(\frac{1}{|\xi_j|} + \frac{1}{|\xi_i-\xi_j|}\right) \tag{3.17}$$

Note that $|\xi_i| = |Z_i| = |q_i - q_0| > m$, $|\xi_i - \xi_j| = |q_i - q_0 - q_j + q_0| > m$, and $|\xi_i| \leq |q_i| + |q_0| < 2M$ So

$$|\xi_i|^2 \leq 1 + \epsilon|\mu_i| + \epsilon\frac{4M(N-1)\max(|\mu_j|)}{m} \tag{3.18}$$

Similarly,

$$|\xi_i| \geq (1+\epsilon|\mu_i|)\frac{1}{|\xi_i|} - \epsilon\sum_{j\neq i}|\mu_j|\left(\frac{1}{|\xi_j|}+\frac{1}{|\xi_i-\xi_j|}\right) \tag{3.19}$$

$$|\xi_i|^2 \geq (1+\epsilon|\mu_i|) - \epsilon|\xi_i|\sum_{j\neq i}|\mu_j|\left(\frac{1}{|\xi_j|}+\frac{1}{|\xi_i-\xi_j|}\right) \tag{3.20}$$

$$\geq (1+\epsilon|\mu_i|) - \epsilon\frac{4M(N-1)\max(|\mu_j|)}{m} \tag{3.21}$$

Thus $|\xi_i|^2 = 1+\mathcal{O}(\epsilon)$. Taking the limits of (3.17) and (3.20) as $\epsilon \to 0$, we see that $|\bar{\xi_i}| = |\bar{Z}_i| = 1$ for all i. Also since we're assuming center of vorticity is at the origin

$$q_0 + \epsilon\sum_{j=1}^{N}\mu_j q_j = 0 \tag{3.22}$$

$$|q_0| \leq \epsilon N\max(|\mu_j|)M \tag{3.23}$$

So $|Z_0| = |q_0| = \mathcal{O}(\epsilon)$, and $\bar{Z}_0 = 0$.

□

Note that for a different angular velocity, the small vortices would limit to a circle with a different radius around the origin.

3.4 The Potential Function V

Based on the potential function used in [8] and [11], we derive a function V that gives the locations of relative equilibria in the $(1+N)$-vortex problem. However, here we need to take a "weighted" gradient to compensate for the mixed signs in the circulations.

Let μ be an $N \times N$ diagonal matrix with entries $\mu_i \neq 0$.

Lemma 3.3. *Let $(r,\theta) = (1,...,1,\theta_1,...\theta_N)$ be a relative equilibrium of the $(1+N)$-vortex problem. Then θ is a solution to the equation $\mu^{-1}\nabla V = 0$ where*

$$V(\theta) = -\sum_{i<j}\mu_i\mu_j[\cos(\theta_i-\theta_j) + \tfrac{1}{2}\log(2-2\cos(\theta_i-\theta_j))] \tag{3.24}$$

Proof. Let Z^ϵ be a sequence of relative equilibria in heliocentric coordinates of the full $(N+1)$-vortex problem which converges to Z as $\epsilon \to 0$. Since relative equilibria rotate rigidly around the center of vorticity (which we assume to be at the origin) $Z_i^\epsilon \cdot \dot{Z}_i^\epsilon = 0$. In the following calculation, we leave out the dependence on ϵ.

$$0 = Z_i \cdot \dot{Z}_i \tag{3.25}$$

$$0 = Z_i \cdot \frac{Z_i^\perp}{|Z_i|^2} + \epsilon\mu_i \frac{Z_i \cdot Z_i^\perp}{|Z_i|^2} + \epsilon \sum_{j\neq i} \mu_j \left(\frac{Z_i \cdot Z_j^\perp}{|Z_j|^2} + \frac{Z_i \cdot (Z_i - Z_j)^\perp}{|Z_i - Z_j|^2} \right) \tag{3.26}$$

Note $Z_i \cdot Z_i^\perp = 0$, thus

$$0 = \epsilon \sum_{j\neq i} \mu_j \left(\frac{Z_i \cdot Z_j^\perp}{|Z_j|^2} - \frac{Z_i \cdot (Z_j)^\perp}{|Z_i - Z_j|^2} \right) \tag{3.27}$$

In polar coordinates this becomes

$$0 = \epsilon \sum_{j\neq i} \mu_j r_i r_j \sin(\theta_i - \theta_j) \left(\frac{1}{r_j^2} - \frac{1}{r_i^2 + r_j^2 - 2r_i r_j \cos(\theta_i - \theta_j)} \right) \tag{3.28}$$

Divide by ϵ, and then let $r_j \to 1$ as $\epsilon \to 0$

$$0 = \sum_{j\neq i} \mu_j \sin(\theta_i - \theta_j) \left(1 - \frac{1}{2 - 2\cos(\theta_i - \theta_j)} \right) \tag{3.29}$$

Let $V = -\sum \mu_i \mu_j \left[\cos(\theta_i - \theta_j) + \frac{1}{2} \log(2 - 2\cos(\theta_i - \theta_j)) \right]$.
Therefore θ is a solution to the equations $\mu_i^{-1} \dfrac{\partial V}{\partial \theta_i} = 0$, i.e. $\mu^{-1} \nabla V = 0$.

□

Note that solutions to $\mu^{-1}\nabla V = 0$ are the same as solutions to $\nabla V = 0$.

Lemma 3 asserts that if we have a relative equilibrium of the $(1+N)$-vortex problem, it has the form $(\rho, \phi) = (1, ..., 1, \phi_1, ..., \phi_N)$ where $\phi = (\phi_1, ..., \phi_N)$ is a critical point of the potential function V. The next theorem states the existence of a convergent sequence of relative equilibria of the $(N+1)$-vortex problem for each relative equilibrium defined by a nondegenerate critical point of V. In other words, all nondegenerate critical points of V are relative equilibria of the $(1+N)$-vortex problem.

For this theorem, we need the system in polar coordinates. The equations for Heliocentric coordinates in polar coordinates are

$$\begin{aligned}\dot{r}_i &= \epsilon \sum_{j\neq i} \mu_j r_j \sin(\theta_i - \theta_j)\left(\frac{1}{r_j^2} - \frac{1}{r_i^2 + r_j^2 - 2r_i r_j \cos(\theta_i - \theta_j)}\right) \\ &= \epsilon F_i(r, \theta, \epsilon) \qquad (3.30)\\ \dot{\theta}_i &= (1+\epsilon\mu_i)\frac{1}{r_i^2} + \epsilon \sum_{j\neq i} \mu_j \frac{r_i^2 r_j \cos(\theta_i - \theta_j) - r_i r_j^2 \cos(2(\theta_i - \theta_j))}{r_i r_j^2 (r_i^2 + r_j^2 - 2r_i r_j \cos(\theta_i - \theta_j))} \\ &= G_i(r, \theta, \epsilon) \qquad (3.31)\end{aligned}$$

These are not rotating coordinates so for a relative equilibrium, $\dot{r}_i = 0$, $\dot{\theta}_i = 1$.

Theorem 3.1. *Let $\phi = (\phi_1, ..., \phi_N)$ be a nondegenerate critical point of V. Then for $\rho = (1, ..., 1)$, the configuration $(\rho, \phi) = (1, ..., 1, \phi_1, ..., \phi_N)$ is a relative equilibrium of the $(1 + N)$-vortex problem, i.e. there exists a sequence of relative equilibria of the $(N + 1)$-vortex problem which converges to (ρ, ϕ) as $\epsilon \to 0$.*

This theorem follows from two applications of the Implicit Function Theorem. Let $F = (F_1, ..., F_N)$ and $G = (G_1, ..., G_N)$. Since $F(\rho, \phi, 0) = (0, ..., 0)$ and $D_\theta F(\rho, \phi, 0) = V_{\theta\theta}(\phi)$ is invertible, the Implicit Function Theorem implies that there are solutions of the $(N+1)$-vortex problem that converge to (ρ, ϕ) as $\epsilon = 0$. Then by applying the Implicit Function Theorem again to $G = (1, ..., 1)$, we see that the vortices all have the same rotation rate, and thus the solutions are indeed relative equilibria of the $(N+1)$-vortex problem. For more details, see [11].

Chapter 4

(1+3)-Vortex Problem

Recall that the relative equilbria of the $(1+N)$-vortex problem occur at critical points of the function

$$V(\theta) = -\sum_{i<j} \mu_i \mu_j \left[\cos(\theta_i - \theta_j) + \tfrac{1}{2}\log(2 - 2\cos(\theta_i - \theta_j)).\right] \tag{4.1}$$

In this section we consider the specific case where $N = 3$.

4.1 Some Linear Algebra

The function $V(\theta)$ has translational symmetry, which corresponds to the rotational symmetry of the $(1+N)$-vortex problem in nonpolar coordinates. From this we can expect that any critical point of $V(\theta)$ is degenerate as the Hessian $V_{\theta\theta}$ will always have at least one zero eigenvalue. Here we define a critical point of V to be *nondegenerate* if $V_{\theta\theta}$ has only one zero eigenvalue. (Again, this amounts to a nondegenerate fixed point in a quotient space.) We will also define a *minimum (maximum)* of V as a critical point where $V_{\theta\theta}$ is positive (negative) semidefinite with a one-dimensional null space.

In order to remove this degeneracy (and for easier calculations), we can remove the symmetry by fixing one coordinate and looking at V on this projection into two dimensions. Define the function $\tilde{V}(\theta_2, \theta_3) = V(0, \theta_2, \theta_3)$. Note that a critical point of $\tilde{V}$ is also a critical point of $V(\theta_1, \theta_2, \theta_3)$ when $\theta_1 = 0$. Since any translation of a critical point of V is again a critical point of V, the critical points of $\tilde{V}$ give a representative of each equivalence class of critical points of V.

The 0 eigenvalue of $V_{\theta\theta}$ has corresponding eigenvector (1,1,1). Using this fact, we can do a change of basis on the quadratic form associated to $V_{\theta\theta}$. Let

$$P = \begin{bmatrix} 1 & 0 & 0 \\ 1 & 1 & 0 \\ 1 & 0 & 1 \end{bmatrix}. \tag{4.2}$$

Then

$$P^T V_{\theta\theta} P = \begin{bmatrix} 0 & 0 & 0 \\ 0 & \multicolumn{2}{c}{\multirow{2}{*}{$\tilde{V}_{\theta\theta}$}} \\ 0 & & \end{bmatrix} \tag{4.3}$$

Theorem 4.1. *Conjugate symmetric matrices have the same number of zero, positive, and negative eigenvalues.*

Since $P^T V_{\theta\theta} P$ clearly has one 0 eigenvalue and the same eigenvalues as $\tilde{V}_{\theta\theta}$ we can use $\tilde{V}_{\theta\theta}$ to find and classify critical points of V.

4.2 Bifurcation curves for the $(1+3)$-vortex problem

This thesis focuses on bifurcations that arise from small, smooth changes in one of the parameters μ_i. These bifurcations denote qualitative changes in the nature of the function V. One such change is a change in the number of critical points of V, which corresponds to a change in the number of families of relative equilibria of the $(1+N)$-vortex problem. This is illustrated in Figure 4.1 which shows a saddle-node bifurcation in the critical points of $\tilde{V}$. Another such change is a change in the type of critical point of V, a saddle point switching to a maximum or a minimum, for example. This is illustrated in Figure 4.2.

Bifurcations occur in two ways: at degenerate critical points and at singularity. At a nondegenerate critical point in the interior of the domain of V, the critical point will continue to nearby values of μ_i by the Implicit Function Theorem. However, this is not the case at degenerate critical points, hence the equations for degenerate critical points define where bifurcations of V can occur. For a smooth, bounded function on a compact domain, bifurcations only occur at degenerate critical points. However V is

not bounded on a compact domain, so not all bifurcations occur at degenerate critical points. Some occur at the singularity on the boundary of the domain of V. In the following sections, we first find both types of bifurcations.

Degenerate critical points are solutions to the following three equations: $\tilde{V}_{\theta_2} = 0, \tilde{V}_{\theta_3} = 0, \det(\tilde{V}_{\theta\theta}) = 0$. We want to find the values of μ_1, μ_2, μ_3 where there are degenerate critical points. To do so, we rewrite these equations as polynomial equations and find a Groebner basis while eliminating the position variables and leaving only the circulation parameters.

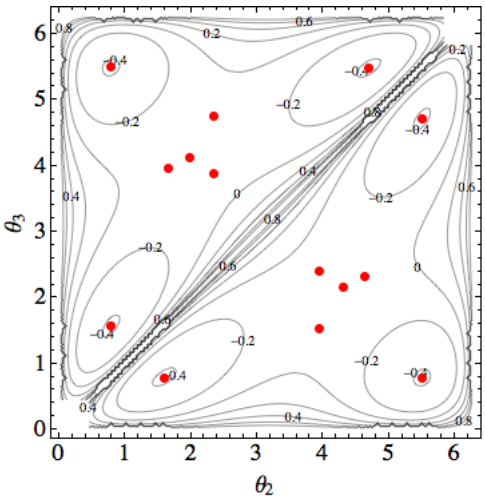

(a) $\mu_1 = 0.569655$
$\mu_2 = 0.569655$
$\mu_3 = 0.592441$

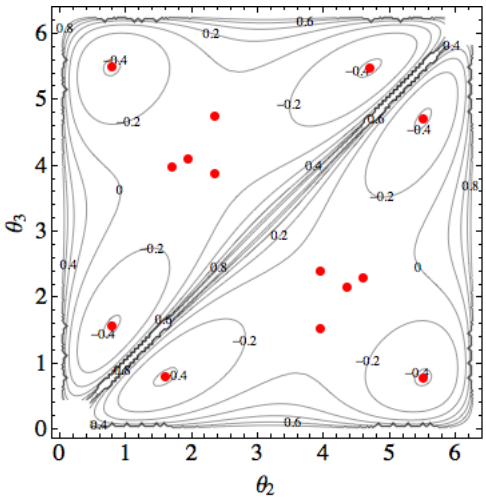

(b) $\mu_1 = 0.567733$
$\mu_2 = 0.567733$
$\mu_3 = 0.59612$

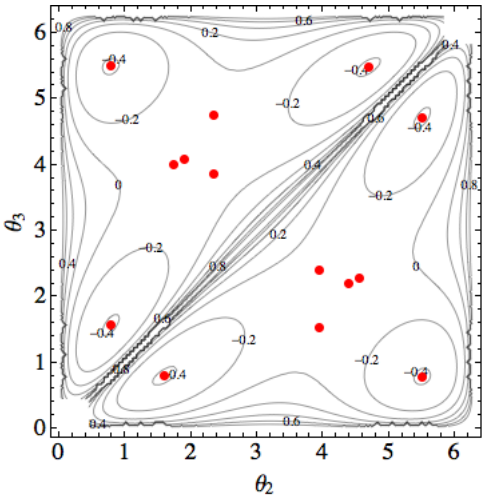

(c) $\mu_1 = 0.565812$
$\mu_2 = 0.565812$
$\mu_3 = 0.599761$

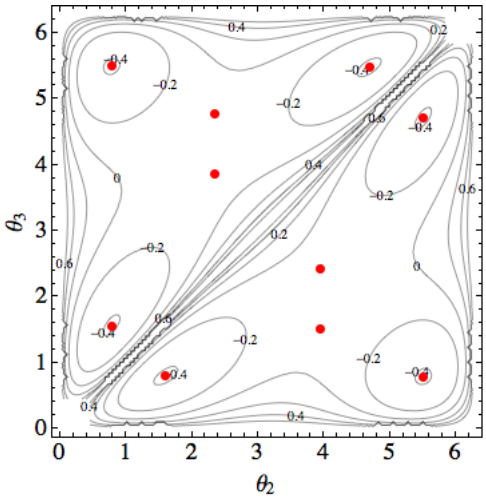

(d) $\mu_1 = 0.563893$
$\mu_2 = 0.563893$
$\mu_3 = 0.603365$

Figure 4.1: Saddle-Node Bifurcation for V

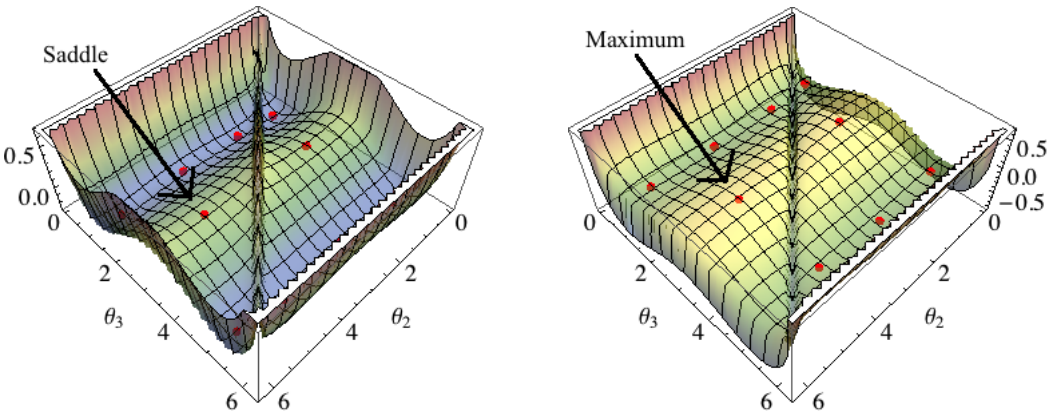

(a) $\mu_1 = 0.70565$
$\mu_2 = 0.06415$
$\mu_3 = 0.70565$

(b) $\mu_1 = 0.70565$
$\mu_2 = -0.06415$
$\mu_3 = 0.70565$

Figure 4.2: Change in type of critical point: saddles to max/min

4.2.1 Some Groebner Basics

This section briefly outlines some ideas in algebraic geometry that are used to find bifurcations at degenerate critical points. For more exposition, see [29].

Let k be a field and let F be a set of polynomials in $k[x_1, ..., x_n]$, and let $I = (F)$ be the ideal generated by F. Geometrically, the set of zeros of F is called the **variety** of F and denoted $Var(F)$.

Theorem 4.2. *If $I = (F)$ is the ideal generated by F in $k[x_1, ..., x_n]$, then $Var(I) = Var(F)$.*

Hence the problem of finding the zeros of F and the geometry of the varieties are related. In order to simplify the problem, we look at a different generating set for the ideal $I = (F)$.

Definition 4.1. *A **monomial order** is a total ordering on monomials $x_1^{\alpha_1} \cdots x_n^{\alpha_n}$, $\alpha_i \in \mathbb{Z}_{\geq 0}$ in a polynomial ring such that if $\alpha = (\alpha_1, ..., \alpha_n) > \beta = (\beta_1, ...\beta_n)$, then $\alpha + \gamma > \beta + \gamma$ for any $\gamma \in \mathbb{Z}^n_{\geq 0}$, and the ordering is a well-ordering. Moreover, an **elimination ordering** is a monomial ordering where $x_1^{\alpha_1} \cdots x_k^{\alpha_k} > x_{k+1}^{\beta_{k+1}} \cdots x_n^{\beta_n}$ whenever one of $\alpha_i > 0$ for $i = 1, ..., k$.*

Definition 4.2. *A **Groebner basis** of an ideal I is a set of polynomials that generate the ideal I and $\forall f \in I$ there is some g in the basis such that the leading term of g divides the leading term of f.*

Theorem 4.3. *Every ideal in $k[x_1, ..., x_n]$ has a Groebner basis with respect to a given monomial ordering.*

Buchberger's Algorithm allows us to find a Groebner basis, often giving a polynomial in the basis with only one variable (or at least fewer variables than the starting polynomial). This "elimination" is based on the choice of monomial order. A Groebner basis can also be used to guarantee elimination of certain variables from a system of polynomial equations.

Theorem 4.4. *Let G be Groebner basis for $I \subset k[x_1, .., x_k, x_{k+1}, ..., x_n]$ and an elimination order with $x_1^{\alpha_1} \cdots x_k^{\alpha_k} > x_{k+1}^{\beta_{k+1}} \cdots x_n^{\beta_n}$, then $G \cap I_k$ is the Groebner basis for the elimination ideal $I_k = I \cap k[x_{k+1}, ..., x_n]$*

4.2.2 Bifurcation Curve via Groebner Basis

In order to use these techniques from algebraic geometry, we need polynomial equations equivalent to $\frac{1}{\mu_2}\tilde{V}_{\theta_2}$, $\frac{1}{\mu_3}\tilde{V}_{\theta_3}$ and $\frac{1}{\mu_1\mu_2\mu_3}\det(\tilde{V}_{\theta\theta})$.[1] The following is an example calculation on $\tilde{V}_{\theta_2}$ and the results for all three equations are Appendix A. These algebraic manipulations were done in Mathematica.

$$\begin{aligned}\tfrac{1}{\mu_2}\tilde{V}_{\theta_2} =& [\mu_1 \sin\theta_2 - 2\mu_1 \cos\theta_2 \sin\theta_2 - \mu_1 \cos(\theta_2-\theta_3)\sin\theta_2 + 2\mu_1 \cos\theta_2 \cos(\theta_2-\theta_3)\sin\theta_2 \\ &+ \mu_3 \sin(\theta_2-\theta_3) - \mu_3 \cos\theta_2 \sin(\theta_2-\theta_3) - 2\mu_3 \cos(\theta_2-\theta_3)\sin(\theta_2-\theta_3) \\ &+2\mu_3 \cos\theta_2 \cos(\theta_2-\theta_3)\sin(\theta_2-\theta_3)] \,/[2(-1+\cos\theta_2)(-1+\cos(\theta_2-\theta_3))]\end{aligned} \tag{4.4}$$

Except for when $\cos\theta_2 = 1$, $\cos\theta_3 = 1$ (which occurs in $\tilde{V}_{\theta_3}$), and $\cos(\theta_2-\theta_3) = 1$, the solutions to these equations will be zeros of the numerator. We can consider only the numerator for now and later take these conditions into account.

First we want to transform these equations into polynomial equations. To start, expand out the terms $\cos(\theta_2-\theta_3)$ and $\sin(\theta_2-\theta_3)$ in terms of $\cos\theta_2, \sin\theta_2, \cos\theta_3$, and $\sin\theta_3$ and make the following substitutions:

$$s_2 = \sin\theta_2, \quad s_3 = \sin\theta_3, \quad c_2 = \cos\theta_2, \quad c_3 = \cos\theta_3 \tag{4.5}$$

Now the expression is a polynomial in s_2, s_3, c_2, c_3. $\frac{1}{\mu_2}\tilde{V}_{\theta_2}$ becomes

$$\begin{aligned}p_1 =& 2\mu_1 s_2 - 4c_2\mu_1 s_2 + c_3\mu_1 s_2 - 2c_2c_3\mu_1 s_2 + 3c_2^2c_3\mu_1 s_2 + 2c_3\mu_3 s_2 - 2c_2c_3\mu_3 s_2 + c_3^2\mu_3 s_2 \\ &- 4c_2c_3^2\mu_3 s_2 + 3c_2^2c_3^2\mu_3 s_2 - c_3\mu_1 s_2^3 - c_3^2\mu_3 s_2^3 - \mu_1 s_3 + c_2\mu_1 s_3 + c_2^2\mu_1 s_3 - c_2^3\mu_1 s_3 \\ &+ \mu_3 s_3 - 2c_2\mu_3 s_3 + c_2^2\mu_3 s_3 - 2c_2c_3\mu_3 s_3 + 4c_2^2c_3\mu_3 s_3 - 2c_2^3c_3\mu_3 s_3 - \mu_1 s_2^2 s_3 \\ &+ 3c_2\mu_1 s_2^2 s_3 - \mu_3 s_2^2 s_3 - 4c_3\mu_3 s_2^2 s_3 + 6c_2c_3\mu_3 s_2^2 s_3 - \mu_3 s_2 s_3^2 + 4c_2\mu_3 s_2 s_3^2 \\ &- 3c_2^2\mu_3 s_2 s_3^2 + \mu_3 s_2^3 s_3^2\end{aligned} \tag{4.6}$$

Because $s_2^2 + c_2^2 = 1$ and $s_3^2 + c_3^2 = 1$, we can use the tangent double angle formulas to do a change of variables to t_2, t_3 by

$$s_2 = \frac{2t_2}{1+t_2^2}, \quad c_2 = \frac{t_2^2-1}{1+t_2^2}, \quad s_3 = \frac{2t_3}{1+t_3^2}, \quad c_3 = \frac{t_3^2-1}{1+t_3^2}. \tag{4.7}$$

[1] Note that by dividing the determinate by $\mu_1\mu_2\mu_3$, we are removing the degeneracy that occurs when $\mu_i = 0$ from this calculation.

This change of variables also sends the terms $\cos\theta_2 = 1$ and $\cos\theta_3 = 1$ to infinity so these two singularity conditions from earlier are not a concern right now. (There is still an issue with the noncompactness of the domain, and we address this in the next section.) Then we take a common denominator and look at the numerator of the new expression

$$\begin{aligned} p_2 = &-8(t_2-t_3)(-\mu_3 - 3\mu_1 t_2^2 + 3\mu_3 t_2^2 + \mu_1 t_2^4 + 3\mu_1 t_2 t_3 - \\ &9\mu_3 t_2 t_3 - \mu_1 t_2^3 t_3 + 3\mu_3 t_2^3 t_3 + 3\mu_3 t_3^2 - 3\mu_1 t_2^2 t_3^2 - 9\mu_3 t_2^2 t_3^2 + \mu_1 t_2^4 t_3^2 + 3\mu_1 t_2 t_3^3 + \\ &3\mu_3 t_2 t_3^3 - \mu_1 t_2^3 t_3^3 - \mu_3 t_2^3 t_3^3) \end{aligned} \tag{4.8}$$

We can factor out the term $(t_2 - t_3)$ since it depends only on the position variables t_2, t_3, the variables we eventually want to eliminate. Geometrically, eliminating variables when we calculate the Groebner basis is the projection of the variety onto a smaller space. However, if the projection is the whole of the smaller space, that doesn't tell us anything. Algebraically, this corresponds to a common factor of the system of polynomials that depends only on the variables being eliminated. We call these *trivial solutions*. Taking the Groebner Basis while the polynomials contain this factor would give the 0-ideal. Hence we want to remove this factor in some way before calculating the Groebner basis of the elimination ideal. This is the first time we come across a trivial solution where the system would be 0 for all values of μ_1, μ_2, μ_3. These are the solutions where $\cos(\theta_2 - \theta_3) = 1$, the last singularity condition, which we deal with in the next section.

$$\begin{aligned} p_3 = &-\mu_3 - 3\mu_1 t_2^2 + 3\mu_3 t_2^2 + \mu_1 t_2^4 + 3\mu_1 t_2 t_3 - 9\mu_3 t_2 t_3 - \mu_1 t_2^3 t_3 + 3\mu_3 t_2^3 t_3 + 3\mu_3 t_3^2 \\ &- 3\mu_1 t_2^2 t_3^2 - 9\mu_3 t_2^2 t_3^2 + \mu_1 t_2^4 t_3^2 + 3\mu_1 t_2 t_3^3 + 3\mu_3 t_2 t_3^3 - \mu_1 t_2^3 t_3^3 - \mu_3 t_2^3 t_3^3 \end{aligned} \tag{4.9}$$

Again, the same manipulations are used to derive polynomials q_3 and h_3 corresponding to the equations for $\frac{1}{\mu_3}\tilde{V}_{\theta_3}$ and $\frac{1}{\mu_1\mu_2\mu_3}\det(\tilde{V}_{\theta\theta})$, and these polynomials are given in Appendix A.

The last reparameterization still gives some trivial solutions, namely $t_2 t_3 + 1 = 0$. To eliminate these, we include a new polynomial $w(t_2 - t_3) - 1$ in the set. The inclusion of a polynomial of this form is a trick used in the proof of Hilbert's Nullstellenstaz in [29]. By including a polynomial where the zero set does *not* include the solutions

$t_2 = t_3$, such solutions will not be in the variety generated by the Groebner Basis when we compute it and eliminate the extra variable w.

Thus the next step is to compute a Groebner basis on the ideal generated by $\{p_3, q_3, h_3, w(t_2 - t_3) - 1\}$ in μ_1, μ_2, μ_3 and eliminate the variables t_2, t_3, w, which was done using the GroebnerBasis command Mathematica with the built in elimination ordering. There is one polynomial f in the Groebner basis, a degree 18 polynomial in μ_1, μ_2, μ_3. It is included in Appendix A. This is the curve shown in Figure 4.4.

4.2.3 Bifurcation at Singularity

From numerical exploration it is apparent that bifurcations also occur when $\cos(\theta_2) = 1$, $\cos(\theta_3) = 1$, and $\cos(\theta_2 - \theta_3) = 1$. This is illustrated in Figure 4.3. In the first three pictures, two of the critical points "slide" off the domain. We can see that there are values of μ_i where the V is fairly flat at the corners of $(0, 2\pi) \times (0, 2\pi)$ and the gradient of V has a limit of 0 at the singularities.

The function $\tilde{V}$ has singularities when $\theta_2 = \theta_3$, $\theta_2 = 0 \pm 2\pi n$ and $\theta_3 = 0 \pm 2\pi m$, so it is not bounded on a compact domain. Bifurcations can also occur at these singularities but the critical points that emerge out of singularities are not degenerate, and hence they were not included in the previous Groebner Basis calculation. We want to find the values of μ_i where this bifurcation at singularity occurs.

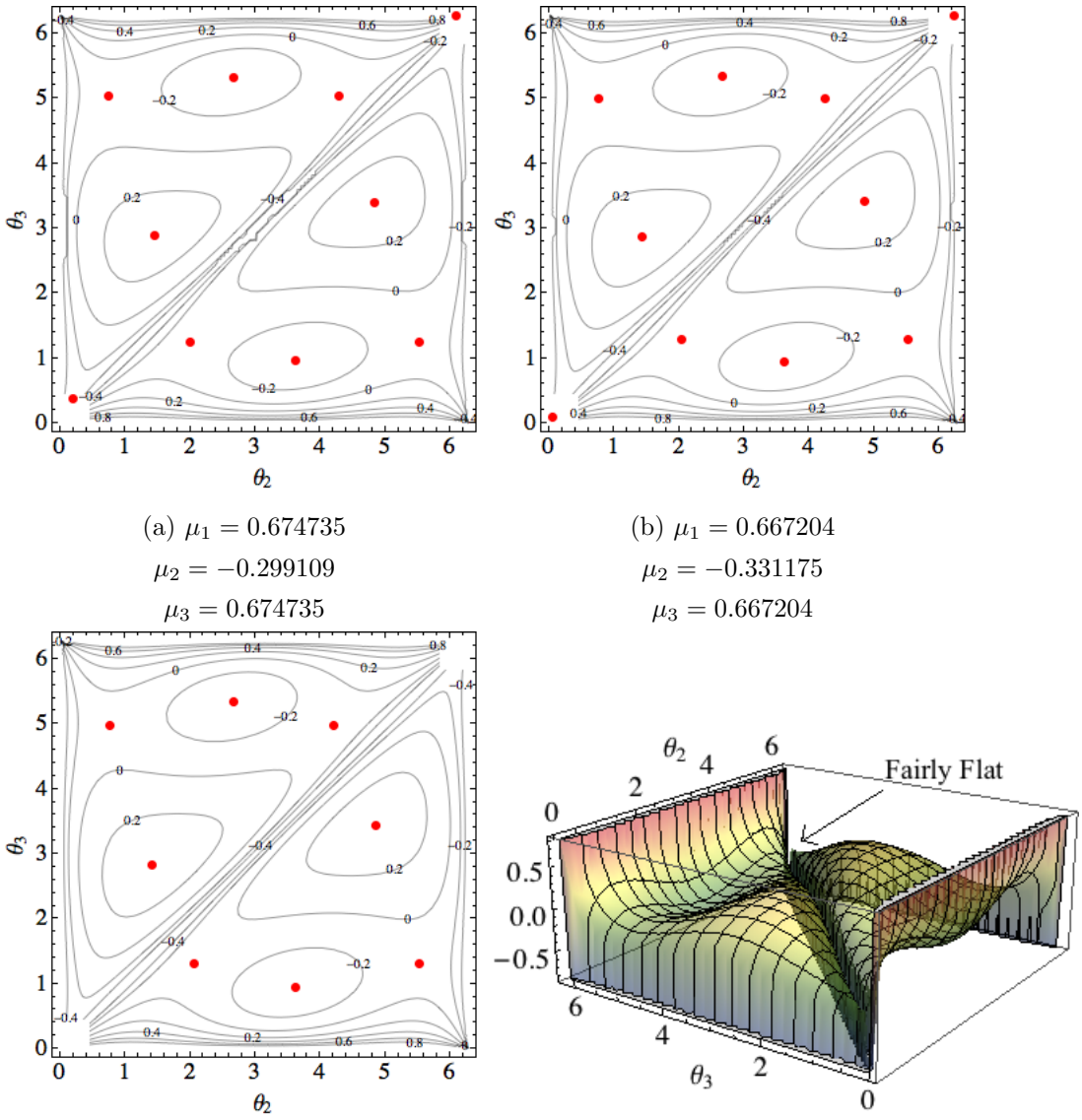

(a) $\mu_1 = 0.674735$
$\mu_2 = -0.299109$
$\mu_3 = 0.674735$

(b) $\mu_1 = 0.667204$
$\mu_2 = -0.331175$
$\mu_3 = 0.667204$

(c) $\mu_1 = 0.659061$
$\mu_2 = -0.362322$
$\mu_3 = 0.659061$

(d) $\mu_1 = 0.674735$
$\mu_2 = -0.299109$
$\mu_3 = 0.674735$

Figure 4.3: Bifurcation at Singularity

To find a curve that gives values of μ_i corresponding to these bifurcations, we go back to equations p_1 and q_1 as found in Appendix A. Again we can use the tangent double angle formulas to do a change of variables to u_2, u_3 by

$$s_2 = \frac{2u_2}{1+u_2^2},\ c_2 = \frac{1-u_2^2}{1+u_2^2},\ s_3 = \frac{2u_3}{1+u_3^2},\ c_3 = \frac{1-u_3^2}{1+u_3^2}.$$

so $\cos(\theta_2) = 1$ when $u_2 = 0$ and $\cos(\theta_3) = 1$ when $u_3 = 0$.

$$\begin{aligned} p =& \mu_1 u_2 + \mu_3 u_2 - 3\mu_1 u_2^3 - 3\mu_3 u_2^3 - \mu_1 u_3 + 3\mu_1 u_2^2 u_3 + 9\mu_3 u_2^2 u_3 - 3\mu_3 u_2^4 u_3 + \mu_1 u_2 u_3^2 \\ &- 3\mu_3 u_2 u_3^2 - 3\mu_1 u_2^3 u_3^2 + 9\mu_3 u_2^3 u_3^2 - \mu_1 u_3^3 + 3\mu_1 u_2^2 u_3^3 - 3\mu_3 u_2^2 u_3^3 + \mu_3 u_2^4 u_3^3, \end{aligned} \tag{4.10}$$

$$\begin{aligned} q =& \mu_1 u_2 + \mu_1 u_2^3 - \mu_1 u_3 - \mu_2 u_3 - \mu_1 u_2^2 u_3 + 3\mu_2 u_2^2 u_3 - 3\mu_1 u_2 u_3^2 - 9\mu_2 u_2 u_3^2 - 3\mu_1 u_2^3 u_3^2 \\ &+ 3\mu_2 u_2^3 u_3^2 + 3\mu_1 u_3^3 + 3\mu_2 u_3^3 + 3\mu_1 u_2^2 u_3^3 - 9\mu_2 u_2^2 u_3^3 + 3\mu_2 u_2 u_3^4 - \mu_2 u_2^3 u_3^4 \end{aligned} \tag{4.11}$$

This places the singularities at the origin. Now we have 2 polynomials $p, q \in \mathbb{R}[\mu_1, \mu_2, \mu_3, u_2, u_3]$ where $p = q = 0$ when $u_2 = u_3 = 0$ for all μ_i. However, we want to find the "nontrivial" solutions at $u_2 = u_3 = 0$. These are solutions where the μ_i force $p = q = 0$ at $u_2 = u_3 = 0$, meaning they are limits of solutions with $(u_2, u_3) \neq (0, 0)$. A trick for finding the nontrivial solutions is as follows: We can write the two polynomials as the matrix equation

$$\begin{bmatrix} p(u_2,0)/u_2 & (p(u_2,u_3) - p(u_2,0))/u_3 \\ q(u_2,0)/u_2 & (q(u_2,u_3) - q(u_2,0))/u_3 \end{bmatrix} \begin{bmatrix} u_2 \\ u_3 \end{bmatrix} = \begin{bmatrix} 0 \\ 0 \end{bmatrix}. \tag{4.12}$$

Note that the entries of this matrix are polynomials since there is a factor of u_2 or u_3 where appropriate. Nontrivial solutions of this system occur when the determinant of this matrix is equal to 0.

$$\begin{aligned} \det =& -\mu_1\mu_2 - \mu_1\mu_3 - \mu_2\mu_3 + 6\mu_1\mu_2 u_2^2 - 7\mu_1\mu_3 u_2^2 + 6\mu_2\mu_3 u_2^2 - 9\mu_1\mu_2 u_2^4 - 3\mu_1\mu_3 u_2^4 \\ &- 9\mu_2\mu_3 u_2^4 + 3\mu_1\mu_3 u_2^6 - 4\mu_1^2 u_2 u_3 - 9\mu_1\mu_2 u_2 u_3 - 9\mu_2\mu_3 u_2 u_3 + 8\mu_1^2 u_2^3 u_3 \\ &+ 30\mu_1\mu_2 u_2^3 u_3 + 30\mu_2\mu_3 u_2^3 u_3 + 12\mu_1^2 u_2^5 u_3 - 9\mu_1\mu_2 u_2^5 u_3 - 9\mu_2\mu_3 u_2^5 u_3 + 4\mu_1^2 u_3^2 \\ &+ 3\mu_1\mu_2 u_3^2 + 3\mu_1\mu_3 u_3^2 + 3\mu_2\mu_3 u_3^2 - 8\mu_1^2 u_2^2 u_3^2 - 18\mu_1\mu_2 u_2^2 u_3^2 - 3\mu_1\mu_3 u_2^2 u_3^2 \\ &- 18\mu_2\mu_3 u_2^2 u_3^2 - 12\mu_1^2 u_2^4 u_3^2 + 27\mu_1\mu_2 u_2^4 u_3^2 - 7\mu_1\mu_3 u_2^4 u_3^2 + 27\mu_2\mu_3 u_2^4 u_3^2 - \mu_1\mu_3 u_2^6 u_3^2 \\ &+ 3\mu_1\mu_2 u_2 u_3^3 + 3\mu_2\mu_3 u_2 u_3^3 - 10\mu_1\mu_2 u_2^3 u_3^3 - 10\mu_2\mu_3 u_2^3 u_3^3 + 3\mu_1\mu_2 u_2^5 u_3^3 + 3\mu_2\mu_3 u_2^5 u_3^3 \end{aligned}$$

Evaluating the determinant at $u_2 = u_3 = 0$, we get a bifurcation curve

$$\mu_1\mu_2 + \mu_1\mu_3 + \mu_2\mu_3 = 0 \tag{4.13}$$

which we'll call the *harmonic curve*.

4.2.4 Stereographic Projection of Bifurcation Curves

Looking at the equations for $\nabla\tilde{V} = 0$ and $\det(\tilde{V}_{\theta\theta}) = 0$, it is apparent that the ratio of the μ_i affects the number of critical points, not the μ_i themselves, so we can normalize the size of μ_1, μ_2, μ_3 and consider only the unit sphere in the parameter space. To examine the bifurcation curves, we'll take a stereographic projection that puts $(\mu_1, \mu_2\, \mu_3) = \frac{1}{\sqrt{3}}(1,1,1)$ at the origin $(u, v) = (0, 0)$.

$$\begin{aligned} V_1 &= (1, 0, -1)/\sqrt{2} \\ V_2 &= (1, -2, 1)/\sqrt{6} \\ V_3 &= (1, 1, 1)/\sqrt{3} \end{aligned} \tag{4.14}$$

$$\begin{aligned} x_0 &= 2u/(1 + u^2 + v^2) \\ y_0 &= 2v/(1 + u^2 + v^2) \\ z_0 &= (1 - u^2 - v^2)/(1 + u^2 + v^2) \end{aligned} \tag{4.15}$$

$$(\mu_1, \mu_2, \mu_3) = [V_1\ V_2\ V_3]^{-1}.(x_0, y_0, z_0) \tag{4.16}$$

$$\mu_1 = \frac{3\sqrt{2}u - \sqrt{3}u^2 + \sqrt{3}(1 + \sqrt{2}v - v^2)}{3(1 + u^2 + v^2)} \tag{4.17}$$

$$\mu_2 = -\frac{-1 + u^2 + 2\sqrt{2}v + v^2}{\sqrt{3}(1 + u^2 + v^2)} \tag{4.18}$$

$$\mu_3 = \frac{-3\sqrt{2}u - \sqrt{3}u^2 + \sqrt{3}(1 + \sqrt{2}v - v^2)}{3(1 + u^2 + v^2)} \tag{4.19}$$

Using this change of variables, we can rewrite the bifurcation curves and plot them.

In Figure 4.4, the curve f has three parts, and the dashed curve labeled h is the "harmonic curve." The outer circle is the curve $\mu_1 + \mu_2 + \mu_3 = 0$. (This is the equator

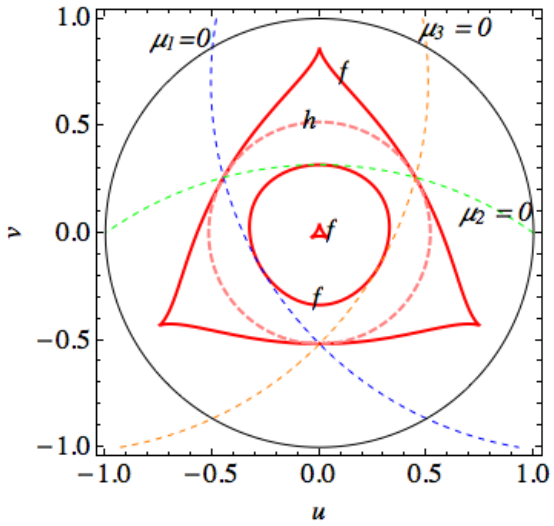

Figure 4.4: Stereographic Projection of Bifurcation Curves

of the sphere given $\frac{1}{\sqrt{3}}(1,1,1)$ is the north pole. We need only consider half the sphere because of the symmetry of V for the circulation parameters.) The three dashed curves show when one of the $\mu_i = 0$. These curves are included for reference and also because they show where a bifurcation in the classification of critical points occurs. Recall that when calculating an equivalent polynomial equations $\det(\tilde{V}_{\theta\theta})$, a factor of $\mu_1\mu_2\mu_3$ was removed. When $\mu_i = 0$ for $i = 1, 2, 3$, one of the eigenvalues of $\tilde{V}_{\theta\theta}$ passes through zero and changes sign.

4.3 Counting Components

To get a good idea of what is going on in this bifurcation diagram, we want to rigorously count the components and then consider a representative point in each component. The symmetry in the stereographic projection can be reduced by fixing an ordering of the vortices, hence we need only consider one third of of the diagram. Using again the tangent double angle identities to "unwrap" the circle gives the change of coordinates:

$$u = \frac{2rt}{\sqrt{2}(1+t^2)}, \; v = \frac{r(1-t^2)}{\sqrt{2}(1+t^2)}, \; r > 0 \tag{4.20}$$

$$\mu_1 = \frac{2\sqrt{3}(1+t^2) - \sqrt{3}r^2(1+t^2) + 2r(\sqrt{3}+6t-\sqrt{3}t^2)}{3(2+r^2)(1+t^2)}$$
$$\mu_2 = \frac{4r(-1+t^2) + 2(1+t^2) - r^2(1+t^2)}{\sqrt{3}(2+r^2)(1+t^2)} \tag{4.21}$$
$$\mu_3 = -\frac{-2\sqrt{3}(1+t^2) + \sqrt{3}r^2(1+t^2) + 2r(-\sqrt{3}+6t+\sqrt{3}t^2)}{3(2+r^2)(1+t^2)}$$

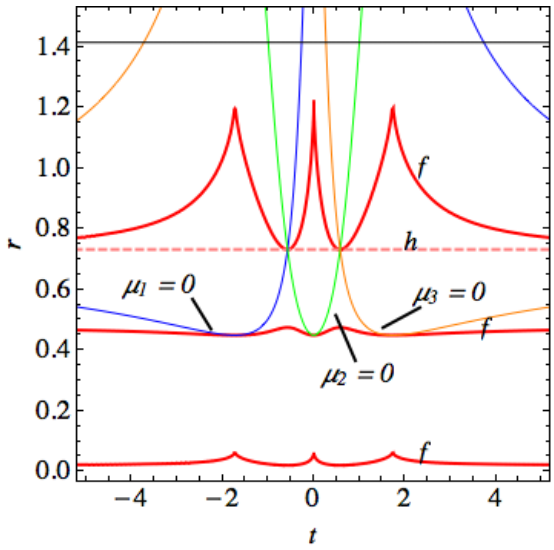

Figure 4.5: "Straightened out" Bifurcation Diagram

Figure 4.5 is this "straightened out" bifurcation diagram. Here r along the vertical axis is the radius of the coordinate (u, v) and t along the horizontal axis gives the stereographic projection of the point (u, v) onto the u-axis. In order to count the number of components we show that the bifurcations curves are four graphs over t and then count the number of roots using an algorithm from algebraic geometry described in the next section.

4.3.1 Sturm Algorithm for Counting Real Roots

Let $P \in \mathbb{R}[x]$ be a polynomial in one variable with coefficients in $\mathbb{R}$. Define a sequence $(P_0, P_1, ..., P_k)$ called the Sturm sequence by $P_0 = P$, $P_1 = P'$ and $P_{i+1} = P_i Q_i - P_{i-1}$, where P_{i+1} is the negative remainder of Euclidean division, $\deg P_{i+1} < \deg P_i$ and P_k is a nonzero constant.

Let $a \in \mathbb{R}$. Then one can evaluate the Sturm sequence at a, $(P_0(a), P_1(a), ..., P_k(a))$. Define $v_P(a)$ as the number of sign changes of the sequence, ignoring any zeros. The following theorem gives the number of real roots in an interval.

Theorem 4.5 (Sturm)**.** *Let $(a, b) \subset \mathbb{R}$ where $P(a) \neq 0$ and $P(b) \neq 0$. Then the number of real roots in the interval (a, b) is $v_P(a) - v_P(b)$.*

This algorithm works specifically when P has no repeated roots, but it can be adapted for P with multiple roots. Instead define the Sturm sequence as $(P_0/P_k, P_1/P_k, ..., P_{k-1}/P_k, 1)$. Then Sturm's theorem still holds, where $v_P(a) - v_P(b)$ is the number of *distinct* real roots in the interval (a, b).

For details, see [30].

4.3.2 Five Components

To rigorously count components, first we show that the curve of the Groebner basis polynomial $f(r, t) = 0$ and the harmonic curve $h(r, t) = 0$ are graphs over the t-axis. The harmonic curve

$$h(r, t) = \mu_1\mu_2 + \mu_1\mu_3 + \mu_2\mu_3 = \frac{4 - 8r^2 + r^4}{(2 + r^2)^2} = 0 \tag{4.22}$$

is constant, $r = 1 + \sqrt{3}$, and is thus a graph. To check if $f(r, t) = 0$ is a graph, we look for vertical tangents and singularities. Since $f(r, t)$ is a polynomial there are no singularities. Vertical tangents occur where $f(r, t)$ and $\frac{d}{dr}(f(r, t))$ have a common 0. Here we can look at the resultant of these two polynomials as polynomials in r. The resultant is a polynomial in t and is always positive.

Define a polynomial $g(r, t) = f(r, t)h(r, t)$. Since we know these curves are graphs, we want to count the roots for fixed t. The number of roots is the number of bifurcations for each value of t, and we can use the Sturm Algorithm for counting real roots. The code used to implement the Sturm Algorthim in Mathematica is in Appendix B. There are four real roots of g for $t \neq \pm 1/\sqrt{3}$ and three at $t = \pm\sqrt{3}$ where f and the harmonic curve h have a common root.

Figure 4.6 has a closer view of the middle portion $-1 \leq t \leq 1$ and the components are numbered for reference. There are five components. Components 3 and 5 have been split into 3a, 3b, 5a and 5b, based on where there are changes in the signs of the vorticity.

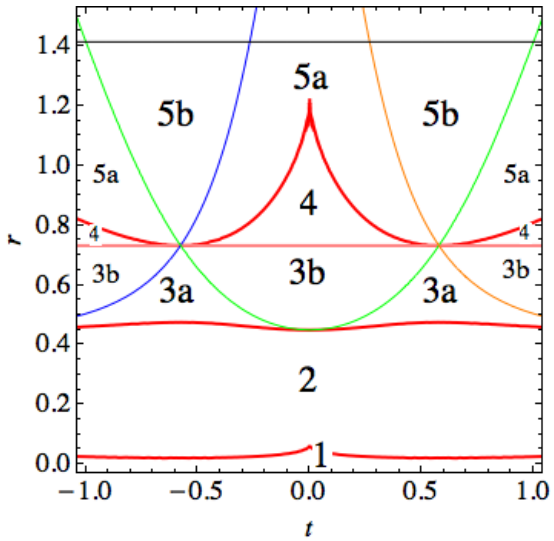

Figure 4.6: Counting Components

We can consider the portion of the diagram $\frac{-1}{\sqrt{3}} \leq t \leq \frac{1}{\sqrt{3}}$ and get representative of each component.

Using the change of coordinates above, we can pick nice integer values for μ_1, μ_2, μ_3, thus allowing for exact computations, and find (r, t) to get representatives of each component. In the next section, for each representative, we look at the number of critical points of V which corresponds to the number of families of relative equilibria.

Table 4.1: Component Representatives

component	(μ_1, μ_2, μ_3)	(t, r)
1	(1,1,1)	(0,0)
2	(2,1,2)	$(\ 0,\ -5+3\sqrt{3})$
3a	(2,1,9)	$(\frac{1}{7}(3\sqrt{3}-2\sqrt{19}), -4\sqrt{\frac{3}{19}}+\sqrt{\frac{86}{19}})$
3b	(2,-1,3)	$(\frac{7-2\sqrt{13}}{\sqrt{3}}, \frac{-4+\sqrt{42}}{\sqrt{13}})$
4	(3,-2,3)	$(0, \frac{1}{5}(-4+\sqrt{66})$
5a	(1,-2,3)	$(\frac{-4+\sqrt{19}}{\sqrt{3}}, \frac{-2+\sqrt{42}}{\sqrt{19}})$
5b	(-1,-3,10)	$(\frac{1}{11}(-14+5\sqrt{3}), \frac{1}{7}(-2\sqrt{3}+\sqrt{110}))$

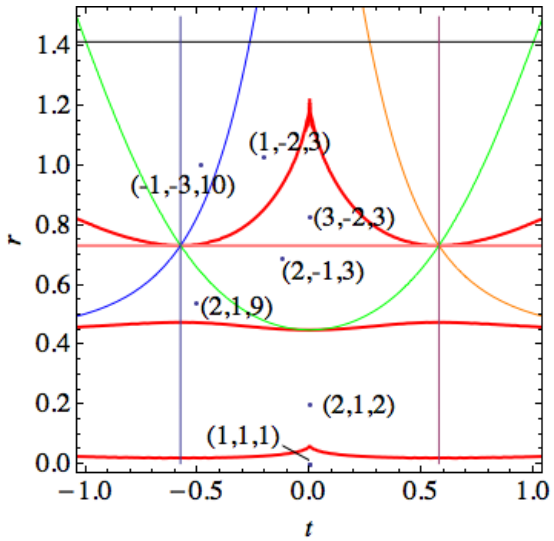

Figure 4.7: Component Representatives

4.4 Families of Relative Equilibria

In this section, we use a method for counting real roots to determine the exact number of critical points in each component of the bifurcation diagram. We'll examine the corresponding families of relative equilibria.

4.4.1 Hermite Method for Counting Roots

This section outlines the Hermite method for counting roots of polynomials. The method for one polynomial is described in detail in [30]. Below we outline the Hermite method for a set of polynomials which is in Chapter 2 of [31].

Let I be the ideal generated by a set of polynomials in $\mathbb{Q}[x_1, ..., x_n]$. The quotient ring $\mathbb{Q}[x_1, ..., x_n]/I$ is a vector space over $\mathbb{Q}$ and it is finite dimensional (if $Var(I)$ is finite). The Hermite method of counting real roots involves finding a matrix $\mathcal{H}(I)$, the entries of which are constructed from basis elements of the vector space $\mathbb{Q}[x_1, ..., x_n]/I$.

First, find the Groebner basis G of the ideal I with respect to a certain lexicographic order. The basis B for $\mathbb{Q}[x_1, ..., x_n]/I$ is a set of monomials that are not in the ideal of leading terms $\langle LT(I)\rangle$ of G (with respect to that same lexicographic order),

$$B = \{x^\alpha : x^\alpha \notin \langle LT(I)\rangle\}.$$

These are essentially all the monomials with exponents less than the exponents of the leading terms of the Groebner basis. For a basis element $f_i \in B$, there is a corresponding linear map m_i over the vector space $\mathbb{Q}[x_1, ..., x_n]/I$.

Define the matrix $\mathcal{H}(I)$ with entries $\mathcal{H}_{ij} = Tr(m_i \cdot m_j)$.

Theorem 4.6. *The signature of the matrix $\mathcal{H}(I)$ is the number of distinct real roots of the polynomials generating I. The rank of $\mathcal{H}(I)$ is the number of distinct roots over $\mathbb{C}$.*

There exist a couple definitions of the signature of a matrix, but here we define signature as the dimension of the positive definite subspace minus the dimension of the negative definite subspace. To determine the signature, calculate a sequence $1, \delta_1, ..., \delta_d$, where δ_i is the ith principle minor of $\mathcal{H}(I)$. Then Jacobi's theorem says signature of $\mathcal{H}(I)$ is d minus 2 times the number of sign changes in the sequence.

The computation for Hermite's method was done by modifying a Mathematica implementation of Moeckel's. The code for this method is in Appendix B.

4.4.2 Critical points of V for $N = 3$

The equations for bifurcations tell us when the number of critical points changes. Thus we can calculate the number of critical points for representative values of (μ_1, μ_2, μ_3) to find the number of critical points at all values of μ_i in each component. To apply the Hermite Method for counting roots, the equations for critical points $\nabla\tilde{V} = 0$ need to be rewritten as polynomial equations, and then evaluated at the component representative values of μ_i to calculate the number of roots in t_2, t_3. Luckily, we already did this to find the bifurcation curve for degenerate critical points. Taking polynomials p_3 and q_3, we can evaluate them at each component representative to get polynomials in t_2, t_3. Then we apply the Hermite method to the set of polynomials $\{p_3, q_3, w * (t_2 - t_3) - 1\} \in \mathbb{Z}[t_2, t_3, w]$, eliminating w when finding the Groebner basis in t_2 and t_3. The Hermite method involves only exact symbolic computations with integers, using the code found in Appendix B. Table 4.2 gives the results for each component.

Again, Hermite's method does only exact computations with integers. However, it is nice to be able to visualize V and see the roots of the polynomial equations which correspond to critical points of V. Figure 4.8 shows a contour plot of V made in Mathematica for each component representative. From component 1 to component 2,

Table 4.2: Number of Roots in Each Component

component	(μ_1, μ_2, μ_3)	Roots in $\mathbb{R}$	Roots in $\mathbb{C}$
1	(1,1,1)	14	14
2	(2,1,2)	10	14
3a	(2,1,9)	10	14
3b	(2,-1,3)	10	14
4	(3,-2,3)	8	14
5a	(1,-2,3)	8	14
5b	(-1,-3,10)	8	14

we see that there are four fewer critical points because of a saddle-node bifurcation. From component 2 to 3, there is no change in the number of critical points. However, the type of critical points switches from components 2 or 3a to 3b. The saddles become minima or maxima, and the minima and maxima become saddles. This is just the switch of μ_2 from positive to negative. From component 3 to 4, the number of critical points decreases by two, as two critical points "slide" off into the singularity at the boundary of the domain of V. From components 4 to 5, there is no change in the number of critical points, but in component 5b, we see that the saddles and maxima/minima switch as now μ_3 is negative as well.

Remark: The lack of change in the number of real critical points from components 2 to 3 and 4 to 5 is evidence that there is a degenerate complex valued critical point of V.

Component 1 - $(1,1,1)$					
14 Critical points					
max.	2	min.	6	saddle	6

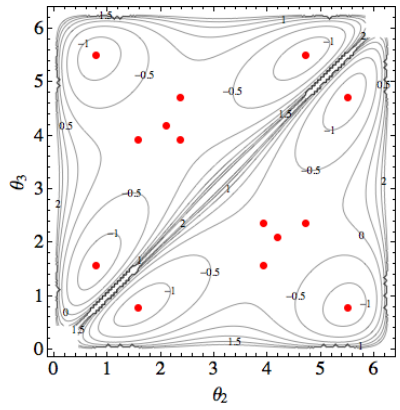

$\tilde{V}(\theta_2, \theta_3)$

Component 2 - $(2,1,2)$					
10 Critical points					
max.	0	min.	6	saddle	4

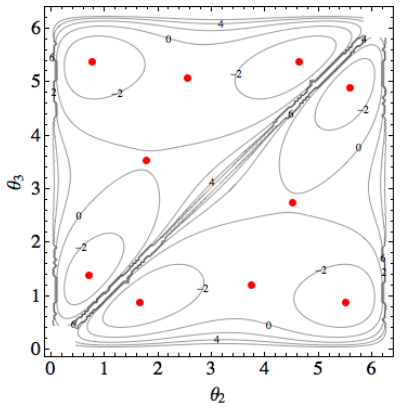

$\tilde{V}(\theta_2, \theta_3)$

Component 3a - $(2,1,9)$					
10 Critical points					
max.	0	min.	6	saddle	4

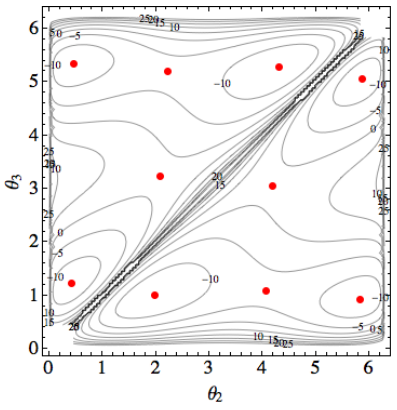

$\tilde{V}(\theta_2, \theta_3)$

Component 3b - $(2,-1,3)$					
10 Critical points					
max.	2	min.	2	saddle	6

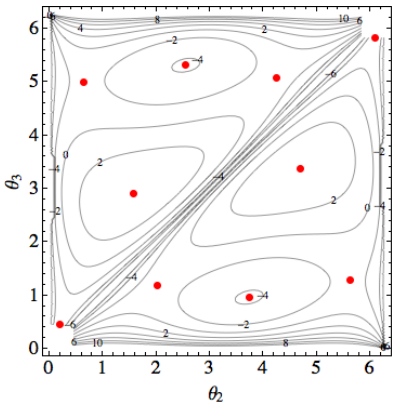

$\tilde{V}(\theta_2, \theta_3)$

Component 4 - $(3, -2, 3)$					
8 Critical points					
max.	2	min.	2	saddle	4

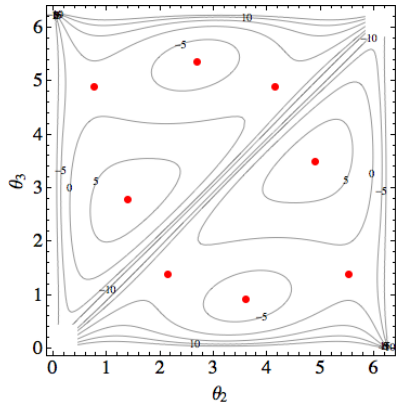

$\tilde{V}(\theta_2, \theta_3)$

Component 5a - $(1, -2, 3)$					
8 Critical points					
max.	2	min.	2	saddle	4

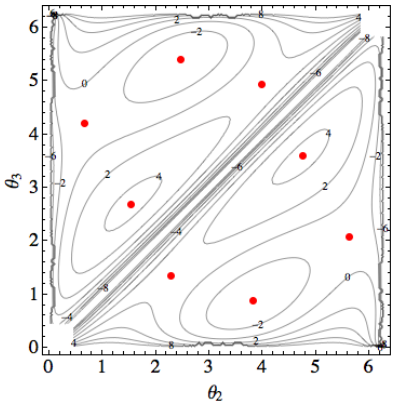

$\tilde{V}(\theta_2, \theta_3)$

Component 5b - $(-1, -3, 10)$					
8 Critical points					
max.	2	min.	2	saddle	4

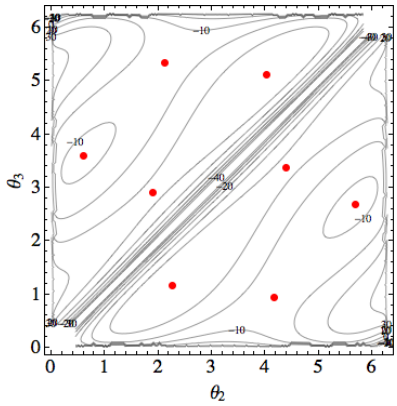

$\tilde{V}(\theta_2, \theta_3)$

Figure 4.8: Contour Plots of $\tilde{V}$ at Each Component Representative

Chapter 5

Linear Stability

Theorem 3.1 asserts that the nondegenerate relative equilibria of the $(1+N)$-vortex problem are the limiting configurations of relative equilibria of the $(N+1)$-vortex problem for $\epsilon > 0$. In this chapter, we look at the linear stability of the relative equilibria configurations of the $(N+1)$-vortex problem that continue from relative equilibria of the $(1+N)$-vortex problem.

5.1 Conditions for Linear Stability

Recall that the equations of motion in polar-heliocentric coordinates are

$$\dot{r}_i = \epsilon \sum_{j \neq i} \mu_j r_j \sin(\theta_i - \theta_j) \left(\frac{1}{r_j^2} - \frac{1}{r_i^2 + r_j^2 - 2 r_i r_j \cos(\theta_i - \theta_j)} \right) \tag{5.1}$$

$$\dot{\theta}_i = (1 + \epsilon \mu_i) \frac{1}{r_i^2} + \epsilon \sum_{j \neq i} \mu_j \frac{r_i^2 r_j \cos(\theta_i - \theta_j) - r_i r_j^2 \cos(2(\theta_i - \theta_j))}{r_i r_j^2 (r_i^2 + r_j^2 - 2 r_i r_j \cos(\theta_i - \theta_j))} \tag{5.2}$$

At a relative equilibrium configuration, $\dot{r}_i = 0$ and $\dot{\theta}_i = 1$. To get a true fixed point, put the system in rotating coordinates.

$$\dot{r}_i = \epsilon \sum_{j \neq i} \mu_j r_j \sin(\theta_i - \theta_j) \left(\frac{1}{r_j^2} - \frac{1}{r_i^2 + r_j^2 - 2 r_i r_j \cos(\theta_i - \theta_j)} \right) \tag{5.3}$$

$$\dot{\theta}_i = -\omega + (1 + \epsilon \mu_i) \frac{1}{r_i^2} + \epsilon \sum_{j \neq i} \mu_j \frac{r_i^2 r_j \cos(\theta_i - \theta_j) - r_i r_j^2 \cos(2(\theta_i - \theta_j))}{r_i r_j^2 (r_i^2 + r_j^2 - 2 r_i r_j \cos(\theta_i - \theta_j))} \tag{5.4}$$

We assume $\omega = 1$, and then at a relative equilibrium $\dot{r}_i = 0$ and $\dot{\theta}_i = 0$.

Let $(\rho^\epsilon, \phi^\epsilon)$ be a sequence of relative equilibria of the $(N+1)$-vortex problem which converges to a relative equilibrium $(\rho, \phi) = (1, ..., 1, \phi_1, ..., \phi_N)$ of the $(1+N)$-vortex problem as $\epsilon \to 0$, and let ϕ be a nondegenerate critical point of V. At $(\rho^\epsilon, \phi^\epsilon)$, we can apply Lemma 3.2 that $r_i = 1 + \mathcal{O}(\epsilon)$ for ϵ sufficiently small, and get that for the linearized system $(\dot{\delta r}, \dot{\delta\theta}) = M(\delta r, \delta\theta)$, M is made up of four $n \times n$ blocks:

$$M = \begin{pmatrix} \epsilon A + \mathcal{O}(\epsilon^2) & \epsilon\mu^{-1}V_{\theta\theta} + \mathcal{O}(\epsilon^2) \\ -2I + \mathcal{O}(\epsilon) & \epsilon D + \mathcal{O}(\epsilon^2) \end{pmatrix} \tag{5.5}$$

where A and D are $n \times n$ matrices of the form:

$$a_{ii} = \sum_{j \neq i} \mu_j \frac{\sin(\theta_i - \theta_j)}{2 - 2\cos(\theta_i - \theta_j)} \qquad d_{ii} = -\sum_{j \neq i} \mu_j \sin(\theta_i - \theta_j) \tag{5.6}$$

$$a_{ij} = -\mu_j \sin(\theta_i - \theta_j) \qquad d_{ij} = \mu_j \sin(\theta_i - \theta_j) \tag{5.7}$$

5.1.1 Invariant Subspace of M

M has a two-dimensional invariant subspace spanned by $v = (0, .., 0, 1, .., 1) \in \mathbb{C}^{2N}$ and $\mathcal{J}v = (1, ..., 1, 0, ..., 0) \in \mathbb{C}^{2N}$. The eigenvalues corresponding to this invariant subspace are two zero eigenvalues and give a nontrivial Jordan block in the diagonalization of M. Thus a relative equilibrium point is never a conventional stable fixed point. The instability is associated to the fact that relative equilibrium configurations are members of families of such configurations with different rotational frequencies. Thus, as above, we will define linear stability by restricting to the complementary subspace.

Note that M is Hamiltonian on this complementary subspace in the sense that $\Omega(v, Mw) = -\Omega(Mv, w)$ where Ω is the skew inner product defined in Chapter 2.

5.1.2 Eigenvalues of M and Theorem

Let $\lambda \in \mathbf{C}$ be nonzero and consider the matrix

$$M - \lambda I = \begin{pmatrix} -\lambda I + \epsilon A + \mathcal{O}(\epsilon^2) & \epsilon\mu^{-1}V_{\theta\theta} + \mathcal{O}(\epsilon^2) \\ -2I + \mathcal{O}(\epsilon) & -\lambda I + \epsilon D + \mathcal{O}(\epsilon^2) \end{pmatrix} \tag{5.8}$$

Lemma 5.1 (Lemma 4 in [11])**.** *Let A, B, C and D be real $n \times n$ matrices and define*

$$M = \begin{pmatrix} A & B \\ C & D \end{pmatrix}.$$

Then $\det M = \det(A)\det(D - CA^{-1}B) = \det(D)\det(A - BD^{-1}C)$ *whenever* A *and* D *are invertible.*

From the previous section, we know that M has at least two zero eigenvalues, so consider $\det(M - \lambda I)$ in the region where $|\lambda| \geq c\sqrt{\epsilon}$ for small $c > 0$. Applying this lemma yields

$$\begin{aligned}\det(M - \lambda I) &= \det(-\lambda I + \epsilon A + \mathcal{O}(\epsilon^2))\det((-\lambda I + \epsilon D + \mathcal{O}(\epsilon^2)) \\ &\quad - (-2I + \mathcal{O}(\epsilon))(-\lambda I + \epsilon A + \mathcal{O}(\epsilon^2))^{-1}(\epsilon\mu^{-1}V_{\theta\theta} + \mathcal{O}(\epsilon^2))) \\ &= \det(\lambda I + \mathcal{O}(\epsilon))\det(\lambda I + \tfrac{2}{\lambda}\epsilon\mu^{-1}V_{\theta\theta} + \mathcal{O}(\epsilon)) \\ &= \det(I + \tfrac{1}{\lambda}\mathcal{O}(\epsilon))\det(\lambda^2 I + 2\epsilon\mu^{-1}V_{\theta\theta} + \lambda\mathcal{O}(\epsilon))\end{aligned} \tag{5.9}$$

Since λ depends on ϵ, we keep it on the $\mathcal{O}(\epsilon)$ terms. The only way this determinant can be zero is if $\lambda = \mathcal{O}(\sqrt{\epsilon})$. Let $\lambda = \sqrt{\epsilon}\gamma(\epsilon)$ and define $\lim_{\epsilon\to 0}\gamma(\epsilon) = \gamma_0$. Then

$$\begin{aligned}\det(M - \lambda I) &= \det(I + \mathcal{O}(\sqrt{\epsilon}))\det(\epsilon\gamma^2 + 2\epsilon\mu^{-1}V_{\theta\theta} + \mathcal{O}(\epsilon^{3/2})) \\ &= (1 + \mathcal{O}(\sqrt{\epsilon}))\det(\epsilon\gamma^2 + 2\epsilon\mu^{-1}V_{\theta\theta} + \mathcal{O}(\epsilon^{3/2}))\end{aligned} \tag{5.10}$$

Thus for $\det(M - \lambda I) = 0$, $\det(\epsilon\gamma^2 + 2\epsilon\mu^{-1}V_{\theta\theta} + \mathcal{O}(\epsilon^{3/2})) = 0$. The $\det(M - \lambda I)$ is a polynomial of degree $2N$ in λ.

$$\det(\epsilon\gamma^2 + 2\epsilon\mu^{-1}V_{\theta\theta} + \mathcal{O}(\epsilon^{3/2})) = \epsilon^N \det(\gamma^2 I + 2\mu^{-1}V_{\theta\theta} + \mathcal{O}(\sqrt{\epsilon})) = 0 \tag{5.11}$$

In the limit $\epsilon \to 0$ this polynomial becomes

$$\det(\gamma_0^2 I + 2\mu^{-1}V_{\theta\theta}) = 0 \tag{5.12}$$

So for small ϵ the eigenvalues of $2\mu^{-1}V_{\theta\theta}$ will determine the spectral stability of the relative equilibria.

Theorem 5.1. *Let* $(\rho^\epsilon, \phi^\epsilon)$ *be a sequence of relative equilibria of the* $(N+1)$*-vortex problem which converges to a relative equilibrium* $(\rho, \phi) = (1, ..., 1, \phi_1, ..., \phi_N)$ *of the* $(1+N)$*-vortex problem as* $\epsilon \to 0$*, and let* ϕ *be a nondegenerate critical point of* V*. For* ϵ *sufficiently small,* $(\rho^\epsilon, \phi^\epsilon)$ *is nondegenerate and is linearly stable if and only if* $\mu^{-1}V_{\theta\theta}$ *has* $N - 1$ *nonzero positive eigenvalues.*

Proof. Note that the eigenvalues of $2\mu^{-1}V_{\theta\theta}$ have the same signs as the eigenvalues of $\mu^{-1}V_{\theta\theta}$ and that $\mu^{-1}V_{\theta\theta}$ always has one 0 eigenvalue because $(1, 1, 1..., 1)$ is still an eigenvector for eigenvalue 0. Let $\zeta = -\gamma_0^2$ be a nonzero eigenvalue of $\mu^{-1}V_{\theta\theta}$.

Assume that $\mu^{-1}V_{\theta\theta}$ has a negative or complex-valued eigenvalue ζ. Then for ϵ sufficiently small, $\gamma(\epsilon)$ must have nonzero real part, and therefore $\lambda = \sqrt{\epsilon}\gamma(\epsilon)$ has nonzero real part and the relative equilibrium is not linearly stable.

Now assume that $\mu^{-1}V_{\theta\theta}$ has $N-1$ positive eigenvalues (and one zero eigenvalue). To prove stability, we verify that the hypothesis of Lemma 2.1 holds. The calculation is exactly like the analogous part of the proof in [11].

□

5.2 Linear Stability for $(1+3)$-Vortices

In this section, we consider when $\mu^{-1}V_{\theta\theta}$ has $N-1$ positive eigenvalues, specifically looking at the case when $N = 3$. We give a negative result, and then find that values of μ_i that give at least one stable family of relative equilibria using a (minimally) numerical method.

5.2.1 Stability by Inner Products

When $\mu_i > 0$ for all i, the condition for stability given in Theorem 5.1 is the as same as the condition that ϕ is a minimum of $\tilde{V}$ since we can define an inner product $\langle v, w\rangle = v^T\mu w$ and then the quadratic form $\mu^{-1}\tilde{V}_{\theta\theta}$ is positive definite with respect to this inner product. When $\mu_i < 0$ for all i, condition for stability given in Theorem 5.1 is the same as the condition that ϕ is a maximum of $\tilde{V}$ with respect to the same inner product above, only now the inner product is negative definite. When μ_i have mixed signs, it is not so obvious. The issue is that the inner product is indefinite.

5.2.2 A negative result

Let $N = 3$. Then $\det(\mu^{-1}V_{\theta\theta} - \lambda I)$ is a cubic polynomial with one factor $-\lambda$. Taking a common denominator, we can write $\det(\mu^{-1}V_{\theta\theta} - \lambda I) = -\lambda(\frac{a\lambda^2+b\lambda+c}{a})$, and clear the denominator to find roots of $-\lambda(a\lambda^2 + b\lambda + c)$. The two nonzero eigenvalues are given

by $\lambda = -(b \pm \sqrt{b^2 - 4ac})/2a$ where a, b, c depend on μ_i, θ_i. To get two positive real eigenvalues there are three conditions: $b^2 - 4ac \geq 0$ (real eigenvalues), $b/a < 0$ (at least one positive eigenvalue) and $ac > 0$ (both eigenvalues positive). The idea is to find the set of μ_i where at least one of the critical points of $V(\theta)$ satisfies these three conditions.

One way to do this take the equations for critical points and each condition, rewrite them as polynomial equations, and then calculate three Groebner bases that eliminate the position variables (hoping there's only one polynomial in each Groebner basis), just like in Chapter 4. These polynomials are given in Appendix 4. However, trying to do this calculation on the $b^2 - 4ac$ condition did not work in Mathematica - the algorithms for a Groebner basis took up too much memory for a personal computer. Additionally, trying to use resultants of polynomials did not work for the same reason.

5.2.3 The t-map

The equations for $\mu^{-1}\nabla V = 0$ can be viewed as an $N \times N$ system of linear equations in μ_i:

$$T(\theta) \begin{bmatrix} \mu_1 \\ \vdots \\ \mu_N \end{bmatrix} = \begin{bmatrix} 0 \\ \vdots \\ 0 \end{bmatrix} \tag{5.13}$$

where $T(\theta)$ is an $N \times N$ matrix. In the same way we did this in Chapter 4, we can make these equations polynomial equations. We can take the numerators of each coordinate in ∇V and make the change of variables

$$\sin(\theta_i) = \frac{2t_i}{t_i^2 + 1}, \qquad \cos(\theta_i) = \frac{t_i^2 - 1}{t_i^2 + 1}$$

Now we get an $N \times N$ system of linear equations in μ_i

$$T(t_i) \begin{bmatrix} \mu_1 \\ \vdots \\ \mu_N \end{bmatrix} = \begin{bmatrix} 0 \\ \vdots \\ 0 \end{bmatrix} \tag{5.14}$$

where $T(t_i)$ is an $N \times N$ matrix with entries that are polynomials in t_i. For $N = 3$,

$$T(t_1, t_2, t_3) = \begin{bmatrix} 0 & \tau_3(t_1 - t_3) & -\tau_2(t_1 - t_2) \\ -\tau_3(t_2 - t_3) & 0 & \tau_1(t_1 - t_2) \\ \tau_2(t_2 - t_3) & -\tau_1(t_1 - t_3) & 0 \end{bmatrix} \tag{5.15}$$

Where

$$\tau_1 = (1+t_1^2)(1+t_2t_3)(1-3t_2^2+8t_2t_3-3t_3^2+t_2^2t_3^2) \tag{5.16}$$

$$\tau_2 = -(1+t_2^2)(1+t_1t_3)(1-3t_1^2+8t_1t_3-3t_3^2+t_1^2t_3^2) \tag{5.17}$$

$$\tau_3 = (1+t_1t_2)(1-3t_1^2+8t_1t_2-3t_2^2+t_1^2t_2^2)(1+t_3^2) \tag{5.18}$$

Using Mathematica, the nullspace of T is

$$\begin{bmatrix} \mu_1 \\ \mu_2 \\ \mu_3 \end{bmatrix} = \begin{bmatrix} \tau_1(t_1-t_2)(t_1-t_3) \\ \tau_2(t_1-t_2)(t_2-t_3) \\ \tau_3(t_1-t_3)(t_2-t_3) \end{bmatrix} = t(t_1,t_2,t_3). \tag{5.19}$$

Thus given (t_1, t_2, t_3) there is a unique (up to scaling) set of circulation parameters (μ_1, μ_2, μ_3) where (t_1, t_2, t_3) is a critical point of V. We'll call this the t-map.

5.2.4 Stability Conditions

Using the t-map, polynomial equations for each condition can be rewritten completely in terms of (t_1, t_2, t_3). These are given in Appendix C. Setting $t_1 = 0$ (reducing by rotational symmetry), the varieties of each condition are shown in Figure 5.1. Figure 5.1d shows all three varieties together and the shaded regions in the (t_2, t_3) coordinate plane where the configurations are stable, i.e. $b/a < 0$, $ac > 0$ and $b^2 - 4ac > 0$. We see stable configurations in a region around the line of singularities where $t_2 = t_3$. We also see two regions of stability away from the origin and centered around the line $t_2 = -t_3$. In the next section, these regions of stability are examined in more depth.

First, we will look at stability in the circulation parameters. We use a numerical method to do this. For each condition polynomial, we used the Solve function in Mathematica to symbolically solve for points in the variety of each polynomial equation. The builtin Solve is most accurate in only one dimension, so we fixed one of t_1, t_2, t_3 to be 0 (this is the same as reducing by rotational symmetry), and then set another of the variables to a mesh of variable size made of 180 points in the interval [-20,20], and solved for the third. Running through various permutations of t_1, t_2, t_3 gave a large set of points in the variety of each polynomial.

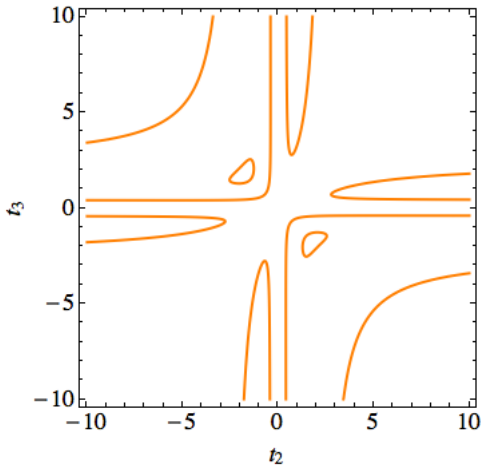

(a) $ac = 0$

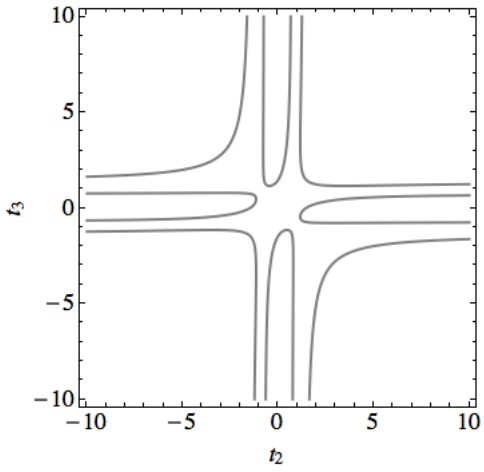

(b) $b/a = 0$

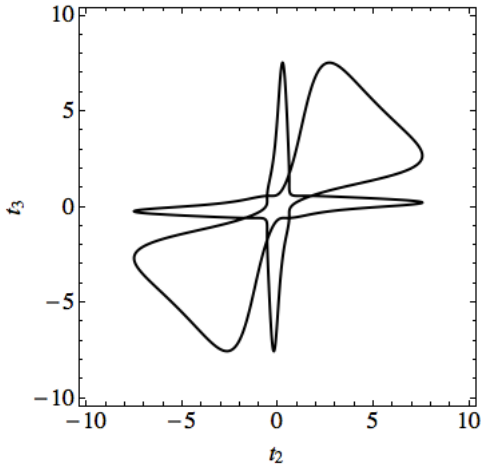

(c) $b^2 - 4ac = 0$

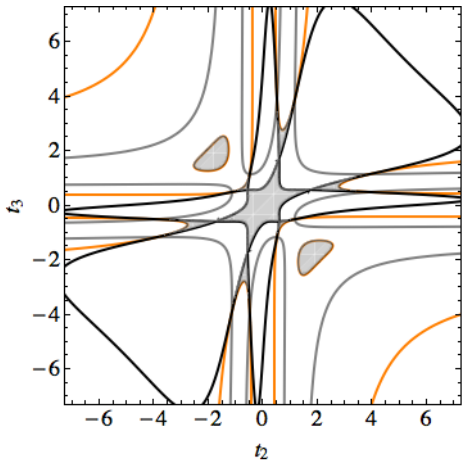

(d) Shaded Regions correspond to stable configurations

Figure 5.1: Stability conditions in (t_2, t_3)-coordinates

From there, we put these values into the t-map to get μ_1, μ_2, μ_3 and normalized these to the unit sphere. Figure 5.2 gives the stereographic projection of these points.

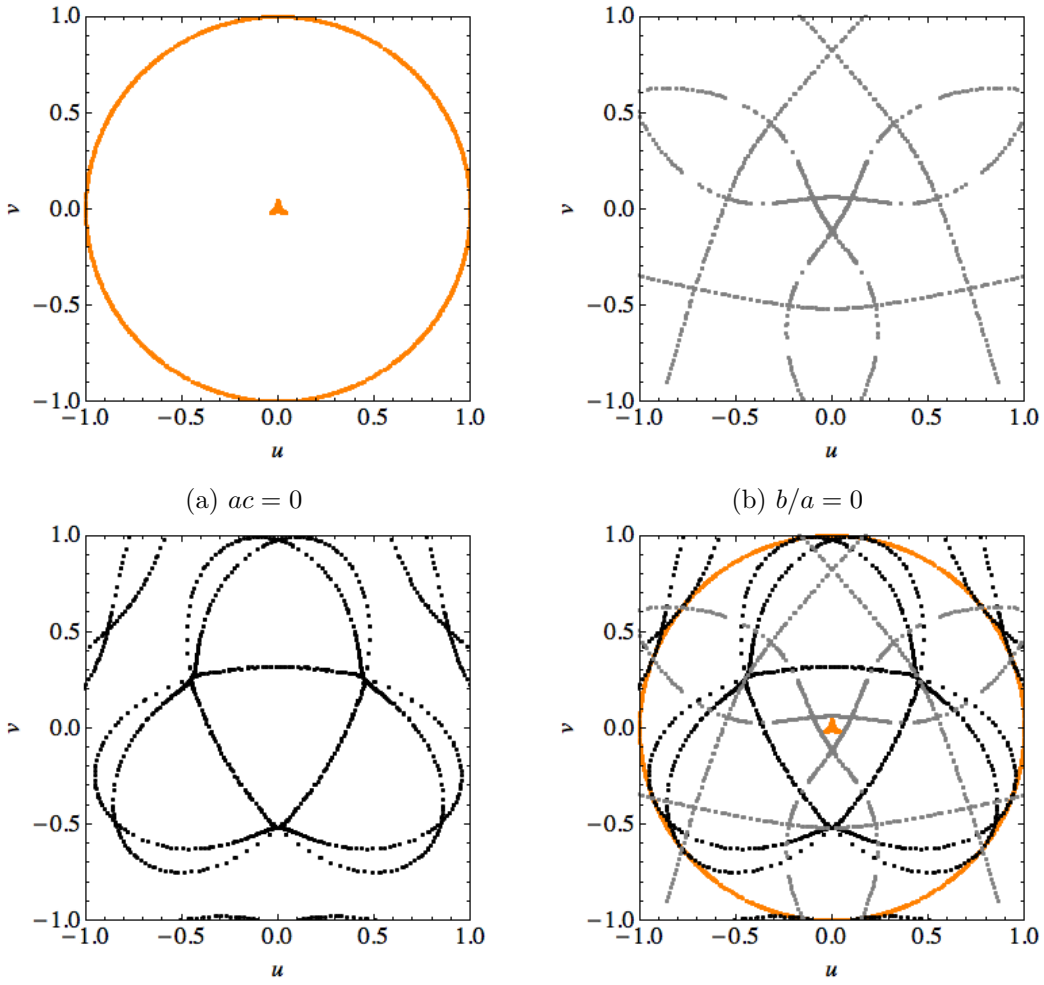

(a) $ac = 0$ (b) $b/a = 0$

(c) $b^2 - 4ac = 0$ (d) All Three Varieties

Figure 5.2: Points in the Variety of the Stability Conditions

Figure 5.2a shows the variety of $ac = 0$, which includes a little triangular shape near $\mu_1 = \mu_2 = \mu_3$, the same as for real-valued degenerate critical points, as well as a factor of the "equator" $\mu_1 + \mu_2 + \mu_3 = 0$. Figure 5.2b shows the variety of $b/a = 0$, the trace of $\mu^{-1}V_{\theta\theta}$. Figure 5.2c shows the variety of $b^2 - 4ac = 0$. It is interesting to note that this curve follows part of the curves $\mu_i = 0$. This is where the positive definite inner

product becomes an indefinite inner product, as mentioned above. Figure 5.3 shows the varieties of the stability conditions with the bifurcation diagram from Chapter 4.

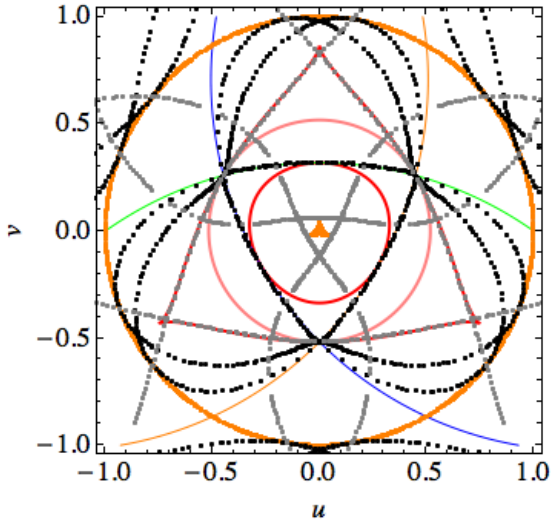

Figure 5.3: Bifurcation Diagram and Varieties of Stability Conditions

Figure 5.4 shows the varieties of the stability conditions in the "straightened out" (t, r) coordinates as given in (4.21). The areas shaded in blue are values of the circulation parameters that have stable relative equilibria points. The data used to examine how stability changes across the diagram is included in Appendix C.

If we examine these values we see that starting from the bottom of Figure 5.4 where $t = 0$ and all μ_i are equal, $b/a < 0$ and $b^2 - 4ac \geq 0$ for all critical points of V and the critical points that correspond to unstable relative equilibria have $ac < 0$. The first change in stability occurs when crossing the $ac = 0$ curve, that corresponds to the saddle-node bifurcation. The next change occurs when crossing the trace curve. Below this curve the trace is negative for all critical points, but now some of critical points which were unstable because $ac < 0$ also have $b/a > 0$. Then the next section is bordered by the $b^2 - 4ac = 0$ curve and lines up with $\mu_i = 0$. The relative equilibria that were previously stable switch to unstable as now $\mu^{-1}V_{\theta\theta}$ has imaginary eigenvalues, and only one of the previously unstable critical points of V becomes stable. This critical point is the critical point near the singularity. Then after the harmonic curve, none of the relative equilibria are stable, as this point slides off the domain. None of the relative

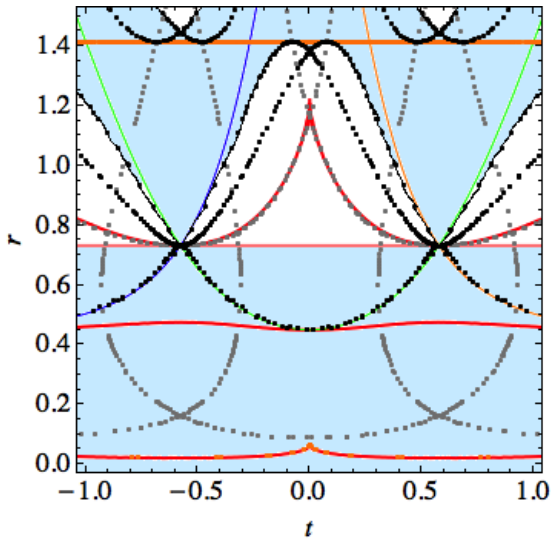

Figure 5.4: Varieties of Stability conditions in (t, r) coordinates. Shaded Regions give at least one stable relative equilibrium configuration

equilibria are stable again until both the trace and real eigenvalue conditions change sign again.

5.2.5 Comparison to stability in the full 4-vortex problem

We were curious how these results compared to stability in the unrestricted 4-vortex problem. Using Mathematica, we created a grid with step size $h = 1/10$ to over the $[-1, 1] \times [-1, 1]$ box in the stereographic projection of the parameter space, and using NSolve in Mathematica found relative equilibria configurations for $\epsilon = 1/10$ and then for $\epsilon = 1/100$. From here, we numerically calculated the eigenvalues of the linearized system at these relative equilibria. Figure 5.5 shows a dot for each point on the grid with at least one stable relative equilibria. Figure 5.6 shows the varieties of the stability conditions along with these results and Figure 5.7 also includes the bifurcation curves from Chapter 4.

We see that curves for stability conditions line up with the boundary between existence and nonexistence of a stable family of relative equilibria, except for the near the harmonic bifurcation curve where there is some space in the grid. This is not troubling for because the stable families of relative equilibria in this region are the families close to

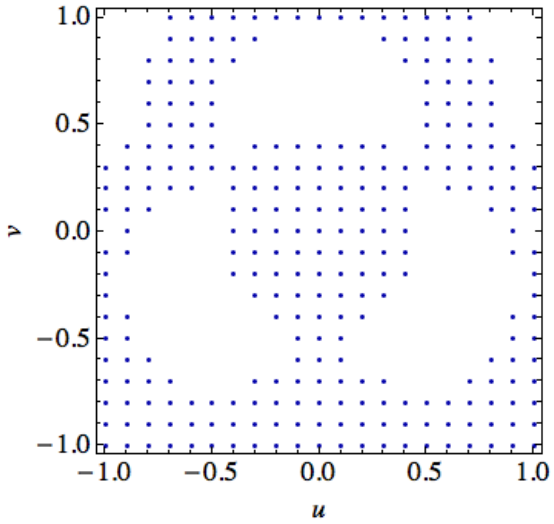

Figure 5.5: Values of circulations with at least one stable relative equilibrium

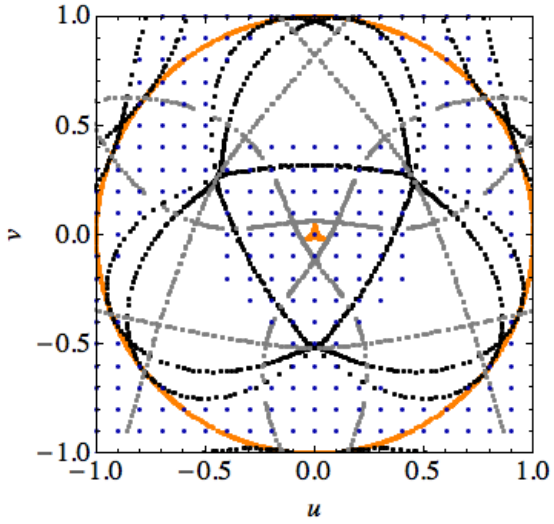

Figure 5.6: Stable Relative Equilibria and Varieties of the Stability Conditions

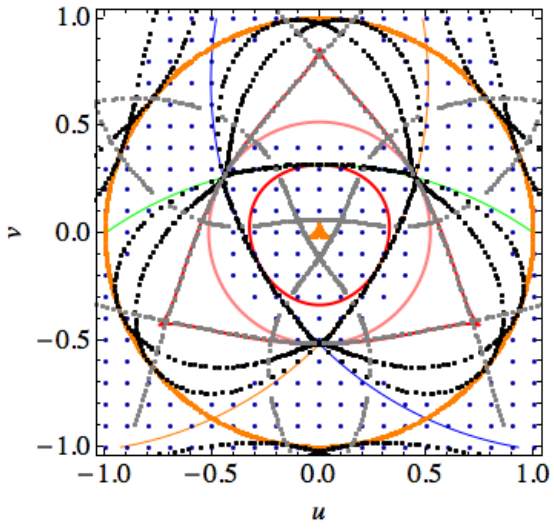

Figure 5.7: Stable Relative Equilibria, Varieties of Stability Conditions, and Bifurcation Curves

the singularity. The built in numerical methods in Mathematica are not robust, particularly near singularities, and $\epsilon = 1/100$ might not be small enough to be "sufficiently" small for the relative equilibrium points continue.

5.2.6 Examples of Families of Stable Relative Equilibria

In Figure 5.1d, the shaded regions correspond to configurations of stable relative equilibria in the (t_2, t_3) coordinates. We can reintroduce polar coordinates into the polynomials for stability conditions using the inverse transformation

$$t_2 = -\tan(\theta_2/2) \qquad t_2 = -\tan(\theta_3/2). \tag{5.20}$$

Setting $\theta_1 = 0$, Figure 5.8a shows the regions where (θ_2, θ_3) are critical points of V that correspond to stable families of relative equilibria. There are regions of stability near the singularity where $\theta_1 = \theta_2 = \theta_3$ as well as some other separated regions. To get some context, Figure 5.8b shows the relative equilibria configurations when $(\mu_1, \mu_2, \mu_3) = (1, 1, 1)$.

The six dots in the larger shaded regions in Figure 5.8b are stable relative equilibria configurations with the three small vortices equally spaced over an angular region of $\pi/2$

radians. These are families v-vii in Figure 5.9a. The region of stability that contains each point are perturbations of these configurations, like families iii-v in Figures 5.9b and 5.9c. Towards the corners of the domain, these shaded regions contain the stable configurations near the singularity, for example, family v in Figure 5.9d. These regions have little triangle-ish regions nearby. The configurations at the point connecting them are configurations with the three small vortices equally spaced over an angular region of $2\pi/3$ radians. These configurations correspond to the points where two of the three circulation parameters $\mu_i = 0$. The triangle-ish regions contain stable relative equilibria that spread out from there, for example see family iii in Figure 5.9g.

The six dots that are not in a shaded region in Figure 5.8b are the unstable relative equilibria that are saddle points of V, families ii-iv in 5.9a. The two dots in small elliptical regions are the relative equilibria configurations in family i in 5.9a that are also unstable. These configurations are regular polygonal configurations. Here they appear in a shaded stability region. This is because the same configurations are maxima of V for $(\mu_1, \mu_2, \mu_3) = (-1, -1, -1)$, and are stable there. The region surrounding these configurations are stable configurations for $\mu_i < 0$ for all i.

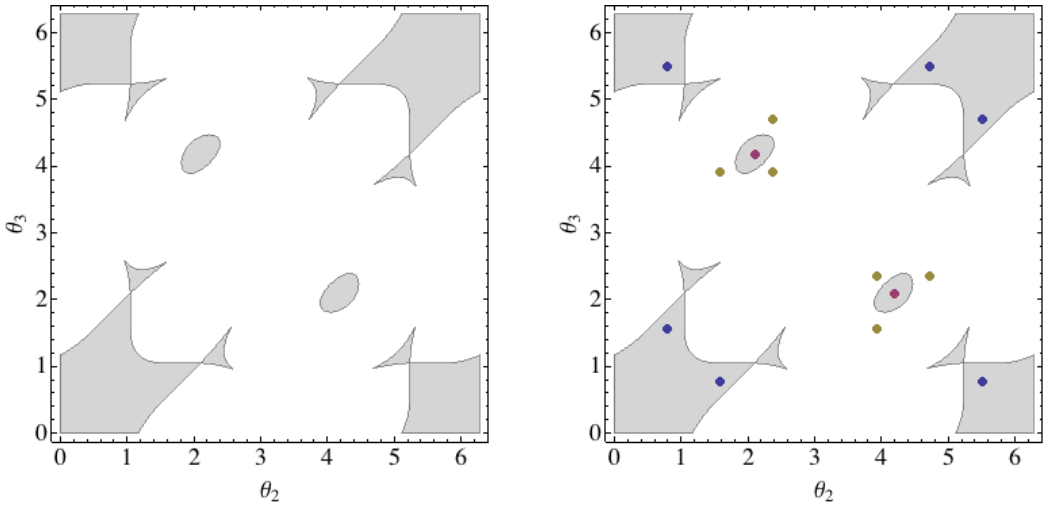

(a) Shaded regions correspond to stable configurations

(b) Relative Equilibria Configurations at (1,1,1)

Figure 5.8: Regions of Stable Configurations in Polar Coordinates

Figure 5.9 has families of relative equilibria for each bifurcation component from

Chapter 4, along with the type of critical point of V and the stability of the fixed point.

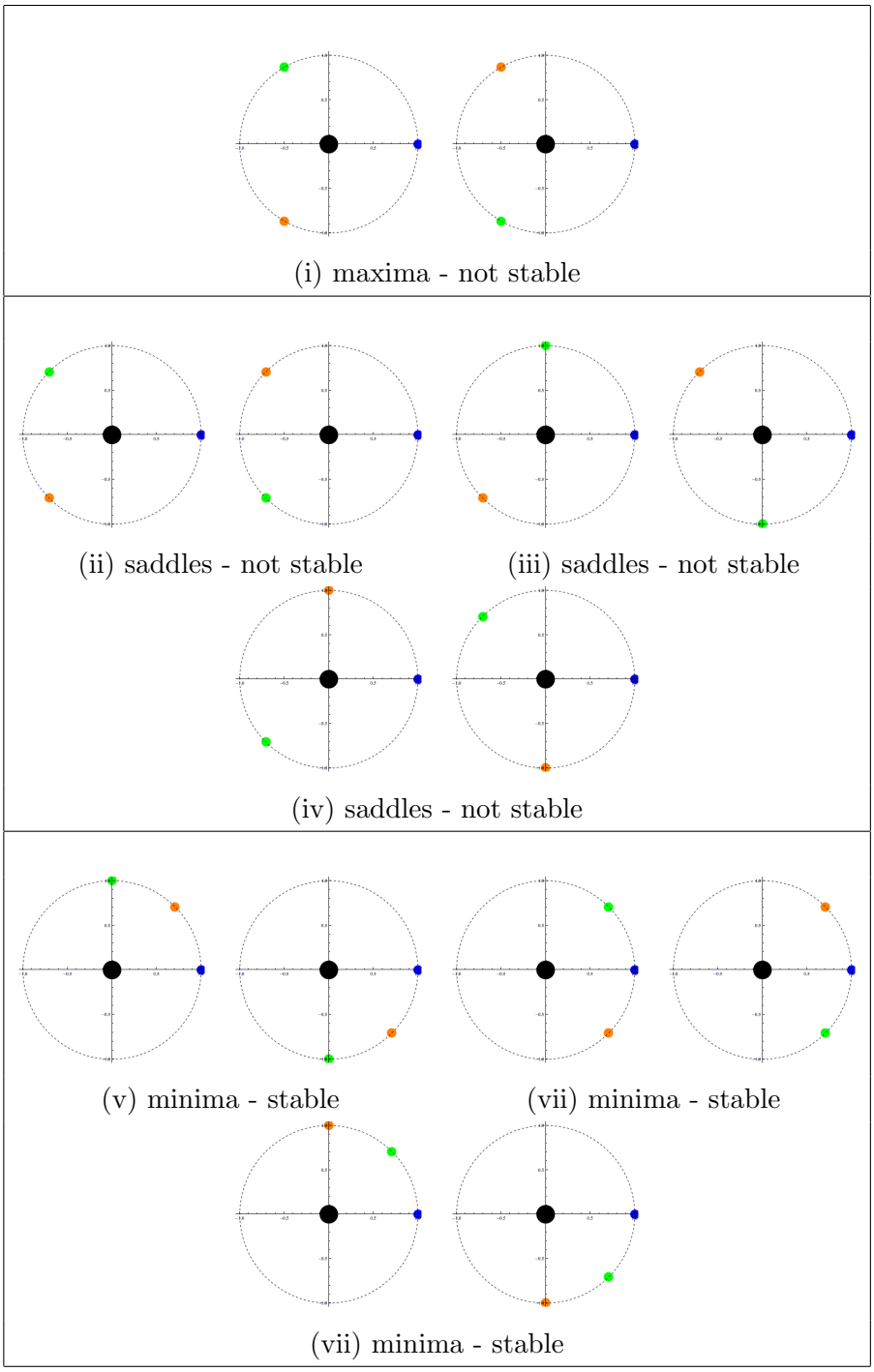

(a) Component 1 - 14 Families

Figure 5.9: Families of Relative Equilibria in Each Component

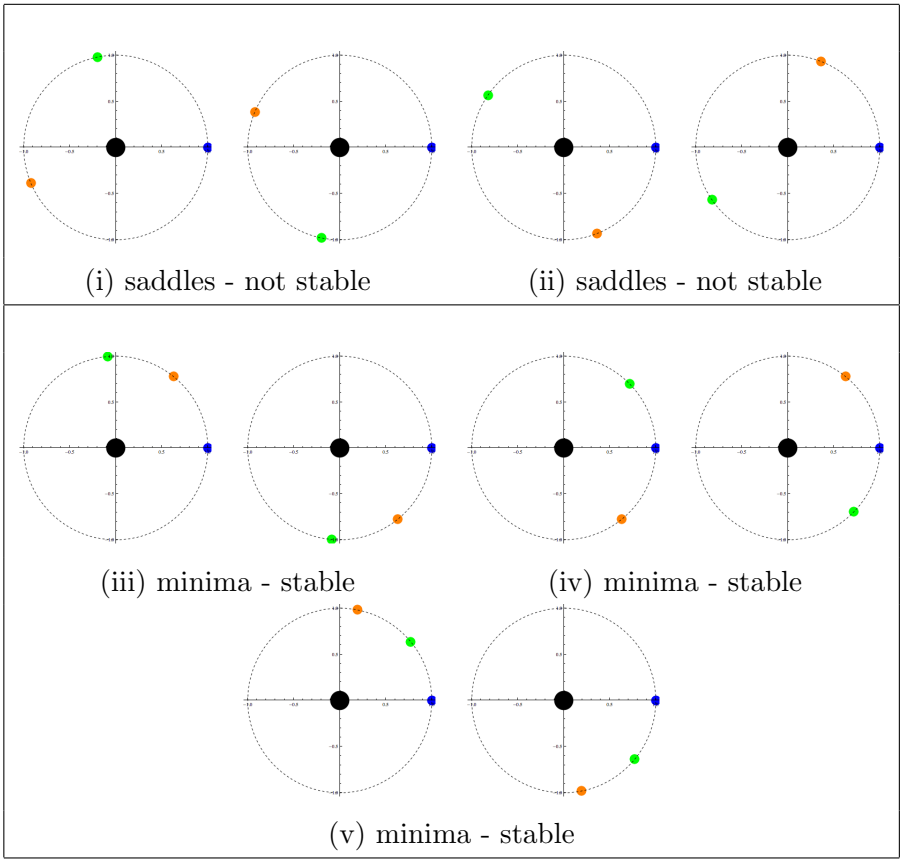

(b) Component 2 - 10 Families

Figure 5.9: Families of Relative Equilibria in Each Component (continued)

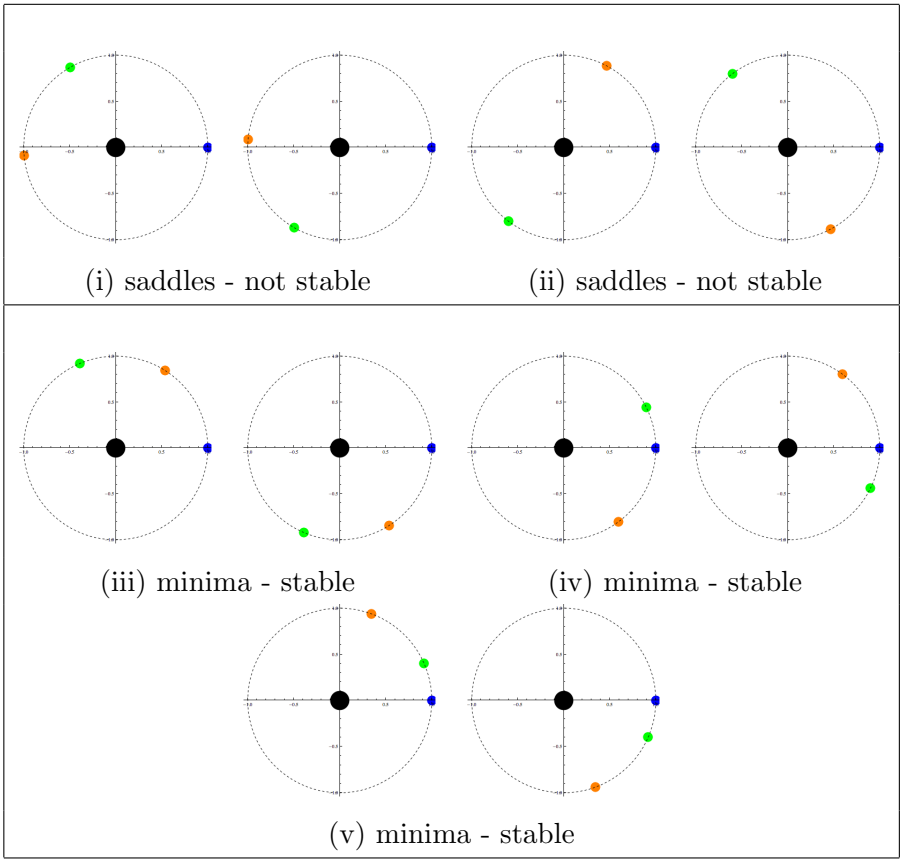

(c) Component 3a - 10 Families

Figure 5.9: Families of Relative Equilibria in Each Component (continued)

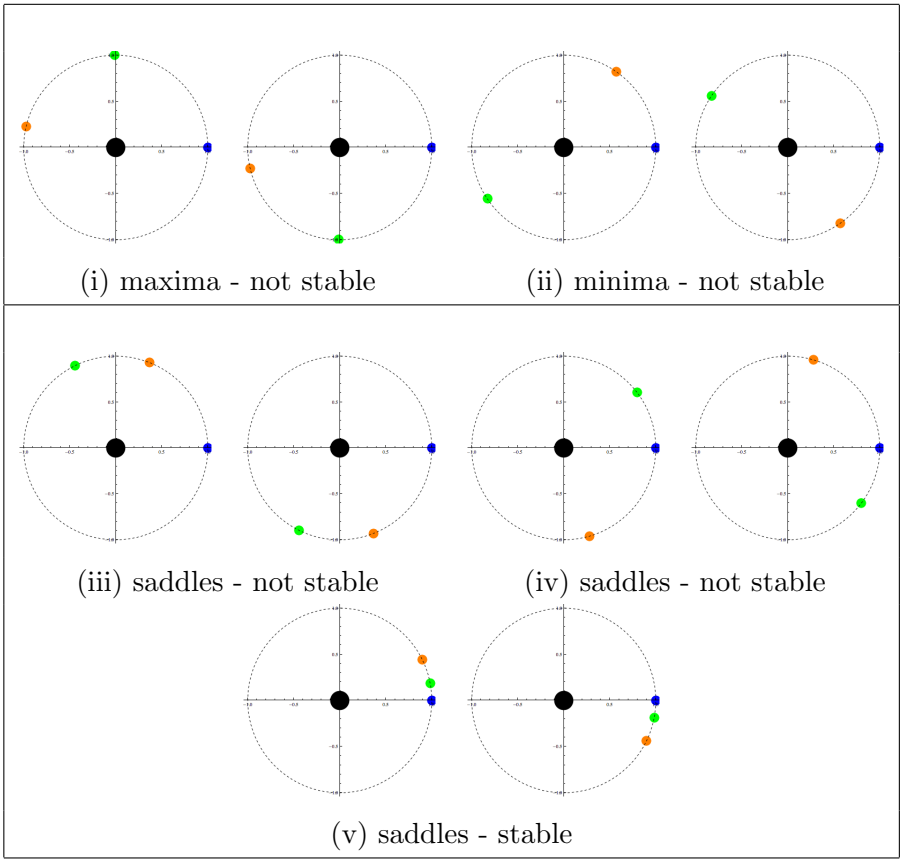

(d) Component 3b - 10 Families

Figure 5.9: Families of Relative Equilibria in Each Component (continued)

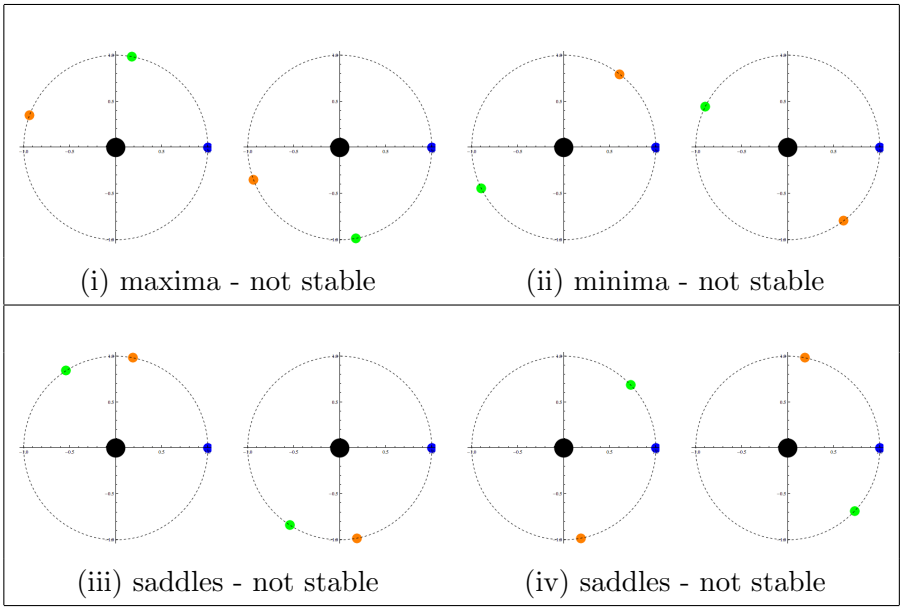

(e) Component 4 - 8 Families

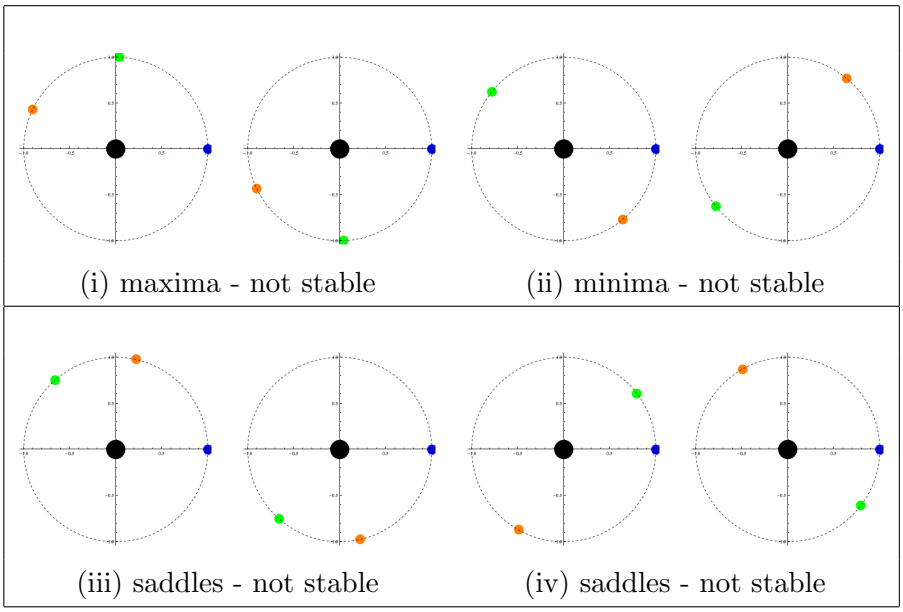

(f) Component 5a - 8 Families

Figure 5.9: Families of Relative Equilibria in Each Component (continued)

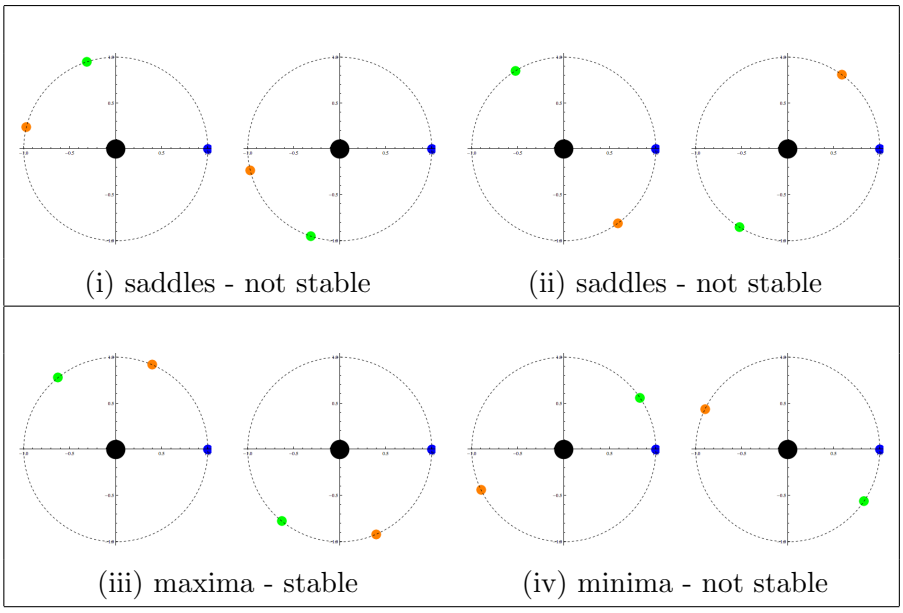

(g) Component 5b - 8 Families

Figure 5.9: Families of Relative Equilibria in Each Component (continued)

Chapter 6

Conclusion

Studying the dynamics of vortex configurations with one large vortex and N smaller vortices has applications to physical electromagnetic systems and atmospheric science, as well as being a historically interesting problem. This dissertation generalized the previous study of these configurations to configurations with a large vortex of strength $\Gamma_0 = 1$ and small vortices of different strengths, $\Gamma_i = \epsilon\mu_i$, $i = 1, ..., N$. Relative equilibria of the $(1 + N)$-vortex problem are defined as limits as $\epsilon \to 0$ of relative equilibria with N small vortices and one large vortex, where in the limit the small vortices become infinitesimal. The large vortex limits to the origin and the small vortices limit to a circle around the origin. The angular positions of the small vortices in the limit are the critical points of a potential function

$$V(\theta_1, ..., \theta_N) = -\sum_{i<j} \left(\cos(\theta_i - \theta_j) + \tfrac{1}{2}\log(2 - 2\cos(\theta_i - \theta_j)\right),$$

and any critical point of V continues to relative equilibria with one large and N small, nonzero vortices. The function V also plays a part in the linear stability of relative equilibria which continue for $\epsilon > 0$ from relative equilibria of the $(1+N)$-vortex problem. These configurations are linearly stable if they continue from a nondegenerate critical point ϕ of V and the weighted Hessian matrix of V at ϕ, $\mu^{-1}V_{\theta\theta}(\phi)$, has $N - 1$ positive eigenvalues.

In the case where $N = 3$, the $(1 + N)$-vortex problem is a subcase of the 4-vortex problem, the smallest number of vortices for which the n-vortex problem is not integrable. The number of critical points of V bifurcates depending on the ratios of the

parameters (μ_1, μ_2, μ_3), and hence there different numbers of relative equilibria for different ratios of circulations. The bifurcation curves for degenerate critical points can be found using algebraic geometry and Groebner bases. There is also another bifurcation where a nondegenate critical point slides off the noncompact domain of V into a singularity. These two curves together give complete picture of the number of relative equilibria when ϵ is sufficiently small. There are regions of 14, 10, and 8 families of relative equilibria.

Linear stability also depends on the values of μ_i. When $\mu_i > 0$ for all i, stable relative equilibria continue from minima of V. When $\mu_i < 0$ for all i, stable relative equilibria continue from maxima of V. Configurations that are minima of V are grouped together on the circle, rather than configurations which are spread out over multiple quadrants. When one of the μ_i is negative, stable configurations are close to the singularity on the boundary of the domain of V. When two μ_i are negative, stable configurations spread away from each other, but there are larger regions where there are no stable relative equilibria. When all μ_i are negative with the opposite sign of the central vortex), stable configurations are perturbations of the regular polygon configuration that occurs when $(\mu_1, \mu_2, \mu_3) = (-1, -1, -1)$.

References

[1] H von Helmholtz. Lxiii. on integrals of the hydrodynamical equations, which express vortex-motion. *The London, Edinburgh, and Dublin Philosophical Magazine and Journal of Science*, 33(226):485–512, 1867.

[2] D Durkin and J Fajans. Experiments on two-dimensional vortex patterns. *Physics of Fluids (1994-present)*, 12(2):289–293, 2000.

[3] James P Kossin, Wayne H Schubert, and Michael T Montgomery. Unstable interactions between a hurricane's primary eyewall and a secondary ring of enhanced vorticity. *Journal of the atmospheric sciences*, 57(24):3893–3917, 2000.

[4] James P Kossin and Wayne H Schubert. Mesovortices, polygonal flow patterns, and rapid pressure falls in hurricane-like vortices. *Journal of the atmospheric sciences*, 58(15):2196–2209, 2001.

[5] H Poincaré. Théorie des tourbillons (carré, paris). 1893.

[6] G Kirchhoff. Lectures on mathematical physics, mechanics. *Teubner, Leipzig*, 1877.

[7] Joseph John Thomson. *A Treatise on the Motion of Vortex Rings: an essay to which the Adams prize was adjudged in 1882, in the University of Cambridge*. Macmillan, 1883.

[8] G. R. Hall. Central configurations in the planar $1 + n$ body problem. preprint, 1988.

[9] Richard Moeckel. Linear Stability of Relative Equilibria with a Dominant Mass. *Journal of Dynamics and Differential Equations*, 6(1), 1994.

[10] HE Cabral and DS Schmidt. Stability of relative equilibria in the problem of n+ 1 vortices. *SIAM Journal on Mathematical Analysis*, 31(2):231–250, 2000.

[11] Anna M Barry, Glen R Hall, and C Eugene Wayne. Relative equilibria of the (1+ n)-vortex problem. *Journal of nonlinear science*, 22(1):63–83, 2012.

[12] Gareth E. Roberts. Stability of relative equilibria in the planar n-vortex problem. preprint, 2013.

[13] Richard Moeckel. Linear Stability Analysis of Some Symmetric Classes of Relative Equilbria. In *Hamiltonian Dynamical Systems*, volume 63 of *IMA Vol. Math. Appl.*, pages 291–317, New York, 1995. Springer.

[14] Walter Gröbli. *Specielle Probleme über die Bewegung geradliniger paralleler Wirbelfäden*. PhD thesis, Druck von Zürcher und Furrer, 1877.

[15] Hassan Aref, Nicholas Rott, and Hans Thomann. Gröbli's solution of the three-vortex problem. *Annual Review of Fluid Mechanics*, 24(1):1–21, 1992.

[16] Bruno Eckhardt. Integrable four vortex motion. *Physics of fluids*, 31(10):2796, 1988.

[17] Nicholas Rott. Constrained three-and four-vortex problems. *Physics of Fluids A: Fluid Dynamics (1989-1993)*, 2(8):1477–1480, 1990.

[18] KA Oneil. Relative equilibrium and collapse configurations of four point vortices. *Regular and Chaotic Dynamics*, 12(2):117–126, 2007.

[19] Marshall Hampton and Richard Moeckel. Finiteness of stationary configurations of the four-vortex problem. *Transactions of the American Mathematical Society*, 361(3):1317–1332, 2009.

[20] Marshall Hampton, Gareth E Roberts, and Manuele Santoprete. Relative equilibria in the four-vortex problem with two pairs of equal vorticities. *Journal of Nonlinear Science*, 24(1):39–92, 2014.

[21] Kenneth R. Meyer and Glen R. Hall. *Introduction to Hamiltonian Dynamical Systems and the N-Body Problem*. Springer-Verlag, New York, 1992.

[22] Richard Moeckel. Celestial Mechanics (Especially Central Configurations). ICTP Lecture Notes, 1994.

[23] Paul K Newton. *The N-vortex problem: analytical techniques*, volume 145. Springer, 2001.

[24] Hassan Aref. Point vortex dynamics: A classical mathematics playground. *Journal of mathematical Physics*, 48:065401, 2007.

[25] V. I. Arnold. *Mathematical Methods of Classical Mechanics*. Springer, New York, 1989.

[26] Vladimir I Arnold. Instability of dynamical systems with several degrees of freedom(instability of motions of dynamic system with five-dimensional phase space). *Soviet Mathematics*, 5:581–585, 1964.

[27] S. Smale. Topology and Mechanics. I. *Invent. Math.*, 10:305–331, 1970.

[28] Richard Moeckel. On central configurations. *Mathematische Zeitschrift*, 205(1):499–517, 1990.

[29] David Cox, John Little, Donal O'Shea, and Moss Sweedler. Ideals, varieties, and algorithms. *American Mathematical Monthly*, 101(6):582–586, 1994.

[30] Michel Coste. An introduction to semialgebraic geometry. In *in Geometry and Robotics, LNCS 391*. Citeseer, 1989.

[31] David A Cox, John B Little, and Donal O'shea. *Using algebraic geometry*. Springer, 1998.

Appendix A

A.1 Equations for degenerate critical points

$\frac{1}{\mu_2}\tilde{V}_{\theta_2} = [\mu_1 \sin\theta_2 - 2\mu_1 \cos\theta_2 \sin\theta_2 - \mu_1 \cos(\theta_2 - \theta_3)\sin\theta_2 + 2\mu_1 \cos\theta_2 \cos(\theta_2 - \theta_3)\sin\theta_2 + \mu_3 \sin(\theta_2 - \theta_3) - \mu_3 \cos\theta_2 \sin(\theta_2 - \theta_3) - 2\mu_3 \cos(\theta_2 - \theta_3)\sin(\theta_2 - \theta_3) + 2\mu_3 \cos\theta_2 \cos(\theta_2 - \theta_3)\sin(\theta_2 - \theta_3)]/[2(-1 + \cos\theta_2)(-1 + \cos(\theta_2 - \theta_3))]$

$\frac{1}{\mu_3}\tilde{V}_{\theta_3} = [-\mu_2 \sin(\theta_2 - \theta_3) + 2\mu_2 \cos(\theta_2 - \theta_3)\sin(\theta_2 - \theta_3) + \mu_2 \cos(\theta_3)\sin(\theta_2 - \theta_3) - 2\mu_2 \cos(\theta_2 - \theta_3)\cos(\theta_3)\sin(\theta_2 - \theta_3) + \mu_1 \sin(\theta_3) - \mu_1 \cos(\theta_2 - \theta_3)\sin(\theta_3) - 2\mu_1 \cos(\theta_3)\sin(\theta_3) + 2\mu_1 \cos(\theta_2 - \theta_3)\cos(\theta_3)\sin(\theta_3)]/[2(-1+\cos(\theta_2-\theta_3))(-1+\cos\theta_3)]$

$\frac{1}{\mu_1\mu_2\mu_3}\det(\tilde{V}_{\theta\theta}) = [\mu_2 \cos(\theta_2)\cos(\theta_2 - \theta_3) - 3\mu_2 \cos(\theta_2)^2 \cos(\theta_2 - \theta_3) + 2\mu_2 \cos(\theta_2)^3 \cos(\theta_2 - \theta_3) - 3\mu_2 \cos(\theta_2)\cos(\theta_2 - \theta_3)^2 + 9\mu_2 \cos(\theta_2)^2 \cos(\theta_2 - \theta_3)^2 - 6\mu_2 \cos(\theta_2)^3 \cos(\theta_2 - \theta_3)^2 + 2\mu_2 \cos(\theta_2)\cos(\theta_2 - \theta_3)^3 - 6\mu_2 \cos(\theta_2)^2 \cos(\theta_2 - \theta_3)^3 + 4\mu_2 \cos(\theta_2)^3 \cos(\theta_2 - \theta_3)^3 + \mu_1 \cos(\theta_2)\cos(\theta_3) - 3\mu_1 \cos(\theta_2)^2 \cos(\theta_3) + 2\mu_1 \cos(\theta_2)^3 \cos(\theta_3) + \mu_3 \cos(\theta_2 - \theta_3)\cos(\theta_3) - 2\mu_1 \cos(\theta_2)\cos(\theta_2 - \theta_3)\cos(\theta_3) - 2\mu_2 \cos(\theta_2)\cos(\theta_2-\theta_3)\cos(\theta_3) - 2\mu_3 \cos(\theta_2)\cos(\theta_2-\theta_3)\cos(\theta_3) + 6\mu_1 \cos(\theta_2)^2 \cos(\theta_2-\theta_3)\cos(\theta_3) + 6\mu_2 \cos(\theta_2)^2 \cos(\theta_2 - \theta_3)\cos(\theta_3) + \mu_3 \cos(\theta_2)^2 \cos(\theta_2 - \theta_3)\cos(\theta_3) - 4\mu_1 \cos(\theta_2)^3 \cos(\theta_2 - \theta_3)\cos(\theta_3) - 4\mu_2 \cos(\theta_2)^3 \cos(\theta_2 - \theta_3)\cos(\theta_3) - 3\mu_3 \cos(\theta_2 - \theta_3)^2 \cos(\theta_3) + \mu_1 \cos(\theta_2)\cos(\theta_2 - \theta_3)^2 \cos(\theta_3) + 6\mu_2 \cos(\theta_2)\cos(\theta_2 - \theta_3)^2 \cos(\theta_3) + 6\mu_3 \cos(\theta_2)\cos(\theta_2 - \theta_3)^2 \cos(\theta_3) - 3\mu_1 \cos(\theta_2)^2 \cos(\theta_2 - \theta_3)^2 \cos(\theta_3) - 18\mu_2 \cos(\theta_2)^2 \cos(\theta_2 - \theta_3)^2 \cos(\theta_3) - 3\mu_3 \cos(\theta_2)^2 \cos(\theta_2 - \theta_3)^2 \cos(\theta_3) +$

$$2\mu_1\cos(\theta_2)^3\cos(\theta_2-\theta_3)^2\cos(\theta_3)+12\mu_2\cos(\theta_2)^3\cos(\theta_2-\theta_3)^2\cos(\theta_3)+2\mu_3\cos(\theta_2-\theta_3)^3\cos(\theta_3)-4\mu_2\cos(\theta_2)\cos(\theta_2-\theta_3)^3\cos(\theta_3)-4\mu_3\cos(\theta_2)\cos(\theta_2-\theta_3)^3\cos(\theta_3)+12\mu_2\cos(\theta_2)^2\cos(\theta_2-\theta_3)^3\cos(\theta_3)+2\mu_3\cos(\theta_2)^2\cos(\theta_2-\theta_3)^3\cos(\theta_3)-8\mu_2\cos(\theta_2)^3\cos(\theta_2-\theta_3)^3\cos(\theta_3)-3\mu_1\cos(\theta_2)\cos(\theta_3)^2+9\mu_1\cos(\theta_2)^2\cos(\theta_3)^2-6\mu_1\cos(\theta_2)^3\cos(\theta_3)^2-3\mu_3\cos(\theta_2-\theta_3)\cos(\theta_3)^2+6\mu_1\cos(\theta_2)\cos(\theta_2-\theta_3)\cos(\theta_3)^2+\mu_2\cos(\theta_2)\cos(\theta_2-\theta_3)\cos(\theta_3)^2+6\mu_3\cos(\theta_2)\cos(\theta_2-\theta_3)\cos(\theta_3)^2-18\mu_1\cos(\theta_2)^2\cos(\theta_2-\theta_3)\cos(\theta_3)^2-3\mu_2\cos(\theta_2)^2\cos(\theta_2-\theta_3)\cos(\theta_3)^2-3\mu_3\cos(\theta_2)^2\cos(\theta_2-\theta_3)\cos(\theta_3)^2+12\mu_1\cos(\theta_2)^3\cos(\theta_2-\theta_3)\cos(\theta_3)^2+2\mu_2\cos(\theta_2)^3\cos(\theta_2-\theta_3)\cos(\theta_3)^2+9\mu_3\cos(\theta_2-\theta_3)^2\cos(\theta_3)^2-3\mu_1\cos(\theta_2)\cos(\theta_2-\theta_3)^2\cos(\theta_3)^2-3\mu_2\cos(\theta_2)\cos(\theta_2-\theta_3)^2\cos(\theta_3)^2-18\mu_3\cos(\theta_2)\cos(\theta_2-\theta_3)^2\cos(\theta_3)^2+9\mu_1\cos(\theta_2)^2\cos(\theta_2-\theta_3)^2\cos(\theta_3)^2+9\mu_2\cos(\theta_2)^2\cos(\theta_2-\theta_3)^2\cos(\theta_3)^2+9\mu_3\cos(\theta_2)^2\cos(\theta_2-\theta_3)^2\cos(\theta_3)^2-6\mu_1\cos(\theta_2)^3\cos(\theta_2-\theta_3)^2\cos(\theta_3)^2-6\mu_2\cos(\theta_2)^3\cos(\theta_2-\theta_3)^2\cos(\theta_3)^2-6\mu_3\cos(\theta_2-\theta_3)^3\cos(\theta_3)^2+2\mu_2\cos(\theta_2)\cos(\theta_2-\theta_3)^3\cos(\theta_3)^2+12\mu_3\cos(\theta_2)\cos(\theta_2-\theta_3)^3\cos(\theta_3)^2-6\mu_2\cos(\theta_2)^2\cos(\theta_2-\theta_3)^3\cos(\theta_3)^2-6\mu_3\cos(\theta_2)^2\cos(\theta_2-\theta_3)^3\cos(\theta_3)^2+4\mu_2\cos(\theta_2)^3\cos(\theta_2-\theta_3)^3\cos(\theta_3)^2+2\mu_1\cos(\theta_2)\cos(\theta_3)^3-6\mu_1\cos(\theta_2)^2\cos(\theta_3)^3+4\mu_1\cos(\theta_2)^3\cos(\theta_3)^3+2\mu_3\cos(\theta_2-\theta_3)\cos(\theta_3)^3-4\mu_1\cos(\theta_2)\cos(\theta_2-\theta_3)\cos(\theta_3)^3-4\mu_3\cos(\theta_2)\cos(\theta_2-\theta_3)\cos(\theta_3)^3+12\mu_1\cos(\theta_2)^2\cos(\theta_2-\theta_3)\cos(\theta_3)^3+2\mu_3\cos(\theta_2)^2\cos(\theta_2-\theta_3)\cos(\theta_3)^3-8\mu_1\cos(\theta_2)^3\cos(\theta_2-\theta_3)\cos(\theta_3)^3-6\mu_3\cos(\theta_2-\theta_3)^2\cos(\theta_3)^3+2\mu_1\cos(\theta_2)\cos(\theta_2-\theta_3)^2\cos(\theta_3)^3+12\mu_3\cos(\theta_2)\cos(\theta_2-\theta_3)^2\cos(\theta_3)^3-6\mu_1\cos(\theta_2)^2\cos(\theta_2-\theta_3)^2\cos(\theta_3)^3-6\mu_3\cos(\theta_2)^2\cos(\theta_2-\theta_3)^2\cos(\theta_3)^3+4\mu_1\cos(\theta_2)^3\cos(\theta_2-\theta_3)^2\cos(\theta_3)^3+4\mu_3\cos(\theta_2-\theta_3)^3\cos(\theta_3)^3-8\mu_3\cos(\theta_2)\cos(\theta_2-\theta_3)^3\cos(\theta_3)^3+4\mu_3\cos(\theta_2)^2\cos(\theta_2-\theta_3)^3\cos(\theta_3)^3+\mu_2\cos(\theta_2-\theta_3)\sin(\theta_2)^2-3\mu_2\cos(\theta_2-\theta_3)^2\sin(\theta_2)^2+2\mu_2\cos(\theta_2-\theta_3)^3\sin(\theta_2)^2+\mu_1\cos(\theta_3)\sin(\theta_2)^2-2\mu_1\cos(\theta_2-\theta_3)\cos(\theta_3)\sin(\theta_2)^2-2\mu_2\cos(\theta_2-\theta_3)\cos(\theta_3)\sin(\theta_2)^2+\mu_1\cos(\theta_2-\theta_3)^2\cos(\theta_3)\sin(\theta_2)^2+6\mu_2\cos(\theta_2-\theta_3)^2\cos(\theta_3)\sin(\theta_2)^2-4\mu_2\cos(\theta_2-\theta_3)^3\cos(\theta_3)\sin(\theta_2)^2-3\mu_1\cos(\theta_3)^2\sin(\theta_2)^2+6\mu_1\cos(\theta_2-\theta_3)\cos(\theta_3)^2\sin(\theta_2)^2+\mu_2\cos(\theta_2-\theta_3)\cos(\theta_3)^2\sin(\theta_2)^2-3\mu_1\cos(\theta_2-\theta_3)^2\cos(\theta_3)^2\sin(\theta_2)^2-3\mu_2\cos(\theta_2-\theta_3)^2\cos(\theta_3)^2\sin(\theta_2)^2+2\mu_2\cos(\theta_2-\theta_3)^3\cos(\theta_3)^2\sin(\theta_2)^2+2\mu_1\cos(\theta_3)^3\sin(\theta_2)^2-4\mu_1\cos(\theta_2-\theta_3)\cos(\theta_3)^3\sin(\theta_2)^2+2\mu_1\cos(\theta_2-\theta_3)^2\cos(\theta_3)^3\sin(\theta_2)^2+\mu_2\cos(\theta_2)\sin(\theta_2-\theta_3)^2-3\mu_2\cos(\theta_2)^2\sin(\theta_2-\theta_3)^2+2\mu_2\cos(\theta_2)^3\sin(\theta_2-\theta_3)^2+\mu_3\cos(\theta_3)\sin(\theta_2-\theta_3)^2-2\mu_2\cos(\theta_2)\cos(\theta_3)\sin(\theta_2-$$

$$\theta_3)^2 - 2\mu_3\cos(\theta_2)\cos(\theta_3)\sin(\theta_2 - \theta_3)^2 + 6\mu_2\cos(\theta_2)^2\cos(\theta_3)\sin(\theta_2 - \theta_3)^2 + \mu_3\cos(\theta_2)^2\cos(\theta_3)\sin(\theta_2 - \theta_3)^2 - 4\mu_2\cos(\theta_2)^3\cos(\theta_3)\sin(\theta_2 - \theta_3)^2 - 3\mu_3\cos(\theta_3)^2\sin(\theta_2 - \theta_3)^2 + \mu_2\cos(\theta_2)\cos(\theta_3)^2\sin(\theta_2 - \theta_3)^2 + 6\mu_3\cos(\theta_2)\cos(\theta_3)^2\sin(\theta_2 - \theta_3)^2 - 3\mu_2\cos(\theta_2)^2\cos(\theta_3)^2\sin(\theta_2 - \theta_3)^2 - 3\mu_3\cos(\theta_2)^2\cos(\theta_3)^2\sin(\theta_2 - \theta_3)^2 + 2\mu_2\cos(\theta_2)^3\cos(\theta_3)^2\sin(\theta_2 - \theta_3)^2 + 2\mu_3\cos(\theta_3)^3\sin(\theta_2 - \theta_3)^2 - 4\mu_3\cos(\theta_2)\cos(\theta_3)^3\sin(\theta_2 - \theta_3)^2 + 2\mu_3\cos(\theta_2)^2\cos(\theta_3)^3\sin(\theta_2 - \theta_3)^2 + \mu_2\sin(\theta_2)^2\sin(\theta_2 - \theta_3)^2 - 2\mu_2\cos(\theta_3)\sin(\theta_2)^2\sin(\theta_2 - \theta_3)^2 + \mu_2\cos(\theta_3)^2\sin(\theta_2)^2\sin(\theta_2 - \theta_3)^2 + \mu_1\cos(\theta_2)\sin(\theta_3)^2 - 3\mu_1\cos(\theta_2)^2\sin(\theta_3)^2 + 2\mu_1\cos(\theta_2)^3\sin(\theta_3)^2 + \mu_3\cos(\theta_2 - \theta_3)\sin(\theta_3)^2 - 2\mu_1\cos(\theta_2)\cos(\theta_2 - \theta_3)\sin(\theta_3)^2 - 2\mu_3\cos(\theta_2)\cos(\theta_2 - \theta_3)\sin(\theta_3)^2 + 6\mu_1\cos(\theta_2)^2\cos(\theta_2 - \theta_3)\sin(\theta_3)^2 + \mu_3\cos(\theta_2)^2\cos(\theta_2 - \theta_3)\sin(\theta_3)^2 - 4\mu_1\cos(\theta_2)^3\cos(\theta_2 - \theta_3)\sin(\theta_3)^2 - 3\mu_3\cos(\theta_2 - \theta_3)^2\sin(\theta_3)^2 + \mu_1\cos(\theta_2)\cos(\theta_2 - \theta_3)^2\sin(\theta_3)^2 + 6\mu_3\cos(\theta_2)\cos(\theta_2 - \theta_3)^2\sin(\theta_3)^2 - 3\mu_1\cos(\theta_2)^2\cos(\theta_2 - \theta_3)^2\sin(\theta_3)^2 - 3\mu_3\cos(\theta_2)^2\cos(\theta_2 - \theta_3)^2\sin(\theta_3)^2 + 2\mu_1\cos(\theta_2)^3\cos(\theta_2 - \theta_3)^2\sin(\theta_3)^2 + 2\mu_3\cos(\theta_2 - \theta_3)^3\sin(\theta_3)^2 - 4\mu_3\cos(\theta_2)\cos(\theta_2 - \theta_3)^3\sin(\theta_3)^2 + 2\mu_3\cos(\theta_2)^2\cos(\theta_2 - \theta_3)^3\sin(\theta_3)^2 + \mu_1\sin(\theta_2)^2\sin(\theta_3)^2 - 2\mu_1\cos(\theta_2 - \theta_3)\sin(\theta_2)^2\sin(\theta_3)^2 + \mu_1\cos(\theta_2 - \theta_3)^2\sin(\theta_2)^2\sin(\theta_3)^2 + \mu_3\sin(\theta_2 - \theta_3)^2\sin(\theta_3)^2 - 2\mu_3\cos(\theta_2)\sin(\theta_2 - \theta_3)^2\sin(\theta_3)^2 + \mu_3\cos(\theta_2)^2\sin(\theta_2 - \theta_3)^2\sin(\theta_3)^2]/[4(-1+\cos(\theta_2))^2(-1+\cos(\theta_2 - \theta_3))^2(-1+\cos(\theta_3))^2]$$

A.2 Polynomials p_1, q_1

$$\begin{aligned} p_1 =& 2\mu_1 s_2 - 4c_2\mu_1 s_2 + c_3\mu_1 s_2 - 2c_2c_3\mu_1 s_2 + 3c_2^2c_3\mu_1 s_2 + 2c_3\mu_3 s_2 - 2c_2c_3\mu_3 s_2 \\ &+ c_3^2\mu_3 s_2 - 4c_2c_3^2\mu_3 s_2 + 3c_2^2c_3^2\mu_3 s_2 - c_3\mu_1 s_2^3 - c_3^2\mu_3 s_2^3 - \mu_1 s_3 + c_2\mu_1 s_3 + c_2^2\mu_1 s_3 \\ &- c_2^3\mu_1 s_3 + \mu_3 s_3 - 2c_2\mu_3 s_3 + c_2^2\mu_3 s_3 - 2c_2c_3\mu_3 s_3 + 4c_2^2c_3\mu_3 s_3 - 2c_2^3c_3\mu_3 s_3 \\ &- \mu_1 s_2^2 s_3 + 3c_2\mu_1 s_2^2 s_3 - \mu_3 s_2^2 s_3 - 4c_3\mu_3 s_2^2 s_3 + 6c_2c_3\mu_3 s_2^2 s_3 - \mu_3 s_2 s_3^2 + 4c_2\mu_3 s_2 s_3^2 \\ &- 3c_2^2\mu_3 s_2 s_3^2 + \mu_3 s_2^3 s_3^2 \end{aligned}$$

$$
\begin{aligned}
q_1 = &-\mu_1 s_2 + c_3\mu_1 s_2 + c_3^2\mu_1 s_2 - c_3^3\mu_1 s_2 + \mu_2 s_2 - 2c_3\mu_2 s_2 - 2c_2c_3\mu_2 s_2 + c_3^2\mu_2 s_2 \\
&+ 4c_2c_3^2\mu_2 s_2 - 2c_2c_3^3\mu_2 s_2 + 2\mu_1 s_3 + c_2\mu_1 s_3 - 4c_3\mu_1 s_3 - 2c_2c_3\mu_1 s_3 \\
&+ 3c_2c_3^2\mu_1 s_3 + 2c_2\mu_2 s_3 + c_2^2\mu_2 s_3 - 2c_2c_3\mu_2 s_3 - 4c_2^2c_3\mu_2 s_3 + 3c_2^2c_3^2\mu_2 s_3 \\
&- \mu_2 s_2^2 s_3 + 4c_3\mu_2 s_2^2 s_3 - 3c_3^2\mu_2 s_2^2 s_3 - \mu_1 s_2 s_3^2 + 3c_3\mu_1 s_2 s_3^2 - \mu_2 s_2 s_3^2 - 4c_2\mu_2 s_2 s_3^2 \\
&+ 6c_2c_3\mu_2 s_2 s_3^2 - c_2\mu_1 s_3^3 - c_2^2\mu_2 s_3^3 + \mu_2 s_2^2 s_3^3
\end{aligned}
$$

A.3 Polynomials p_3, q_3, h_3 used to calculate Groebner Basis

$$
\begin{aligned}
p_3 = {} & \mu_3 + 3\mu_1 t_2^2 - 3\mu_3 t_2^2 - \mu_1 t_2^4 - 3\mu_1 t_2 t_3 + 9\mu_3 t_2 t_3 + \mu_1 t_2^3 t_3 - 3\mu_3 t_2^3 t_3 - 3\mu_3 t_3^2 + 3\mu_1 t_2^2 t_3^2 + \\
& 9\mu_3 t_2^2 t_3^2 - \mu_1 t_2^4 t_3^2 - 3\mu_1 t_2 t_3^3 - 3\mu_3 t_2 t_3^3 + \mu_1 t_2^3 t_3^3 + \mu_3 t_2^3 t_3^3
\end{aligned}
$$

$$
\begin{aligned}
q_3 = {} & -\mu_2 + 3\mu_2 t_2^2 + 3\mu_1 t_2 t_3 - 9\mu_2 t_2 t_3 + 3\mu_1 t_2^3 t_3 + 3\mu_2 t_2^3 t_3 - 3\mu_1 t_3^2 + 3\mu_2 t_3^2 - 3\mu_1 t_2^2 t_3^2 - \\
& 9\mu_2 t_2^2 t_3^2 - \mu_1 t_2 t_3^3 + 3\mu_2 t_2 t_3^3 - \mu_1 t_2^3 t_3^3 - \mu_2 t_2^3 t_3^3 + \mu_1 t_3^4 + \mu_1 t_2^2 t_3^4
\end{aligned}
$$

$$
\begin{aligned}
h_3 = {} & -3\mu_2 - 3\mu_3 + 9\mu_1 t_2^2 - 12\mu_2 t_2^2 - 21\mu_3 t_2^2 - 9\mu_1 t_2^4 + 46\mu_2 t_2^4 - 9\mu_3 t_2^4 - 21\mu_1 t_2^6 - 12\mu_2 t_2^6 + \\
& 9\mu_3 t_2^6 - 3\mu_1 t_2^8 - 3\mu_2 t_2^8 - 18\mu_1 t_2 t_3 + 24\mu_2 t_2 t_3 + 24\mu_3 t_2 t_3 + 18\mu_1 t_2^3 t_3 - 120\mu_2 t_2^3 t_3 - 48\mu_3 t_2^3 t_3 + \\
& 42\mu_1 t_2^5 t_3 + 136\mu_2 t_2^5 t_3 - 72\mu_3 t_2^5 t_3 + 6\mu_1 t_2^7 t_3 + 24\mu_2 t_2^7 t_3 + 9\mu_1 t_3^2 - 21\mu_2 t_3^2 - 12\mu_3 t_3^2 - 18\mu_1 t_2^2 t_3^2 + \\
& 132\mu_2 t_2^2 t_3^2 + 132\mu_3 t_2^2 t_3^2 - 12\mu_1 t_2^4 t_3^2 - 182\mu_2 t_2^4 t_3^2 + 108\mu_3 t_2^4 t_3^2 + 18\mu_1 t_2^6 t_3^2 - 12\mu_2 t_2^6 t_3^2 - 36\mu_3 t_2^6 t_3^2 + \\
& 3\mu_1 t_2^8 t_3^2 + 3\mu_2 t_2^8 t_3^2 + 18\mu_1 t_2 t_3^3 - 48\mu_2 t_2 t_3^3 - 120\mu_3 t_2 t_3^3 - 18\mu_1 t_2^3 t_3^3 + 48\mu_2 t_2^3 t_3^3 + 48\mu_3 t_2^3 t_3^3 - \\
& 42\mu_1 t_2^5 t_3^3 + 112\mu_2 t_2^5 t_3^3 + 168\mu_3 t_2^5 t_3^3 - 6\mu_1 t_2^7 t_3^3 + 16\mu_2 t_2^7 t_3^3 - 9\mu_1 t_3^4 - 9\mu_2 t_3^4 + 46\mu_3 t_3^4 - 12\mu_1 t_2^2 t_3^4 + \\
& 108\mu_2 t_2^2 t_3^4 - 182\mu_3 t_2^2 t_3^4 + 42\mu_1 t_2^4 t_3^4 - 198\mu_2 t_2^4 t_3^4 - 198\mu_3 t_2^4 t_3^4 + 52\mu_1 t_2^6 t_3^4 + 12\mu_2 t_2^6 t_3^4 + 30\mu_3 t_2^6 t_3^4 + \\
& 7\mu_1 t_2^8 t_3^4 + 7\mu_2 t_2^8 t_3^4 + 42\mu_1 t_2 t_3^5 - 72\mu_2 t_2 t_3^5 + 136\mu_3 t_2 t_3^5 - 42\mu_1 t_2^3 t_3^5 + 168\mu_2 t_2^3 t_3^5 + 112\mu_3 t_2^3 t_3^5 - \\
& 98\mu_1 t_2^5 t_3^5 - 24\mu_2 t_2^5 t_3^5 - 24\mu_3 t_2^5 t_3^5 - 14\mu_1 t_2^7 t_3^5 - 8\mu_2 t_2^7 t_3^5 - 21\mu_1 t_3^6 + 9\mu_2 t_3^6 - 12\mu_3 t_3^6 + 18\mu_1 t_2^2 t_3^6 - \\
& 36\mu_2 t_2^2 t_3^6 - 12\mu_3 t_2^2 t_3^6 + 52\mu_1 t_2^4 t_3^6 + 30\mu_2 t_2^4 t_3^6 + 12\mu_3 t_2^4 t_3^6 + 14\mu_1 t_2^6 t_3^6 + 12\mu_2 t_2^6 t_3^6 + 12\mu_3 t_2^6 t_3^6 + \\
& \mu_1 t_2^8 t_3^6 + \mu_2 t_2^8 t_3^6 + 6\mu_1 t_2 t_3^7 + 24\mu_3 t_2 t_3^7 - 6\mu_1 t_2^3 t_3^7 + 16\mu_3 t_2^3 t_3^7 - 14\mu_1 t_2^5 t_3^7 - 8\mu_3 t_2^5 t_3^7 - 2\mu_1 t_2^7 t_3^7 - \\
& 3\mu_1 t_3^8 - 3\mu_3 t_3^8 + 3\mu_1 t_2^2 t_3^8 + 3\mu_3 t_2^2 t_3^8 + 7\mu_1 t_2^4 t_3^8 + 7\mu_3 t_2^4 t_3^8 + \mu_1 t_2^6 t_3^8 + \mu_3 t_2^6 t_3^8
\end{aligned}
$$

A.4 Groebner Basis

$$f(\mu_1,\mu_2,\mu_3) = 4251528\mu_1^{15}\mu_2^3 + 531441\mu_1^{14}\mu_2^4 + 5275044\mu_1^{13}\mu_2^5 - 13094298\mu_1^{12}\mu_2^6 + 4212162\mu_1^{11}\mu_2^7 - 10018647\mu_1^{10}\mu_2^8 + 17685540\mu_1^9\mu_2^9 - 10018647\mu_1^8\mu_2^{10} + 4212162\mu_1^7\mu_2^{11} - 13094298\mu_1^6\mu_2^{12} + 5275044\mu_1^5\mu_2^{13} + 531441\mu_1^4\mu_2^{14} + 4251528\mu_1^3\mu_2^{15} + 12754584\mu_1^{15}\mu_2^2\mu_3 - 50624676\mu_1^{13}\mu_2^4\mu_3 - 97080930\mu_1^{12}\mu_2^5\mu_3 - 131082948\mu_1^{11}\mu_2^6\mu_3 - 65994912\mu_1^{10}\mu_2^7\mu_3 - 40565934\mu_1^9\mu_2^8\mu_3 - 40565934\mu_1^8\mu_2^9\mu_3 - 65994912\mu_1^7\mu_2^{10}\mu_3 - 131082948\mu_1^6\mu_2^{11}\mu_3 - 97080930\mu_1^5\mu_2^{12}\mu_3 - 50624676\mu_1^4\mu_2^{13}\mu_3 + 12754584\mu_1^2\mu_2^{15}\mu_3 + 12754584\mu_1^{15}\mu_2\mu_3^2 - 1062882\mu_1^{14}\mu_2^2\mu_3^2 - 172580544\mu_1^{13}\mu_2^3\mu_3^2 - 231581430\mu_1^{12}\mu_2^4\mu_3^2 - 214751736\mu_1^{11}\mu_2^5\mu_3^2 + 19240011\mu_1^{10}\mu_2^6\mu_3^2 + 236748096\mu_1^9\mu_2^7\mu_3^2 + 348690906\mu_1^8\mu_2^8\mu_3^2 + 236748096\mu_1^7\mu_2^9\mu_3^2 + 19240011\mu_1^6\mu_2^{10}\mu_3^2 - 214751736\mu_1^5\mu_2^{11}\mu_3^2 - 231581430\mu_1^4\mu_2^{12}\mu_3^2 - 172580544\mu_1^3\mu_2^{13}\mu_3^2 - 1062882\mu_1^2\mu_2^{14}\mu_3^2 + 12754584\mu_1\mu_2^{15}\mu_3^2 + 4251528\mu_1^{15}\mu_3^3 - 172580544\mu_1^{13}\mu_2^2\mu_3^3 - 296449308\mu_1^{12}\mu_2^3\mu_3^3 - 46485414\mu_1^{11}\mu_2^4\mu_3^3 + 253964160\mu_1^{10}\mu_2^5\mu_3^3 + 667359540\mu_1^9\mu_2^6\mu_3^3 + 816231654\mu_1^8\mu_2^7\mu_3^3 + 816231654\mu_1^7\mu_2^8\mu_3^3 + 667359540\mu_1^6\mu_2^9\mu_3^3 + 253964160\mu_1^5\mu_2^{10}\mu_3^3 - 46485414\mu_1^4\mu_2^{11}\mu_3^3 - 296449308\mu_1^3\mu_2^{12}\mu_3^3 - 172580544\mu_1^2\mu_2^{13}\mu_3^3 + 4251528\mu_2^{15}\mu_3^3 + 531441\mu_1^{14}\mu_3^4 - 50624676\mu_1^{13}\mu_2\mu_3^4 - 231581430\mu_1^{12}\mu_2^2\mu_3^4 - 46485414\mu_1^{11}\mu_2^3\mu_3^4 + 376811352\mu_1^{10}\mu_2^4\mu_3^4 + 808252182\mu_1^9\mu_2^5\mu_3^4 + 545541021\mu_1^8\mu_2^6\mu_3^4 + 208376712\mu_1^7\mu_2^7\mu_3^4 + 545541021\mu_1^6\mu_2^8\mu_3^4 + 808252182\mu_1^5\mu_2^9\mu_3^4 + 376811352\mu_1^4\mu_2^{10}\mu_3^4 - 46485414\mu_1^3\mu_2^{11}\mu_3^4 - 231581430\mu_1^2\mu_2^{12}\mu_3^4 - 50624676\mu_1\mu_2^{13}\mu_3^4 + 531441\mu_2^{14}\mu_3^4 + 5275044\mu_1^{13}\mu_3^5 - 97080930\mu_1^{12}\mu_2\mu_3^5 - 214751736\mu_1^{11}\mu_2^2\mu_3^5 + 253964160\mu_1^{10}\mu_2^3\mu_3^5 + 808252182\mu_1^9\mu_2^4\mu_3^5 + 121574736\mu_1^8\mu_2^5\mu_3^5 - 2031990768\mu_1^7\mu_2^6\mu_3^5 - 2031990768\mu_1^6\mu_2^7\mu_3^5 + 121574736\mu_1^5\mu_2^8\mu_3^5 + 808252182\mu_1^4\mu_2^9\mu_3^5 + 253964160\mu_1^3\mu_2^{10}\mu_3^5 - 214751736\mu_1^2\mu_2^{11}\mu_3^5 - 97080930\mu_1\mu_2^{12}\mu_3^5 + 5275044\mu_2^{13}\mu_3^5 - 13094298\mu_1^{12}\mu_3^6 - 131082948\mu_1^{11}\mu_2\mu_3^6 + 19240011\mu_1^{10}\mu_2^2\mu_3^6 + 667359540\mu_1^9\mu_2^3\mu_3^6 + 545541021\mu_1^8\mu_2^4\mu_3^6 - 2031990768\mu_1^7\mu_2^5\mu_3^6 - 3904381852\mu_1^6\mu_2^6\mu_3^6 - 2031990768\mu_1^5\mu_2^7\mu_3^6 + 545541021\mu_1^4\mu_2^8\mu_3^6 + 667359540\mu_1^3\mu_2^9\mu_3^6 + 19240011\mu_1^2\mu_2^{10}\mu_3^6 - 131082948\mu_1\mu_2^{11}\mu_3^6 - 13094298\mu_2^{12}\mu_3^6 + 4212162\mu_1^{11}\mu_3^7 - 65994912\mu_1^{10}\mu_2\mu_3^7 + 236748096\mu_1^9\mu_2^2\mu_3^7 + 816231654\mu_1^8\mu_2^3\mu_3^7 + 208376712\mu_1^7\mu_2^4\mu_3^7 - 2031990768\mu_1^6\mu_2^5\mu_3^7 - 2031990768\mu_1^5\mu_2^6\mu_3^7 + 208376712\mu_1^4\mu_2^7\mu_3^7 + 816231654\mu_1^3\mu_2^8\mu_3^7 + 236748096\mu_1^2\mu_2^9\mu_3^7 - 65994912\mu_1\mu_2^{10}\mu_3^7 + 4212162\mu_2^{11}\mu_3^7 - 10018647\mu_1^{10}\mu_3^8 - 40565934\mu_1^9\mu_2\mu_3^8 + 348690906\mu_1^8\mu_2^2\mu_3^8 + 816231654\mu_1^7\mu_2^3\mu_3^8 + 545541021\mu_1^6\mu_2^4\mu_3^8 + 121574736\mu_1^5\mu_2^5\mu_3^8 + 545541021\mu_1^4\mu_2^6\mu_3^8 + 816231654\mu_1^3\mu_2^7\mu_3^8 + 348690906\mu_1^2\mu_2^8\mu_3^8 - 40565934\mu_1\mu_2^9\mu_3^8 -$$

$$10018647\mu_2^{10}\mu_3^8 + 17685540\mu_1^9\mu_3^9 - 40565934\mu_1^8\mu_2\mu_3^9 + 236748096\mu_1^7\mu_2^2\mu_3^9 + 667359540\mu_1^6\mu_2^3\mu_3^9 + 808252182\mu_1^5\mu_2^4\mu_3^9 + 808252182\mu_1^4\mu_2^5\mu_3^9 + 667359540\mu_1^3\mu_2^6\mu_3^9 + 236748096\mu_1^2\mu_2^7\mu_3^9 - 40565934\mu_1\mu_2^8\mu_3^9 + 17685540\mu_2^9\mu_3^9 - 10018647\mu_1^8\mu_3^{10} - 65994912\mu_1^7\mu_2\mu_3^{10} + 19240011\mu_1^6\mu_2^2\mu_3^{10} + 253964160\mu_1^5\mu_2^3\mu_3^{10} + 376811352\mu_1^4\mu_2^4\mu_3^{10} + 253964160\mu_1^3\mu_2^5\mu_3^{10} + 19240011\mu_1^2\mu_2^6\mu_3^{10} - 65994912\mu_1\mu_2^7\mu_3^{10} - 10018647\mu_2^8\mu_3^{10} + 4212162\mu_1^7\mu_3^{11} - 131082948\mu_1^6\mu_2\mu_3^{11} - 214751736\mu_1^5\mu_2^2\mu_3^{11} - 46485414\mu_1^4\mu_2^3\mu_3^{11} - 46485414\mu_1^3\mu_2^4\mu_3^{11} - 214751736\mu_1^2\mu_2^5\mu_3^{11} - 131082948\mu_1\mu_2^6\mu_3^{11} + 4212162\mu_2^7\mu_3^{11} - 13094298\mu_1^6\mu_3^{12} - 97080930\mu_1^5\mu_2\mu_3^{12} - 231581430\mu_1^4\mu_2^2\mu_3^{12} - 296449308\mu_1^3\mu_2^3\mu_3^{12} - 231581430\mu_1^2\mu_2^4\mu_3^{12} - 97080930\mu_1\mu_2^5\mu_3^{12} - 13094298\mu_2^6\mu_3^{12} + 5275044\mu_1^5\mu_3^{13} - 50624676\mu_1^4\mu_2\mu_3^{13} - 172580544\mu_1^3\mu_2^2\mu_3^{13} - 172580544\mu_1^2\mu_2^3\mu_3^{13} - 50624676\mu_1\mu_2^4\mu_3^{13} + 5275044\mu_2^5\mu_3^{13} + 531441\mu_1^4\mu_3^{14} - 1062882\mu_1^2\mu_2^2\mu_3^{14} + 531441\mu_2^4\mu_3^{14} + 4251528\mu_1^3\mu_3^{15} + 12754584\mu_1^2\mu_2\mu_3^{15} + 12754584\mu_1\mu_2^2\mu_3^{15} + 4251528\mu_2^3\mu_3^{15}$$

Appendix B

Mathematica Code

B.1 Mathematica Code for Sturm Algorithm

```
(* Construct a Sturm sequence from a given polynomial P in the \
variable x. *)

SturmSequence[P_, x_] :=
 Module[{f = P, g = D[P, x] // Simplify, h, ss},
  ss = {f, g};
  While[Exponent[g, x] > 0,
    h = -PolynomialRemainder[f, g, x];
    ss = ss~Join~{h};
    f = g; g = h;
    ];
  Return[ss];
  ]

(* Count the sign changes in a Sturm sequence evaluated at x = a *)

LeadingCoefficient[P_, x_, sign_: 1] :=
 Module[{ex = Exponent[P, x], lc},
  If[ex == 0, P, (sign)^ex*Coefficient[P, x^ex]]]
```

```
SignChanges[ss_, x_, a_] := Module[{ss1 , changes = 0},
  If[a == Infinity, ss1 = Map[LeadingCoefficient[#, x, 1] &, ss],
   If[a == -Infinity, ss1 = Map[LeadingCoefficient[#, x, -1] &, ss],
    ss1 = (ss /. x -> a)]];
  ss1 = Select[ss1, (# != 0) &];
  For[i = 1, i < Length[ss1], i++,
   If[ss1[[i]]*ss1[[i + 1]] < 0, changes++]];
  Return[changes];
  ]
```

B.2 Mathematica Code for Hermite Algorithm

```
GetExponents[mon_, vars_] := Map[Exponent[mon, #] &, vars]
GetAllExponents[poly_, vars_] := With[{poly1 = Expand[poly]},
  Table[GetExponents[poly[[i]], vars], {i, 1, Length[poly]}] // Union]

LeadingDegRevLexExponent[explist_] := Module[{maxdegree, l},
  deg[v_] := v[[1]] + v[[2]];
  maxdegree = Max[Map[deg, explist]];
  l = Select[explist, (deg[#] == maxdegree) &];
  Sort[l, (#1[[2]] < #2[[2]]) &][[1]]]

MakeCone[{a_, b_}, cmax_, dmax_] :=
 Flatten[Table[{c, d}, {c, a, cmax}, {d, b, dmax}], 1]

MonomialBasis[lexps_, cmax_, dmax_] := Module[{l, i},
  l = MakeCone[{0, 0}, cmax, dmax];
  For[i = 1, i <= Length[lexps], i++,
   l = Complement[l, MakeCone[lexps[[i]], cmax, dmax]];];
  l]
```

```
GetCoefficient[p_, {a_, b_}] := Module[{q},
  q = Expand[p];
  If[{a, b} == {0, 0}, q /. {r1 -> 0, r2 -> 0},
   If[a == 0, Coefficient[q, r2^b] /. {r1 -> 0},
    If[b == 0, Coefficient[q, r1^a] /. {r2 -> 0},
     Coefficient[q, r1^a*r2^b]]]]
  ]



PolyReduceVector[p_, gb_, mb_] := Module[{r},
  r =  PolynomialReduce[p, gb, {r1, r2},
     MonomialOrder -> DegreeReverseLexicographic][[2]];
  Map[GetCoefficient[r, #] &, mb]]

PolyReduceCoefficient[p_, gb_, {a_, b_}] := Module[{r},
  r =  PolynomialReduce[p, gb, {r1, r2},
     MonomialOrder -> DegreeReverseLexicographic][[2]];
  GetCoefficient[r, {a, b}]]

MultMapTrace[f_, gb_, mb_] :=
 Plus @@ Table[
   PolyReduceCoefficient[f*r1^mb[[i, 1]]*r2^mb[[i, 2]], gb,
    mb[[i]]], {i, 1, Length[mb]}]

HermiteForm[q_, gb_, mb_] := Module[{H, i, j, mon},
  H = Table[0, {i, 1, Length[mb]}, {j, 1, Length[mb]}];
  For[i = 1, i <= Length[mb], i++,
   H[[i, i]] =
    MultMapTrace[q*r1^(2 mb[[i, 1]])*r2^(2*mb[[i, 2]]), gb, mb];
   (*Print[{i,i},H[[i,i]]];*)
   For[j = i + 1, j <= Length[mb], j++,
    mon =
```

```
     q*r1^(mb[[i, 1]] + mb[[j, 1]])*r2^(mb[[i, 2]] + mb[[j, 2]]);
    H[[i, j]] = MultMapTrace[mon, gb, mb];
    H[[j, i]] = H[[i, j]];
    (*Print[{i,j},{j,i},H[[i,j]]];*)];];
  H]

ClearCol[A_, i_] := Module[{B = A, d, ri, j},
  ri =  A[[i]];
  d = ri[[i]];
  For[j = i + 1, j <= Length[A], j++,
   B[[j]] = B[[j]] - B[[j, i]]*ri/d;];
  B]

ClearRow[A_, i_] := Transpose[ClearCol[Transpose[A], i]]
ClearCR[A_, i_] := ClearRow[ClearCol[A, i], i]

SwapRow[A_, i_, j_] := Module[{B = A},
  B[[i]] = A[[j]];
  B[[j]] = A[[i]];
  B]

SwapCol[A_, i_, j_] := Transpose[SwapRow[Transpose[A], i, j]]
SwapCR[A_, i_, j_] := SwapRow[SwapCol[A, i, j], i, j]

RowSumDiff[A_, i_, j_] := Module[{B = A, v, w},
  v = A[[i]] + A[[j]];
  w = -A[[i]] + A[[j]];
  B[[i]] = v;
  B[[j]] = w;
  B]
Clear[ColSumDiff]
ColSumDiff[A_, i_, j_] := Transpose[RowSumDiff[Transpose[A], i, j]]
```

```
SumDiffCR[A_, i_, j_] := RowSumDiff[ColSumDiff[A, i, j], i, j]

SymmetricReduce[A_] := Module[{B = A, n = Length[A], i, j, k},
  For[i = 1, i <= n, i++,
   (* if pivot is 0 look for a nonzero diagonal and switch*)

   If[B[[i, i]] == 0, For[j = i + 1, j <= n, j++,
      If[B[[j, j]] != 0, B = SwapCR[B, i, j]; Break[];]; ];];
   (* if pivot is still 0 do a row/col sum/diff *)

   If[B[[i, i]] == 0, For[j = i + 1, j <= n, j++,
      If[B[[i, j]] != 0, B = SumDiffCR[B, i, j]; Break[];];];];
   If[B[[i, i]] != 0, B = ClearCR[B, i];];
   ];
  B]

Sig[A_] := Module[{A1, i, diagsigns, p, n},
  A1 = SymmetricReduce[A];
  diagsigns = Table[Sign[A1[[i, i]]], {i, 1, Length[A1]}];
  Plus @@ diagsigns]
```

Appendix C

Stability Conditions

C.1 Polynomials for Stability Conditions in t_i only

b/a condition $= -(1+t_1^2)(t_1-t_2)^2(1+t_2^2)(t_1-t_3)^2(t_2-t_3)^2(1+t_3^2)(3+18t_1^2-9t_1^4-12t_1t_2+36t_1^3t_2+18t_2^2-24t_1^2t_2^2+22t_1^4t_2^2+36t_1t_2^3-44t_1^3t_2^3-9t_2^4+22t_1^2t_2^4-9t_1^4t_2^4-12t_1t_3+36t_1^3t_3-12t_2t_3-24t_1^2t_2t_3-44t_1^4t_2t_3-24t_1t_2^2t_3+104t_1^3t_2^2t_3+36t_2^3t_3+104t_1^2t_2^3t_3+36t_1^4t_2^3t_3-44t_1t_2^4t_3+36t_1^3t_2^4t_3+18t_3^2-24t_1^2t_3^2+22t_1^4t_3^2-24t_1t_2t_3^2+104t_1^3t_2t_3^2-24t_2^2t_3^2-432t_1^2t_2^2t_3^2-24t_1^4t_2^2t_3^2+104t_1t_2^3t_3^2-24t_1^3t_2^3t_3^2+22t_2^4t_3^2-24t_1^2t_2^4t_3^2+18t_1^4t_2^4t_3^2+36t_1t_3^3-44t_1^3t_3^3+36t_2t_3^3+104t_1^2t_2t_3^3+36t_1^4t_2t_3^3+104t_1t_2^2t_3^3-24t_1^3t_2^2t_3^3-44t_2^3t_3^3-24t_1^2t_2^3t_3^3-12t_1^4t_2^3t_3^3+36t_1t_2^4t_3^3-12t_1^3t_2^4t_3^3-9t_3^4+22t_1^2t_3^4-9t_1^4t_3^4-44t_1t_2t_3^4+36t_1^3t_2t_3^4+22t_2^2t_3^4-24t_1^2t_2^2t_3^4+18t_1^4t_2^2t_3^4+36t_1t_2^3t_3^4-12t_1^3t_2^3t_3^4-9t_2^4t_3^4+18t_1^2t_2^4t_3^4+3t_1^4t_2^4t_3^4)$

$$ac\,\text{condition} = 8192(1+t_1^2)(t_1-t_2)^8(1+t_2^2)(t_1-t_3)^8(t_2-t_3)^8(1+t_3^2)(t_1^2+t_1^4-t_1t_2-t_1^3t_2+t_2^2+3t_1^2t_2^2-6t_1^4t_2^2-t_1t_2^3+15t_1^3t_2^3+t_2^4-6t_1^2t_2^4+t_1^4t_2^4-t_1t_3-t_1^3t_3-t_2t_3-2t_1^2t_2t_3+15t_1^4t_2t_3-2t_1t_2^2t_3-18t_1^3t_2^2t_3-t_2^3t_3-18t_1^2t_2^3t_3-t_1^4t_2^3t_3+15t_1t_2^4t_3-t_1^3t_2^4t_3+t_3^2+3t_1^2t_3^2-6t_1^4t_3^2-2t_1t_2t_3^2-18t_1^3t_2t_3^2+3t_2^2t_3^2+54t_1^2t_2^2t_3^2+3t_1^4t_2^2t_3^2-18t_1t_2^3t_3^2-2t_1^3t_2^3t_3^2-6t_2^4t_3^2+3t_1^2t_2^4t_3^2+t_1^4t_2^4t_3^2-t_1t_3^3+15t_1^3t_3^3-t_2t_3^3-18t_1^2t_2t_3^3-t_1^4t_2t_3^3-18t_1t_2^2t_3^3-2t_1^3t_2^2t_3^3+15t_2^3t_3^3-2t_1^2t_2^3t_3^3-t_1^4t_2^3t_3^3-t_1t_2^4t_3^3-t_1^3t_2^4t_3^3+t_3^4-6t_1^2t_3^4+t_1^4t_3^4+15t_1t_2t_3^4-t_1^3t_2t_3^4-6t_2^2t_3^4+3t_1^2t_2^2t_3^4+t_1^4t_2^2t_3^4-t_1t_2^3t_3^4-t_1^3t_2^3t_3^4+t_2^4t_3^4+t_1^2t_2^4t_3^4)(13+27t_1^2-9t_1^4+9t_1^6+12t_1t_2+72t_1^3t_2-36t_1^5t_2+27t_2^2-15t_1^2t_2^2+153t_1^4t_2^2+3t_1^6t_2^2+72t_1t_2^3-176t_1^3t_2^3+72t_1^5t_2^3-9t_2^4+153t_1^2t_2^4-123t_1^4t_2^4+3t_1^6t_2^4-36t_1t_2^5+72t_1^3t_2^5+12t_1^5t_2^5+9t_2^6+3t_1^2t_2^6+3t_1^4t_2^6+9t_1^6t_2^6+12t_1t_3+72t_1^3t_3-36t_1^5t_3+12t_2t_3+36t_1^2t_2t_3+36t_1^4t_2t_3+12t_1^6t_2t_3+36t_1t_2^2t_3+216t_1^3t_2^2t_3-108t_1^5t_2^2t_3+72t_2^3t_3+216t_1^2t_2^3t_3+216t_1^4t_2^3t_3+72t_1^6t_2^3t_3+36t_1t_2^4t_3+216t_1^3t_2^4t_3-108t_1^5t_2^4t_3-36t_2^5t_3-108t_1^2t_2^5t_3-108t_1^4t_2^5t_3-36t_1^6t_2^5t_3+12t_1t_2^6t_3+72t_1^3t_2^6t_3-36t_1^5t_2^6t_3+27t_3^2-15t_1^2t_3^2+153t_1^4t_3^2+3t_1^6t_3^2+36t_1t_2t_3^2+216t_1^3t_2t_3^2-108t_1^5t_2t_3^2-15t_2^2t_3^2-513t_1^2t_2^2t_3^2+819t_1^4t_2^2t_3^2-123t_1^6t_2^2t_3^2+216t_1t_2^3t_3^2-528t_1^3t_2^3t_3^2+216t_1^5t_2^3t_3^2+153t_2^4t_3^2+819t_1^2t_2^4t_3^2+819t_1^4t_2^4t_3^2+153t_1^6t_2^4t_3^2-108t_1t_2^5t_3^2+216t_1^3t_2^5t_3^2+36t_1^5t_2^5t_3^2+3t_2^6t_3^2-123t_1^2t_2^6t_3^2+153t_1^4t_2^6t_3^2-9t_1^6t_2^6t_3^2+72t_1t_3^3-176t_1^3t_3^3+72t_1^5t_3^3+72t_2t_3^3+216t_1^2t_2t_3^3+216t_1^4t_2t_3^3+72t_1^6t_2t_3^3+216t_1t_2^2t_3^3-528t_1^3t_2^2t_3^3+216t_1^5t_2^2t_3^3-176t_2^3t_3^3-528t_1^2t_2^3t_3^3-528t_1^4t_2^3t_3^3-176t_1^6t_2^3t_3^3+216t_1t_2^4t_3^3-528t_1^3t_2^4t_3^3+216t_1^5t_2^4t_3^3+72t_2^5t_3^3+216t_1^2t_2^5t_3^3+216t_1^4t_2^5t_3^3+72t_1^6t_2^5t_3^3+72t_1t_2^6t_3^3-176t_1^3t_2^6t_3^3+72t_1^5t_2^6t_3^3-9t_3^4+153t_1^2t_3^4-123t_1^4t_3^4+3t_1^6t_3^4+36t_1t_2t_3^4+216t_1^3t_2t_3^4-108t_1^5t_2t_3^4+153t_2^2t_3^4+819t_1^2t_2^2t_3^4+819t_1^4t_2^2t_3^4+153t_1^6t_2^2t_3^4+216t_1t_2^3t_3^4-528t_1^3t_2^3t_3^4+216t_1^5t_2^3t_3^4-123t_2^4t_3^4+819t_1^2t_2^4t_3^4-513t_1^4t_2^4t_3^4-15t_1^6t_2^4t_3^4-108t_1t_2^5t_3^4+216t_1^3t_2^5t_3^4+36t_1^5t_2^5t_3^4+3t_2^6t_3^4+153t_1^2t_2^6t_3^4-15t_1^4t_2^6t_3^4+27t_1^6t_2^6t_3^4-36t_1t_3^5+72t_1^3t_3^5+12t_1^5t_3^5-36t_2t_3^5-108t_1^2t_2t_3^5-108t_1^4t_2t_3^5-36t_1^6t_2t_3^5-108t_1t_2^2t_3^5+216t_1^3t_2^2t_3^5+36t_1^5t_2^2t_3^5+72t_2^3t_3^5+216t_1^2t_2^3t_3^5+216t_1^4t_2^3t_3^5+72t_1^6t_2^3t_3^5-108t_1t_2^4t_3^5+216t_1^3t_2^4t_3^5+36t_1^5t_2^4t_3^5+12t_2^5t_3^5+36t_1^2t_2^5t_3^5+36t_1^4t_2^5t_3^5+12t_1^6t_2^5t_3^5-36t_1t_2^6t_3^5+72t_1^3t_2^6t_3^5+12t_1^5t_2^6t_3^5+9t_3^6+3t_1^2t_3^6+3t_1^4t_3^6+9t_1^6t_3^6+12t_1t_2t_3^6+72t_1^3t_2t_3^6-36t_1^5t_2t_3^6+3t_2^2t_3^6-123t_1^2t_2^2t_3^6+153t_1^4t_2^2t_3^6-9t_1^6t_2^2t_3^6+72t_1t_2^3t_3^6-176t_1^3t_2^3t_3^6+72t_1^5t_2^3t_3^6+3t_2^4t_3^6+153t_1^2t_2^4t_3^6-15t_1^4t_2^4t_3^6+27t_1^6t_2^4t_3^6-36t_1t_2^5t_3^6+72t_1^3t_2^5t_3^6+12t_1^5t_2^5t_3^6+9t_2^6t_3^6-9t_1^2t_2^6t_3^6+27t_1^4t_2^6t_3^6+13t_1^6t_2^6t_3^6)$$

$$b^2 - 4ac \text{ condition} = 4096(1+t_1^2)(t_1-t_2)^8(1+t_2^2)(t_1-t_3)^8(t_2-t_3)^8(1+t_3^2)(9+13t_1^2+58t_1^4-198t_1^6-243t_1^8+9t_1^{10}+32t_1t_2-64t_1^3t_2+768t_1^5t_2+576t_1^7t_2-288t_1^9t_2+13t_2^2+225t_1^2t_2^2-270t_1^4t_2^2+1170t_1^6t_2^2-303t_1^8t_2^2+93t_1^{10}t_2^2-64t_1t_2^3-288t_1^3t_2^3-2528t_1^5t_2^3+6304t_1^7t_2^3-1632t_1^9t_2^3+58t_2^4-270t_1^2t_2^4+1572t_1^4t_2^4-13564t_1^6t_2^4+11458t_1^8t_2^4+298t_1^{10}t_2^4+768t_1t_2^5-2528t_1^3t_2^5+13152t_1^5t_2^5-31648t_1^7t_2^5+3104t_1^9t_2^5-198t_2^6+1170t_1^2t_2^6-13564t_1^4t_2^6+39396t_1^6t_2^6-17054t_1^8t_2^6+298t_1^{10}t_2^6+576t_1t_2^7+6304t_1^3t_2^7-31648t_1^5t_2^7+24032t_1^7t_2^7-2080t_1^9t_2^7-243t_2^8-303t_1^2t_2^8+11458t_1^4t_2^8-17054t_1^6t_2^8+2241t_1^8t_2^8+93t_1^{10}t_2^8-288t_1t_2^9-1632t_1^3t_2^9+3104t_1^5t_2^9-2080t_1^7t_2^9-384t_1^9t_2^9+9t_2^{10}+93t_1^2t_2^{10}+298t_1^4t_2^{10}+298t_1^6t_2^{10}+93t_1^8t_2^{10}+9t_1^{10}t_2^{10}+32t_1t_3-64t_1^3t_3+768t_1^5t_3+576t_1^7t_3-288t_1^9t_3+32t_2t_3+160t_1^2t_2t_3-3168t_1^4t_2t_3-4512t_1^6t_2t_3+2496t_1^8t_2t_3-384t_1^{10}t_2t_3+160t_1t_2^2t_3+3168t_1^3t_2^2t_3+5856t_1^5t_2^2t_3-6624t_1^7t_2^2t_3+768t_1^9t_2^2t_3-64t_2^3t_3+3168t_1^2t_2^3t_3+2176t_1^4t_2^3t_3+6848t_1^6t_2^3t_3-14656t_1^8t_2^3t_3-2080t_1^{10}t_2^3t_3-3168t_1t_2^4t_3+2176t_1^3t_2^4t_3+7360t_1^5t_2^4t_3+56448t_1^7t_2^4t_3-7008t_1^9t_2^4t_3+768t_2^5t_3+5856t_1^2t_2^5t_3+7360t_1^4t_2^5t_3-30464t_1^6t_2^5t_3+48192t_1^8t_2^5t_3+3104t_1^{10}t_2^5t_3-4512t_1t_2^6t_3+6848t_1^3t_2^6t_3-30464t_1^5t_2^6t_3-32448t_1^7t_2^6t_3-7008t_1^9t_2^6t_3+576t_2^7t_3-6624t_1^2t_2^7t_3+56448t_1^4t_2^7t_3-32448t_1^6t_2^7t_3+4672t_1^8t_2^7t_3-1632t_1^{10}t_2^7t_3+2496t_1t_2^8t_3-14656t_1^3t_2^8t_3+48192t_1^5t_2^8t_3+4672t_1^7t_2^8t_3+768t_1^9t_2^8t_3-288t_2^9t_3+768t_1^2t_2^9t_3-7008t_1^4t_2^9t_3-7008t_1^6t_2^9t_3+768t_1^8t_2^9t_3-288t_1^{10}t_2^9t_3-384t_1t_2^{10}t_3-2080t_1^3t_2^{10}t_3+3104t_1^5t_2^{10}t_3-1632t_1^7t_2^{10}t_3-288t_1^9t_2^{10}t_3+13t_3^2+225t_1^2t_3^2-270t_1^4t_3^2+1170t_1^6t_3^2-303t_1^8t_3^2+93t_1^{10}t_3^2+160t_1t_2t_3^2+3168t_1^3t_2t_3^2+5856t_1^5t_2t_3^2-6624t_1^7t_2t_3^2+768t_1^9t_2t_3^2+225t_2^2t_3^2-6939t_1^2t_2^2t_3^2-22422t_1^4t_2^2t_3^2+13098t_1^6t_2^2t_3^2+18309t_1^8t_2^2t_3^2+2241t_1^{10}t_2^2t_3^2+3168t_1t_2^3t_3^2+15200t_1^3t_2^3t_3^2-17952t_1^5t_2^3t_3^2-35552t_1^7t_2^3t_3^2+4672t_1^9t_2^3t_3^2-270t_2^4t_3^2-22422t_1^2t_2^4t_3^2-13708t_1^4t_2^4t_3^2-146860t_1^6t_2^4t_3^2+1722t_1^8t_2^4t_3^2-17054t_1^{10}t_2^4t_3^2+5856t_1t_2^5t_3^2-17952t_1^3t_2^5t_3^2+292704t_1^5t_2^5t_3^2-145248t_1^7t_2^5t_3^2+48192t_1^9t_2^5t_3^2+1170t_2^6t_3^2+13098t_1^2t_2^6t_3^2-146860t_1^4t_2^6t_3^2+271796t_1^6t_2^6t_3^2+1722t_1^8t_2^6t_3^2+11458t_1^{10}t_2^6t_3^2-6624t_1t_2^7t_3^2-35552t_1^3t_2^7t_3^2-145248t_1^5t_2^7t_3^2-47008t_1^7t_2^7t_3^2-14656t_1^9t_2^7t_3^2-303t_2^8t_3^2+18309t_1^2t_2^8t_3^2+1722t_1^4t_2^8t_3^2+1722t_1^6t_2^8t_3^2+18309t_1^8t_2^8t_3^2-303t_1^{10}t_2^8t_3^2+768t_1t_2^9t_3^2+4672t_1^3t_2^9t_3^2+48192t_1^5t_2^9t_3^2-14656t_1^7t_2^9t_3^2+2496t_1^9t_2^9t_3^2+93t_2^{10}t_3^2+2241t_1^2t_2^{10}t_3^2-17054t_1^4t_2^{10}t_3^2+11458t_1^6t_2^{10}t_3^2-303t_1^8t_2^{10}t_3^2-243t_1^{10}t_2^{10}t_3^2-64t_1t_3^3-288t_1^3t_3^3-2528t_1^5t_3^3+6304t_1^7t_3^3-1632t_1^9t_3^3-64t_2t_3^3+3168t_1^2t_2t_3^3+2176t_1^4t_2t_3^3+6848t_1^6t_2t_3^3-14656t_1^8t_2t_3^3-2080t_1^{10}t_2t_3^3+3168t_1t_2^2t_3^3+15200t_1^3t_2^2t_3^3-17952t_1^5t_2^2t_3^3-35552t_1^7t_2^2t_3^3+4672t_1^9t_2^2t_3^3-288t_2^3t_3^3+15200t_1^2t_2^3t_3^3+30400t_1^4t_2^3t_3^3+304320t_1^6t_2^3t_3^3-47008t_1^8t_2^3t_3^3+24032t_1^{10}t_2^3t_3^3+2176t_1t_2^4t_3^3+30400t_1^3t_2^4t_3^3-241344t_1^5t_2^4t_3^3+128064t_1^7t_2^4t_3^3-32448t_1^9t_2^4t_3^3-2528t_2^5t_3^3-17952t_1^2t_2^5t_3^3-241344t_1^4t_2^5t_3^3-101952t_1^6t_2^5t_3^3-145248t_1^8t_2^5t_3^3-31648t_1^{10}t_2^5t_3^3+6848t_1t_2^6t_3^3+304320t_1^3t_2^6t_3^3-$$

$$101952t_1^5t_2^6t_3^3+128064t_1^7t_2^6t_3^3+56448t_1^9t_2^6t_3^3+6304t_2^7t_3^3-35552t_1^2t_2^7t_3^3+128064t_1^4t_2^7t_3^3+128064t_1^6t_2^7t_3^3-35552t_1^8t_2^7t_3^3+6304t_1^{10}t_2^7t_3^3-14656t_1t_2^8t_3^3-47008t_1^3t_2^8t_3^3-145248t_1^5t_2^8t_3^3-35552t_1^7t_2^8t_3^3-6624t_1^9t_2^8t_3^3-1632t_2^9t_3^3+4672t_1^2t_2^9t_3^3-32448t_1^4t_2^9t_3^3+56448t_1^6t_2^9t_3^3-6624t_1^8t_2^9t_3^3+576t_1^{10}t_2^9t_3^3-2080t_1t_2^{10}t_3^3+24032t_1^3t_2^{10}t_3^3-31648t_1^5t_2^{10}t_3^3+6304t_1^7t_2^{10}t_3^3+576t_1^9t_2^{10}t_3^3+58t_3^4-270t_1^2t_3^4+1572t_1^4t_3^4-13564t_1^6t_3^4+11458t_1^8t_3^4+298t_1^{10}t_3^4-3168t_1t_2t_3^4+2176t_1^3t_2t_3^4+7360t_1^5t_2t_3^4+56448t_1^7t_2t_3^4-7008t_1^9t_2t_3^4-270t_2^2t_3^4-22422t_1^2t_2^2t_3^4-13708t_1^4t_2^2t_3^4-146860t_1^6t_2^2t_3^4+1722t_1^8t_2^2t_3^4-17054t_1^{10}t_2^2t_3^4+2176t_1t_2^3t_3^4+30400t_1^3t_2^3t_3^4-241344t_1^5t_2^3t_3^4+128064t_1^7t_2^3t_3^4-32448t_1^9t_2^3t_3^4+1572t_2^4t_3^4-13708t_1^2t_2^4t_3^4+682344t_1^4t_2^4t_3^4-159512t_1^6t_2^4t_3^4+271796t_1^8t_2^4t_3^4+39396t_1^{10}t_2^4t_3^4+7360t_1t_2^5t_3^4-241344t_1^3t_2^5t_3^4+167232t_1^5t_2^5t_3^4-101952t_1^7t_2^5t_3^4-30464t_1^9t_2^5t_3^4-13564t_2^6t_3^4-146860t_1^2t_2^6t_3^4-159512t_1^4t_2^6t_3^4-159512t_1^6t_2^6t_3^4-146860t_1^8t_2^6t_3^4-13564t_1^{10}t_2^6t_3^4+56448t_1t_2^7t_3^4+128064t_1^3t_2^7t_3^4-101952t_1^5t_2^7t_3^4+304320t_1^7t_2^7t_3^4+6848t_1^9t_2^7t_3^4+11458t_2^8t_3^4+1722t_1^2t_2^8t_3^4+271796t_1^4t_2^8t_3^4-146860t_1^6t_2^8t_3^4+13098t_1^8t_2^8t_3^4+1170t_1^{10}t_2^8t_3^4-7008t_1t_2^9t_3^4-32448t_1^3t_2^9t_3^4-30464t_1^5t_2^9t_3^4+6848t_1^7t_2^9t_3^4-4512t_1^9t_2^9t_3^4+298t_2^{10}t_3^4-17054t_1^2t_2^{10}t_3^4+39396t_1^4t_2^{10}t_3^4-13564t_1^6t_2^{10}t_3^4+1170t_1^8t_2^{10}t_3^4-198t_1^{10}t_2^{10}t_3^4+768t_1t_3^5-2528t_1^3t_3^5+13152t_1^5t_3^5-31648t_1^7t_3^5+3104t_1^9t_3^5+768t_2t_3^5+5856t_1^2t_2t_3^5+7360t_1^4t_2t_3^5-30464t_1^6t_2t_3^5+48192t_1^8t_2t_3^5+3104t_1^{10}t_2t_3^5+5856t_1t_2^2t_3^5-17952t_1^3t_2^2t_3^5+292704t_1^5t_2^2t_3^5-145248t_1^7t_2^2t_3^5+48192t_1^9t_2^2t_3^5-2528t_2^3t_3^5-17952t_1^2t_2^3t_3^5-241344t_1^4t_2^3t_3^5-101952t_1^6t_2^3t_3^5-145248t_1^8t_2^3t_3^5-31648t_1^{10}t_2^3t_3^5+7360t_1t_2^4t_3^5-241344t_1^3t_2^4t_3^5+167232t_1^5t_2^4t_3^5-101952t_1^7t_2^4t_3^5-30464t_1^9t_2^4t_3^5+13152t_2^5t_3^5+292704t_1^2t_2^5t_3^5+167232t_1^4t_2^5t_3^5+167232t_1^6t_2^5t_3^5+292704t_1^8t_2^5t_3^5+13152t_1^{10}t_2^5t_3^5-30464t_1t_2^6t_3^5-101952t_1^3t_2^6t_3^5+167232t_1^5t_2^6t_3^5-241344t_1^7t_2^6t_3^5+7360t_1^9t_2^6t_3^5-31648t_2^7t_3^5-145248t_1^2t_2^7t_3^5-101952t_1^4t_2^7t_3^5-241344t_1^6t_2^7t_3^5-17952t_1^8t_2^7t_3^5-2528t_1^{10}t_2^7t_3^5+48192t_1t_2^8t_3^5-145248t_1^3t_2^8t_3^5+292704t_1^5t_2^8t_3^5-17952t_1^7t_2^8t_3^5+5856t_1^9t_2^8t_3^5+3104t_2^9t_3^5+48192t_1^2t_2^9t_3^5-30464t_1^4t_2^9t_3^5+7360t_1^6t_2^9t_3^5+5856t_1^8t_2^9t_3^5+768t_1^{10}t_2^9t_3^5+3104t_1t_2^{10}t_3^5-31648t_1^3t_2^{10}t_3^5+13152t_1^5t_2^{10}t_3^5-2528t_1^7t_2^{10}t_3^5+768t_1^9t_2^{10}t_3^5-198t_3^6+1170t_1^2t_3^6-13564t_1^4t_3^6+39396t_1^6t_3^6-17054t_1^8t_3^6+298t_1^{10}t_3^6-4512t_1t_2t_3^6+6848t_1^3t_2t_3^6-30464t_1^5t_2t_3^6-32448t_1^7t_2t_3^6-7008t_1^9t_2t_3^6+1170t_2^2t_3^6+13098t_1^2t_2^2t_3^6-146860t_1^4t_2^2t_3^6+271796t_1^6t_2^2t_3^6+1722t_1^8t_2^2t_3^6+11458t_1^{10}t_2^2t_3^6+6848t_1t_2^3t_3^6+304320t_1^3t_2^3t_3^6-101952t_1^5t_2^3t_3^6+128064t_1^7t_2^3t_3^6+56448t_1^9t_2^3t_3^6-13564t_2^4t_3^6-146860t_1^2t_2^4t_3^6-159512t_1^4t_2^4t_3^6-159512t_1^6t_2^4t_3^6-146860t_1^8t_2^4t_3^6-13564t_1^{10}t_2^4t_3^6-30464t_1t_2^5t_3^6-101952t_1^3t_2^5t_3^6+167232t_1^5t_2^5t_3^6-241344t_1^7t_2^5t_3^6+7360t_1^9t_2^5t_3^6+39396t_2^6t_3^6+271796t_1^2t_2^6t_3^6-159512t_1^4t_2^6t_3^6+682344t_1^6t_2^6t_3^6-13708t_1^8t_2^6t_3^6+1572t_1^{10}t_2^6t_3^6-32448t_1t_2^7t_3^6+128064t_1^3t_2^7t_3^6-241344t_1^5t_2^7t_3^6+30400t_1^7t_2^7t_3^6+2176t_1^9t_2^7t_3^6-17054t_2^8t_3^6+1722t_1^2t_2^8t_3^6-$$

$$146860t_1^4t_2^8t_3^6 - 13708t_1^6t_2^8t_3^6 - 22422t_1^8t_2^8t_3^6 - 270t_1^{10}t_2^8t_3^6 - 7008t_1t_2^9t_3^6 + 56448t_1^3t_2^9t_3^6 + 7360t_1^5t_2^9t_3^6 + 2176t_1^7t_2^9t_3^6 - 3168t_1^9t_2^9t_3^6 + 298t_2^{10}t_3^6 + 11458t_1^2t_2^{10}t_3^6 - 13564t_1^4t_2^{10}t_3^6 + 1572t_1^6t_2^{10}t_3^6 - 270t_1^8t_2^{10}t_3^6 + 58t_1^{10}t_2^{10}t_3^6 + 576t_1t_3^7 + 6304t_1^3t_3^7 - 31648t_1^5t_3^7 + 24032t_1^7t_3^7 - 2080t_1^9t_3^7 + 576t_2t_3^7 - 6624t_1^2t_2t_3^7 + 56448t_1^4t_2t_3^7 - 32448t_1^6t_2t_3^7 + 4672t_1^8t_2t_3^7 - 1632t_1^{10}t_2t_3^7 - 6624t_1t_2^2t_3^7 - 35552t_1^3t_2^2t_3^7 - 145248t_1^5t_2^2t_3^7 - 47008t_1^7t_2^2t_3^7 - 14656t_1^9t_2^2t_3^7 + 6304t_2^3t_3^7 - 35552t_1^2t_2^3t_3^7 + 128064t_1^4t_2^3t_3^7 + 128064t_1^6t_2^3t_3^7 - 35552t_1^8t_2^3t_3^7 + 6304t_1^{10}t_2^3t_3^7 + 56448t_1t_2^4t_3^7 + 128064t_1^3t_2^4t_3^7 - 101952t_1^5t_2^4t_3^7 + 304320t_1^7t_2^4t_3^7 + 6848t_1^9t_2^4t_3^7 - 31648t_2^5t_3^7 - 145248t_1^2t_2^5t_3^7 - 101952t_1^4t_2^5t_3^7 - 241344t_1^6t_2^5t_3^7 - 17952t_1^8t_2^5t_3^7 - 2528t_1^{10}t_2^5t_3^7 - 32448t_1t_2^6t_3^7 + 128064t_1^3t_2^6t_3^7 - 241344t_1^5t_2^6t_3^7 + 30400t_1^7t_2^6t_3^7 + 2176t_1^9t_2^6t_3^7 + 24032t_2^7t_3^7 - 47008t_1^2t_2^7t_3^7 + 304320t_1^4t_2^7t_3^7 + 30400t_1^6t_2^7t_3^7 + 15200t_1^8t_2^7t_3^7 - 288t_1^{10}t_2^7t_3^7 + 4672t_1t_2^8t_3^7 - 35552t_1^3t_2^8t_3^7 - 17952t_1^5t_2^8t_3^7 + 15200t_1^7t_2^8t_3^7 + 3168t_1^9t_2^8t_3^7 - 2080t_2^9t_3^7 - 14656t_1^2t_2^9t_3^7 + 6848t_1^4t_2^9t_3^7 + 2176t_1^6t_2^9t_3^7 + 3168t_1^8t_2^9t_3^7 - 64t_1^{10}t_2^9t_3^7 - 1632t_1t_2^{10}t_3^7 + 6304t_1^3t_2^{10}t_3^7 - 2528t_1^5t_2^{10}t_3^7 - 288t_1^7t_2^{10}t_3^7 - 64t_1^9t_2^{10}t_3^7 - 243t_3^8 - 303t_1^2t_3^8 + 11458t_1^4t_3^8 - 17054t_1^6t_3^8 + 2241t_1^8t_3^8 + 93t_1^{10}t_3^8 + 2496t_1t_2t_3^8 - 14656t_1^3t_2t_3^8 + 48192t_1^5t_2t_3^8 + 4672t_1^7t_2t_3^8 + 768t_1^9t_2t_3^8 - 303t_2^2t_3^8 + 18309t_1^2t_2^2t_3^8 + 1722t_1^4t_2^2t_3^8 + 1722t_1^6t_2^2t_3^8 + 18309t_1^8t_2^2t_3^8 - 303t_1^{10}t_2^2t_3^8 - 14656t_1t_2^3t_3^8 - 47008t_1^3t_2^3t_3^8 - 145248t_1^5t_2^3t_3^8 - 35552t_1^7t_2^3t_3^8 - 6624t_1^9t_2^3t_3^8 + 11458t_2^4t_3^8 + 1722t_1^2t_2^4t_3^8 + 271796t_1^4t_2^4t_3^8 - 146860t_1^6t_2^4t_3^8 + 13098t_1^8t_2^4t_3^8 + 1170t_1^{10}t_2^4t_3^8 + 48192t_1t_2^5t_3^8 - 145248t_1^3t_2^5t_3^8 + 292704t_1^5t_2^5t_3^8 - 17952t_1^7t_2^5t_3^8 + 5856t_1^9t_2^5t_3^8 - 17054t_2^6t_3^8 + 1722t_1^2t_2^6t_3^8 - 146860t_1^4t_2^6t_3^8 - 13708t_1^6t_2^6t_3^8 - 22422t_1^8t_2^6t_3^8 - 270t_1^{10}t_2^6t_3^8 + 4672t_1t_2^7t_3^8 - 35552t_1^3t_2^7t_3^8 - 17952t_1^5t_2^7t_3^8 + 15200t_1^7t_2^7t_3^8 + 3168t_1^9t_2^7t_3^8 + 2241t_2^8t_3^8 + 18309t_1^2t_2^8t_3^8 + 13098t_1^4t_2^8t_3^8 - 22422t_1^6t_2^8t_3^8 - 6939t_1^8t_2^8t_3^8 + 225t_1^{10}t_2^8t_3^8 + 768t_1t_2^9t_3^8 - 6624t_1^3t_2^9t_3^8 + 5856t_1^5t_2^9t_3^8 + 3168t_1^7t_2^9t_3^8 + 160t_1^9t_2^9t_3^8 + 93t_2^{10}t_3^8 - 303t_1^2t_2^{10}t_3^8 + 1170t_1^4t_2^{10}t_3^8 - 270t_1^6t_2^{10}t_3^8 + 225t_1^8t_2^{10}t_3^8 + 13t_1^{10}t_2^{10}t_3^8 - 288t_1t_3^9 - 1632t_1^3t_3^9 + 3104t_1^5t_3^9 - 2080t_1^7t_3^9 - 384t_1^9t_3^9 - 288t_2t_3^9 + 768t_1^2t_2t_3^9 - 7008t_1^4t_2t_3^9 - 7008t_1^6t_2t_3^9 + 768t_1^8t_2t_3^9 - 288t_1^{10}t_2t_3^9 + 768t_1t_2^2t_3^9 + 4672t_1^3t_2^2t_3^9 + 48192t_1^5t_2^2t_3^9 - 14656t_1^7t_2^2t_3^9 + 2496t_1^9t_2^2t_3^9 - 1632t_2^3t_3^9 + 4672t_1^2t_2^3t_3^9 - 32448t_1^4t_2^3t_3^9 + 56448t_1^6t_2^3t_3^9 - 6624t_1^8t_2^3t_3^9 + 576t_1^{10}t_2^3t_3^9 - 7008t_1t_2^4t_3^9 - 32448t_1^3t_2^4t_3^9 - 30464t_1^5t_2^4t_3^9 + 6848t_1^7t_2^4t_3^9 - 4512t_1^9t_2^4t_3^9 + 3104t_2^5t_3^9 + 48192t_1^2t_2^5t_3^9 - 30464t_1^4t_2^5t_3^9 + 7360t_1^6t_2^5t_3^9 + 5856t_1^8t_2^5t_3^9 + 768t_1^{10}t_2^5t_3^9 - 7008t_1t_2^6t_3^9 + 56448t_1^3t_2^6t_3^9 + 7360t_1^5t_2^6t_3^9 + 2176t_1^7t_2^6t_3^9 - 3168t_1^9t_2^6t_3^9 - 2080t_2^7t_3^9 - 14656t_1^2t_2^7t_3^9 + 6848t_1^4t_2^7t_3^9 + 2176t_1^6t_2^7t_3^9 + 3168t_1^8t_2^7t_3^9 - 64t_1^{10}t_2^7t_3^9 + 768t_1t_2^8t_3^9 - 6624t_1^3t_2^8t_3^9 + 5856t_1^5t_2^8t_3^9 + 3168t_1^7t_2^8t_3^9 + 160t_1^9t_2^8t_3^9 - 384t_2^9t_3^9 + 2496t_1^2t_2^9t_3^9 - 4512t_1^4t_2^9t_3^9 - 3168t_1^6t_2^9t_3^9 + 160t_1^8t_2^9t_3^9 + 32t_1^{10}t_2^9t_3^9 - 288t_1t_2^{10}t_3^9 + 576t_1^3t_2^{10}t_3^9 + 768t_1^5t_2^{10}t_3^9 - 64t_1^7t_2^{10}t_3^9 + 32t_1^9t_2^{10}t_3^9 + 9t_3^{10} + 93t_1^2t_3^{10} + 298t_1^4t_3^{10} + 298t_1^6t_3^{10} + 93t_1^8t_3^{10} + 9t_1^{10}t_3^{10} - 384t_1t_2t_3^{10} - 2080t_1^3t_2t_3^{10} + 3104t_1^5t_2t_3^{10} - 1632t_1^7t_2t_3^{10} - 288t_1^9t_2t_3^{10} + 93t_2^2t_3^{10} +$$

$$2241t_1^2t_2^2t_3^{10} - 17054t_1^4t_2^2t_3^{10} + 11458t_1^6t_2^2t_3^{10} - 303t_1^8t_2^2t_3^{10} - 243t_1^{10}t_2^2t_3^{10} - 2080t_1t_2^3t_3^{10} + 24032t_1^3t_2^3t_3^{10} - 31648t_1^5t_2^3t_3^{10} + 6304t_1^7t_2^3t_3^{10} + 576t_1^9t_2^3t_3^{10} + 298t_2^4t_3^{10} - 17054t_1^2t_2^4t_3^{10} + 39396t_1^4t_2^4t_3^{10} - 13564t_1^6t_2^4t_3^{10} + 1170t_1^8t_2^4t_3^{10} - 198t_1^{10}t_2^4t_3^{10} + 3104t_1t_2^5t_3^{10} - 31648t_1^3t_2^5t_3^{10} + 13152t_1^5t_2^5t_3^{10} - 2528t_1^7t_2^5t_3^{10} + 768t_1^9t_2^5t_3^{10} + 298t_2^6t_3^{10} + 11458t_1^2t_2^6t_3^{10} - 13564t_1^4t_2^6t_3^{10} + 1572t_1^6t_2^6t_3^{10} - 270t_1^8t_2^6t_3^{10} + 58t_1^{10}t_2^6t_3^{10} - 1632t_1t_2^7t_3^{10} + 6304t_1^3t_2^7t_3^{10} - 2528t_1^5t_2^7t_3^{10} - 288t_1^7t_2^7t_3^{10} - 64t_1^9t_2^7t_3^{10} + 93t_2^8t_3^{10} - 303t_1^2t_2^8t_3^{10} + 1170t_1^4t_2^8t_3^{10} - 270t_1^6t_2^8t_3^{10} + 225t_1^8t_2^8t_3^{10} + 13t_1^{10}t_2^8t_3^{10} - 288t_1t_2^9t_3^{10} + 576t_1^3t_2^9t_3^{10} + 768t_1^5t_2^9t_3^{10} - 64t_1^7t_2^9t_3^{10} + 32t_1^9t_2^9t_3^{10} + 9t_2^{10}t_3^{10} - 243t_1^2t_2^{10}t_3^{10} - 198t_1^4t_2^{10}t_3^{10} + 58t_1^6t_2^{10}t_3^{10} + 13t_1^8t_2^{10}t_3^{10} + 9t_1^{10}t_2^{10}t_3^{10})$$

C.2 Test Points

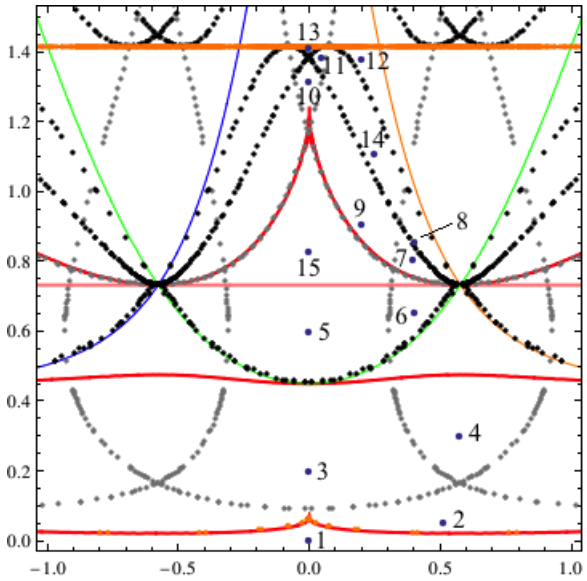

Figure C.1: Test Points for Stability Conditions

After determining values of (μ_1, μ_2, μ_3) at which to test the stability conditions b/a, ac, and $b^2 - 4ac$, we used Mathematica to solve for (t_1, t_2, t_3) at each set of μ_i using the t-map (5.19). We then evaluated the stability conditions at these values of t_i.

Point from Figure C.1	(μ_1, μ_2, μ_3)	(t, r)
1	(1,1,1)	(0,0)
2	(63, 54, 55)	$\left(\frac{-5+\sqrt{73}}{4\sqrt{3}}, \frac{-172+\sqrt{29730}}{\sqrt{73}}\right)$
3	(2, 1, 2)	$(0, -5+3\sqrt{3})$
4	(85, 36, 36)	$(\frac{1}{\sqrt{3}}, \frac{1}{49}(-157+\sqrt{29451}))$
5	(69, -18, 69)	$(0, \frac{1}{29}(-40+\sqrt{3282}))$
6	(97, -7, 23)	$\left(\frac{-67+2\sqrt{2149}}{37\sqrt{3}}, \frac{-113+3\sqrt{3329}}{2\sqrt{2149}}\right)$
7	(96, -21, 13)	$\left(\frac{-151+2\sqrt{10867}}{83\sqrt{3}}, \frac{-88+17\sqrt{102}}{\sqrt{10867}}\right)$
8	(96, -25, 10)	$\left(\frac{1}{43}(-26\sqrt{3}+\sqrt{3877}), -27\sqrt{\frac{3}{3877}}+\sqrt{\frac{9941}{3877}}\right)$
9	(83, -44, 34)	$\left(\frac{-205+2\sqrt{12307}}{49\sqrt{3}}, \frac{-73+3\sqrt{3327}}{\sqrt{12307}}\right)$
10	(45, -77, 45)	$(0, \frac{1}{122}(-13+\sqrt{29937}))$
11	(49, -80, 35)	$\left(\frac{7\sqrt{3}}{122+\sqrt{15031}}, \frac{(-4+3\sqrt{3342})(219430354120+1789792841\sqrt{15031})}{15031(122+\sqrt{15031})^4}\right)$
12	(66, -73, 12)	$\left(\frac{-112+\sqrt{14731}}{27\sqrt{3}}, \frac{-5+\sqrt{29487}}{\sqrt{14731}}\right)$
13	(41, -81, 41)	$(0, \frac{1}{122}(-1+\sqrt{29769}))$
14	(81, -56, 17)	$(\frac{1}{32}(-35\sqrt{3}+\sqrt{4699}), -14\sqrt{\frac{3}{4699}}+\sqrt{\frac{9986}{4699}})$
15	(3, -2, 3)	$(0, \frac{1}{5}(-4+\sqrt{66}))$

Table C.1: Test Points for Stability Conditions

Point from Figure C.1	Critical Point of V (t_1, t_2, t_3)	Stability Conditions		
		b/a	ac	$b^2 - 4ac$
1 (1,1,1)	(0,-1., -0.414214)	-24.2355	149.831	177.618
	(0,-1., 2.41421)	-295.765	-1.00777×10^6	9.25678×10^6
	(0,1., -2.41421)	-295.765	-1.00777×10^6	9.25678×10^6
	(0,1., 0.414214)	-24.2355	149.831	177.618
	(0,-1.73205, 1.73205)	-768.	1.17965×10^6	-8.84756×10^{-9}
	(0,1.73205, -1.73205)	-768.	1.17965×10^6	-8.84756×10^{-9}
	(0,-2.41421, 2.41421)	-3447.68	-4.67534×10^8	4.29451×10^9
	(0,-2.41421, 1.)	-295.765	-1.00777×10^6	9.25678×10^6
	(0,-0.414214, 0.414214)	-8.31631	10.3347	12.2513
	(0,-0.414214, -1.)	-24.2355	149.831	177.618
	(0,0.414214, -0.414214)	-8.31631	10.3347	12.2513
	(0,0.414214, 1.)	-24.2355	149.831	177.618
	(0,2.41421, -2.41421)	-3447.68	-4.67534×10^8	4.29451×10^9
	(0,2.41421, -1.)	-295.765	-1.00777×10^6	9.25678×10^6
2 (63, 54, 55)	(0,-0.41525, -0.974756)	-23.2692	133.989	166.075
	(0,0.41525, 0.974756)	-23.2692	133.989	166.075
	(0,-0.425666, 0.427773)	-8.48186	11.0621	12.0299
	(0,0.425666, -0.427773)	-8.48186	11.0621	12.0299
	(0,-0.914908, 2.92391)	-323.419	-4.80226×10^6	4.0253×10^7
	(0,0.914908, -2.92391)	-323.419	-4.80226×10^6	4.0253×10^7
	(0,-0.982491, -0.418619)	-23.6847	140.519	171.505
	(0,0.982491, 0.418619)	-23.6847	140.519	171.505
	(0,-2.92616, 0.892203)	-262.244	-4.5866×10^6	3.78739×10^7
	(0,2.92616, -0.892203)	-262.244	-4.5866×10^6	3.78739×10^7

Table C.2: Stability Conditions for Test Points

Point from Figure C.1	Critical Point of V (t_1, t_2, t_3)	Stability Conditions		
		b/a	ac	$b^2 - 4ac$
3 (2, 1, 2)	(0,-0.404948, 0.477491)	-8.66817	12.0774	10.7795
	(0,0.404948, -0.477491)	-8.66817	12.0774	10.7795
	(0,-1.09397, -0.477491)	-30.8747	289.175	258.098
	(0,1.09397, 0.477491)	-30.8747	289.175	258.098
	(0,-3.22195, 0.686913)	298.655	-5.23715×10^6	4.33913×10^7
	(0,-1.22055, 4.98455)	-7341.03	-2.65823×10^9	2.47336×10^{10}
	(0,-0.359619, -0.82607)	-16.6199	54.5525	88.3905
	(0,0.359619, 0.82607)	-16.6199	54.5525	88.3905
	(0,1.22055, -4.98455)	-7341.03	-2.65823×10^9	2.47336×10^{10}
	(0,3.22195, -0.686913)	298.655	-5.23715×10^6	4.33913×10^7
4 (85, 36, 36)	(0,-0.434617, -0.874488)	-20.0281	90.2039	119.955
	(0,0.434617, 0.874488)	-20.0281	90.2039	119.955
	(0,-0.874488, -0.434617)	2525.87	-3.00749×10^9	2.44461×10^{10}
	(0,0.874488, 0.434617)	2525.87	-3.00749×10^9	2.44461×10^{10}
	(0,-0.70379, 6.28275)	-20.0281	90.2039	119.955
	(0,0.70379, -6.28275)	-20.0281	90.2039	119.955
	(0,-6.28275, 0.70379)	2525.87	-3.00749×10^9	2.44461×10^{10}
	(0,6.28275, -0.70379)	2525.87	-3.00749×10^9	2.44461×10^{10}
	(0,-0.485229, 0.485229)	-9.10276	14.7056	8.82696
	(0,0.485229, -0.485229)	-9.10276	14.7056	8.82696
5 (69, -18, 69)	(0,-0.393489, 0.655209)	-9.28536	20.4624	-21.3878
	(0,0.393489, -0.655209)	-9.28536	20.4624	-21.3878
	(0,-1.41299, -0.655209)	-62.5174	2406.92	-2515.77
	(0,1.41299,0.655209)	-62.5174	2406.92	-2515.77
	(0,-3.95941, 0.539543)	1389.44	-1.33082×10^7	1.48033×10^8
	(0,-0.923325, -12.5222)	-78644.1	-5.27552×10^{12}	4.40123×10^{13}
	(0,-0.189168, -0.392377)	-5.67936	2.82495	15.9534
	(0,0.189168, 0.392377)	-5.67936	2.82495	15.9534
	(0,0.923325, 12.5222)	-78644.1	-5.27552×10^{12}	4.40123×10^{13}
	(0,3.95941, -0.539543)	1389.44	-1.33082×10^7	1.48033×10^8

Table C.2: Stability Conditions for Test Points(continued)

Point from Figure C.1	Critical Point of V (t_1, t_2, t_3)	Stability Conditions b/a	ac	$b^2 - 4ac$
6 (97, -7, 23)	(0,-0.33286, -0.475848)	-7.92388	7.46629	25.8066
	(0,0.33286, 0.475848)	-7.92388	7.46629	25.8066
	(0,-0.521517, 0.596752)	-9.45183	19.5361	-2.18705
	(0,0.521517, -0.596752)	-9.45183	19.5361	-2.18705
	(0,-0.647291, -35.1966)	1.580×10^6	-4.12655×10^{16}	3.34517×10^{17}
	(0,0.647291, 35.1966)	1.580×10^6	-4.12655×10^{16}	3.34517×10^{17}
	(0,-0.98615, -0.653068)	-32.2498	413.465	-381.277
	(0,0.98615, 0.653068)	-32.2498	413.465	-381.277
	(0,-11.8992, 0.560935)	78655.3	-6.12501×10^{11}	6.05973×10^{12}
	(0,11.8992, -0.560935)	78655.3	-6.12501×10^{11}	6.05973×10^{12}
7 (96, -21, 13)	(0,-0.544957, 0.638803)	-9.43529	21.0238	-5.60998
	(0,0.544957, -0.638803)	-9.43529	21.0238	-5.60998
	(0,-0.614971, -11.5814)	15255.7	-4.11911×10^{11}	3.33863×10^{12}
	(0,0.614971, 11.5814)	15255.7	-4.11911×10^{11}	3.33863×10^{12}
	(0,-4.44718, -2.333)	90322.1	1.8109×10^{11}	-3.566×10^{11}
	(0,4.44718, 2.333)	90322.1	1.8109×10^{11}	-3.566×10^{11}
	(0,-20.6604, 0.5296)	749472.	-1.03699×10^{14}	1.13732×10^{15}
	(0,20.6604, -0.5296)	749472.	-1.03699×10^{14}	1.13732×10^{15}
8 (96, -25, 10)	(0,-0.552387, 0.651164)	-9.41049	21.2445	-5.36969
	(0,0.552387, -0.651164)	-9.41049	21.2445	-5.36969
	(0,-0.605742, -9.72259)	6898.52	-6.30173×10^{10}	5.10353×10^{11}
	(0,0.605742, 9.72259)	6898.52	-6.30173×10^{10}	5.10353×10^{11}
	(0,-7.9851, -2.75498)	1.808×10^6	2.22525×10^{14}	3.78416×10^{13}
	(0,7.9851, 2.75498)	1.808×10^6	2.22525×10^{14}	3.78416×10^{13}
	(0,-26.7496, 0.521081)	2.120×10^6	-1.21386×10^{15}	1.38047×10^{16}
	(0,26.7496, -0.521081)	2.120×10^6	-1.21386×10^{15}	1.38047×10^{16}

Table C.2: Stability Conditions for Test Points (continued)

Point from Figure C.1	Critical Point of V (t_1, t_2, t_3)	Stability Conditions b/a	ac	$b^2 - 4ac$
9 (83, -44, 34)	(0,-0.491055, 0.750258)	-9.03252	26.562	-54.2382
	(0,0.491055, -0.750258)	-9.03252	26.562	-54.2382
	(0,-0.686641, -5.40206)	-1482.08	-2.28365×10^8	1.92447×10^9
	(0,0.686641, 5.40206)	-1482.08	-2.28365×10^8	1.92447×10^9
	(0,-2.81301, -1.35946)	713.725	1.91638×10^7	-1.40379×10^8
	(0,2.81301, 1.35946)	713.725	1.91638×10^7	-1.40379×10^8
	(0,-8.09454, 0.488423)	24005.3	-6.98638×10^9	1.03369×10^{11}
	(0,8.09454, -0.488423)	24005.3	-6.98638×10^9	1.03369×10^{11}
10 (45, -77, 45)	(0,-0.45702, 1.26878)	6.0412	82.8229	-547.442
	(0,0.45702, -1.26878)	6.0412	82.8229	-547.442
	(0,-4.10762, -1.26878)	1320.51	5.85051×10^7	-3.86706×10^8
	(0,4.10762, 1.26878)	1320.51	5.85051×10^7	-3.86706×10^8
	(0,-4.99357, 0.417248)	4477.5	-1.05579×10^7	6.94946×10^8
	(0,-0.71997, -2.98964)	-379.423	-145493.	3.33622×10^6
	(0,0.71997, 2.98964)	-379.423	-145493.	3.33622×10^6
	(0,4.99357, -0.417248)	4477.5	-1.05579×10^7	6.94946×10^8
11 (49, -80, 35)	(0,-0.484384, 1.19479)	1.87369	18.4977	-137.46
	(0,0.484384, -1.19479)	1.87369	18.4977	-137.46
	(0,-0.681393, -2.84422)	-309.024	-23317.8	1.45758×10^6
	(0,0.681393, 2.84422)	-309.024	-23317.8	1.45758×10^6
	(0,-5.56952, -1.45914)	14792.9	9.13142×10^8	1.46197×10^{10}
	(0,5.56952, 1.45914)	14792.9	9.13142×10^8	1.46197×10^{10}
	(0,-6.25671, 0.407093)	10852.3	-2.88817×10^7	5.74278×10^9
	(0,6.25671, -0.407093)	10852.3	-2.88817×10^7	5.74278×10^9
12 (66, -73, 12)	(0,-0.544901, 0.946474)	-6.49228	7.16944	46.2784
	(0,0.544901, -0.946474)	-6.49228	7.16944	46.2784
	(0,-0.610911, -2.99583)	-276.793	-35886.8	1.33654×10^6
	(0,0.610911, 2.99583)	-276.793	-35886.8	1.33654×10^6
	(0,-16.6817, -2.04817)	7.138×10^6	9.24438×10^{14}	6.6536×10^{16}
	(0,16.6817, 2.04817)	7.138×10^6	9.24438×10^{14}	6.6536×10^{16}
	(0,-18.2483, 0.414687)	674764.	-1.42304×10^{12}	1.89609×10^{14}
	(0,18.2483, -0.414687)	674764.	-1.42304×10^{12}	1.89609×10^{14}

Table C.2: Stability Conditions for Test Points (continued)

Point from Figure C.1	Critical Point of V (t_1, t_2, t_3)	Stability Conditions b/a	ac	$b^2 - 4ac$
13 (41, -81, 41)	(0,-0.469381, 1.32959)	9.93756	9.21822	259.81
	(0,0.469381, -1.32959)	9.93756	9.21822	259.81
	(0,-4.78556, -1.32959)	3812.31	2.65716×10^7	7.48905×10^8
	(0,4.78556, 1.32959)	3812.31	2.65716×10^7	7.48905×10^8
	(0,-5.15582, 0.403074)	5186.91	-1.11458×10^6	8.71563×10^8
	(0,-0.703789, -2.78904)	-308.775	-5404.05	1.29479×10^6
	(0,0.703789, 2.78904)	-308.775	-5404.05	1.29479×10^6
	(0,5.15582, -0.403074)	5186.91	-1.11458×10^6	8.71563×10^8
14 (81, -56, 17)	(0,-0.533345, 0.801839)	-8.58102	24.2111	-38.2993
	(0,0.533345, -0.801839)	-8.58102	24.2111	-38.2993
	(0,-0.626769, -4.12382)	-535.273	-7.03967×10^6	6.3503×10^7
	(0,0.626769, 4.12382)	-535.273	-7.03967×10^6	6.3503×10^7
	(0,-8.95828, -2.06403)	703244.	1.99362×10^{13}	5.18802×10^{13}
	(0,8.95828, 2.06403)	703244.	1.99362×10^{13}	5.18802×10^{13}
	(0,-14.9554, 0.459766)	275619.	-1.6777×10^{12}	3.40961×10^{13}
	(0,14.9554, -0.459766)	275619.	-1.6777×10^{12}	3.40961×10^{13}
15 (3, -2, 3)	(0,-0.398176, 0.828336)	-8.55231	37.63	-158.16
	(0,0.398176, -0.828336)	-8.55231	37.63	-158.16
	(0,-1.83013, -0.828336)	-120.535	28061.4	-117943.
	(0,1.83013, 0.828336)	-120.535	28061.4	-117943.
	(0,-4.28089, 0.494157)	2117.54	-1.7057×10^7	2.44275×10^8
	(0,-0.836644, -5.57715)	-3125.36	-7.48257×10^8	6.51916×10^9
	(0,0.836644, 5.57715)	-3125.36	-7.48257×10^8	6.51916×10^9
	(0,4.28089, -0.494157)	2117.54	-1.7057×10^7	2.44275×10^8

Table C.2: Stability Conditions for Test Points (continued)